

Report No. IITRI-U6003-19  
(Final Report)

INVESTIGATION OF LIGHT SCATTERING  
IN HIGHLY REFLECTING PIGMENTED COATINGS

Volume 1  
SUMMARY

May 1, 1963, through September 30, 1966

Contract No. NASr-65(07)  
IITRI Project U6003

G. A. Zerlaut and B. H. Kaye

of

IIT RESEARCH INSTITUTE  
Technology Center  
Chicago, Illinois 60616

for

National Aeronautics and Space Administration  
Office of Advanced Research and Technology  
Washington 25, D.C.

FACILITY FORM 602	<b>N 71-70781</b>	
	(ACCESSION NUMBER)	(THRU)
	<i>122</i>	
	(PAGES)	(CODE)
	<i>CR-116171</i>	
	(NASA CR OR TMX OR AD NUMBER)	(CATEGORY)

Copy No. \_\_\_\_\_

December 1966



## FOREWORD

This is Volume 1 of three volumes of Report No. IITRI-U6003-19 (Final Report) of IITRI Project U6003, Contract No. NASr-65(07), entitled "Investigation of Light Scattering in Highly Reflecting Pigmented Coatings." This report covers the period from May 1, 1963, to September 30, 1966.

The following Quarterly Reports were issued:

IITRI-C6018-3	October 11, 1963
IITRI-C6018-6	January 29, 1964
IITRI-C6018-8	May 5, 1964
IITRI-C6018-11	September 5, 1964
IITRI-C6018-12	December 21, 1964
IITRI-C6018-13	March 10, 1965
IITRI-C6018-14	May 13, 1965
IITRI-C6018-15	August 9, 1965
IITRI-U6003-16	November 9, 1965
IITRI-U6003-17	February 28, 1966
IITRI-U6003-18	May 3, 1966

Because of a divisional reorganization and the accompanying administrative changes, the IITRI number designating this project was changed from C6018 to U6003 on September 1, 1965. The Quarterly Report issued on November 9, 1965, was the first report to bear the new number. Project administration and technical organization were not affected in this change.

The project was under the technical direction of the Research Projects Laboratory of the George C. Marshall Space Flight Center, and Mr. Daniel W. Gates was the cognizant technical manager. The contract was administered by Mr. James J. Gangler of the Office of Advanced Research and Technology, National Aeronautics and Space Administration.

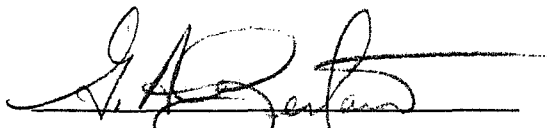
Major contributors to the program were G. A. Zerlaut, project leader, and (alphabetically): T. Church, shape factor analysis; H. Iglarsh, preparation of random models; M. R. Jackson, experimental studies and statistical analyses; Dr. B. H. Kaye, theoretical Monte Carlo and statistical studies; Dr. S. Katz, theoretical (classical) light-scattering studies; V. Raziunas, experimental (classical) studies on silver bromide

suspensions; and J. Stockham, preparation of suspensions.  
Administrative supervision was provided by Dr. T. M. Meltzer,  
Manager, Polymer Research.

Experimental data are recorded in Logbooks C13906, C14085,  
C14644, C16369, and C16765.

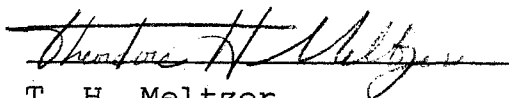
Respectfully submitted,

IIT RESEARCH INSTITUTE



G. A. Zerlaut  
Group Leader  
Polymer Research

Approved by:



T. H. Meltzer  
Manager  
Polymer Research

GAZ/rmc

## ABSTRACT

### INVESTIGATION OF LIGHT SCATTERING IN HIGHLY REFLECTING PIGMENTED COATINGS

#### Volume 1 SUMMARY

The light-scattering theory pertinent to three basic types of "pigmented" systems is reviewed in Section II: (a) systems with real refractive indices in which  $k = 0$ ,  $n^* = n$ , and the particle is transparent at that wavelength ( $k$  is proportional to the absorption coefficient), (b) systems with complex refractive indices in which both  $k$  and  $n$  are finite numbers and the particle both absorbs and scatters incident light, and (c) systems in which the complex refractive index,  $n^*$ , approaches infinity according to either  $n \rightarrow \infty$  or  $k \rightarrow \infty$  and the surface is perfectly reflecting at that wavelength. Application of classical theory to the multiple-scattering problem was essentially confined to theoretical films of spherical particles of real refractive index. Models were therefore proposed and tested by using applicable theory.

Experimental studies of silver bromide dispersions were performed in order to establish relationships between both inherent (refractive index, etc.) and induced (film thickness, concentration, etc.) optical properties of the films. The experiments, which are discussed in Section III, were limited to reflectance and transmittance measurements of various silver bromide suspensions (i.e., both liquid and solid suspensions).

Optical properties of suspensions of particles having narrow size distributions were compared with bimodal mixtures of these sizes. The data indicated that (a) particles of two sizes (a bimodal mixture) acted as independent scatterers in dilute solutions, (b) particles within thin concentrated films (of up to four layers) tended to act as independent scatterers, (c) an actual increase in transmittance at wavelengths corresponding to the first scattering maximum occurred with increasing

concentration of particles in dilute gelatin suspensions, (d) the optical properties predicted from single-particle size measurements were in general agreement with those observed experimentally on bimodal mixtures in concentrated films, (e) the back-scatter coefficient of thin films tended to be slightly higher than that of thicker ones, and (f) the back-scatter intensity obtained from bimodal mixtures was less than that predicted from measurements of monodisperse films.

These last observations tend to support the "ideal" coating model that was subsequently proposed. This model, which consists of several layers of ever-decreasing particle size, was not tested because of difficulties in obtaining colorless, sized fractions of model pigments.

This search for a theory to predict the reflectance properties of paint films revealed that several aspects of current descriptive terminology are insidious barriers to progress. For example, the term "highly reflective paint" can only be defined within a specific context of requirements. Also, false concepts encouraged a search for a technique for applying Mie scattering theory to pigment optics.

The relevance of Mie theory to paint technology is discussed in Section IV. The semantic problems of paint reflectance studies are explored in Section V; it is shown that until randomness, diffuse light, pigment shape, and pigment size are understood better development of paint technology will be accomplished by empirical exploration, which is qualitatively justified a posteriori rather than predicted theoretically.

Some developmental work on the concepts and the techniques of particle shape measurement was carried out. A computer program for investigating the potential use of statistical diameters in shape factor analysis was developed. The shape factor experiments are reported in Section VI.

Possible techniques for simulating particle packing are presented in Section VII, and a general discussion of Monte Carlo techniques as applied to reflectance studies is given in

Section VIII. General considerations concerning the development of a random-walk model for studying energy penetration of a paint film are presented in Section IX.

To study cluster growth in a paint film, a Monte Carlo experiment in two dimensions was developed. From the properties of the model, a statistical derivation of the Lambert-Beer law has been proposed. By use of the model, the possible mechanism by which extender particles can increase the opacity of a given amount of pigment was explored. From statistical reasoning alone, the existence of a critical pigment volume concentration for efficient use of pigment was predicted. The simulated data are given and their implications discussed in Section X.

Early in the development of a possible random-walk model for paint reflectance studies, it was thought that the very small interparticle distances within the paint film would place severe restrictions on any model of this type. Therefore a random screen model was explored. The various aspects of a random screen model are discussed in Section XI.

Various aspects of general studies of technologies such as filtration theory are discussed in Section XII.

## TABLE OF CONTENTS

	Page
I. Introduction	1
II. Classical Light-Scattering Theory	4
A. Concept of Light Scattering by Particles	4
B. Application of Classical Theory to Multiple Scattering	5
III. Experimental Studies of Silver Bromide Dispersions	15
A. Introduction	15
B. Experimental Procedures	15
C. Results and Discussion	16
D. Optical Properties of Films of Various Thicknesses	29
IV. Relevance of Mie Theory for Predicting Reflective Properties of Paint Films	34
V. Semantic Problems in Studying Reflective Properties of Paint Films	45
A. Introduction	45
B. Highly Reflecting Paint Films	45
C. Specification of Pigment Size	46
D. The Concept of Randomness	49
E. Diffuse Light	53
F. Boundary Conditions of Paint Films	54
G. Size Distribution of Pigment Particles Dispersed in Paint Films	55
VI. Measurement of Shape of Particles	57
VII. Simulation of Packing of Pigment Particles in Paint Films	61
VIII. Use of Monte Carlo Methods in Paint Technology	64
IX. Random-Walk Model for Studying Energy Penetration Through Paint Films	66
X. Monte Carlo Studies of Growth in Scattering Centers at Various Concentrations of Pigment	70
A. Simple Model of Monosized Cubic Pigment without Extender	70
B. Simple Model of Noncubic Pigment without Extender	79
C. Simple Model of Monosized Cubic Pigment with Extender	86
D. Partial Encapsulation of Pigment Particles	89

XI.	Random Screen Model for Studying Penetration of Light Through Paint Films	93
	A. Introduction	93
	B. Physical Properties of Random Screens	93
	C. Average Track Length within a Randomly Distributed Paint System	98
XII.	Implications of Monte Carlo Studies of Random Tracks Across a Circle for Filtration Studies	102
	A. Concept of Randomness Applied to Fibrous Filters	102
	B. Use of Random Intercept Diagrams to Devise Monte Carlo Methods for Studying Aerosol Filtration	105
	References	108
	Appendix - Errata in Volumes 2 and 3	110



# LIST OF TABLES

TABLE		Page
1	Attenuation of Light by a Film of Particles of $1-\mu$ Radius and Infinite Refractive Index at a Concentration of $6.7 \times 10^8/\text{cm}^2$	8
2	Conditions for Maximum Scattering by $1-\mu$ Transparent Particles	13
3	Scattering Properties of $1-\mu$ Particles of Various Refractive Indices at Wavelengths Corresponding to Maximum Scattering Cross Sections	14
4	Concentration of $1-\mu$ Particles and Film Thickness Required to Attenuate the Incident Signal to 1%	14
5	Data on Cluster Formation at 0.1 Volume Fraction of Idealized Monosized Pigment Dispersed with and without Theoretical Extender	88
6	Data on Cluster Formation at 0.3 Volume of Idealized Monosized Pigment Dispersed with Various Concentrations of Theoretical Extender	88
7	Available Straight-Through Paths in Randomly Superimposed Screens (Open Space in Original Screen, 0.303)	97

## LIST OF FIGURES

FIGURE	Page
1 Transmission for $1\text{-}\mu$ -Radius Spheres When $m = \alpha$	9
2 Limits of Forward- and Back-Scatter in Films	11
3 Transmittance of AgBr Suspensions in Water	18
4 Particle-Size Measurements from Light Scattering	19
5 Transmittance of Dilute Suspensions of AgBr Mixtures (Batches 25 and 30)	20
6 Scattering Extrema Versus Thickness of Gelatin Suspensions	23
7 Transmittance of Concentrated Gelatin Films	24
8 Optical Density of AgBr Suspensions (Batches 25 and 30)	25
9 Optical Density of a Mixture of Batches 26 and 30	27
10 Back-Scatter Intensity of AgBr Suspensions (Batches 25 and 26)	28
11 Back-Scatter Intensity at Various Thicknesses (Batch 26)	30
12 Thickness Versus Back-Scatter Intensity (Batch 26)	31
13 Schematic of Multilayer Coating and Resultant Optical Density of Layers	33
14 Relative Intensity in Single-Slit Diffraction for Three Values of Slit Width of the Ratio $\alpha/\lambda$	35
15 Combined Interference and Diffraction Pattern for Slits 5 Wavelengths Wide and 50 Wavelengths Apart	36
16 Diffraction Patterns for Two Beams Passing through the Same Slit	38
17 Screens Containing Randomly Spaced Parallel Slits of Equal Width	40
18 Diffraction by Rectangular Apertures	42
19 Claimed Universal Effective Extinction Curve for Pigment Particles	46
20 Different Dispersion States within a Pigment Film	48
21 Three Methods of Drawing Random Intercepts in a Circle	50
22 Lines Drawn between Two Random Numbers Selected on the Perimeter of a Circle	51
23 Lines Drawn Perpendicular to Radius for Randomly Selected Angles to a Fixed Direction	52

FIGURE		Page
24	Frequency of Occurrence of Porosities Less Than Stated Size	63
25	Relationship between Volume Fraction of Solids and Interparticle Distance in a Monosized Maximum Interparticle Distance Array	68
26	Monte Carlo Block Plotting Experiment at 35% Concentration	73
27	Number of Scattering Centers at Various Volume Concentrations for Randomly Distributed Monosized Particles	76
28	Absolute Number of Scattering Centers per Unit Volume	77
29	Number of Different Sized Clusters at Various Volume Concentrations for Randomly Distributed Monosized Particles	78
30	Absolute Number of Scattering Centers per Unit Volume	80
31	20% Coverage by Particles Having 2:1 Shape Ratio	82
32	Absolute Number of Scattering Centers per Unit Volume for Particles Having 2:1 Shape Ratio	83
33	Number of Different Sized Clusters at Various Volume Concentrations Formed from Particles Having 2:1 Shape Ratio	84
34	Simulated Pigment-Extender System: 30% Pigment, 10% Extender	87
35	Size Distributions of Clusters Formed at Various Volume Concentrations for Idealized Monosized Pigment Dispersed with and without Extender	90
36	Possible Configurations of Two Partially Encapsulated Particles	92
37	Basic Screen (Open Area, 0.303)	94
38	Two Randomly Superimposed Screens (Open Area, 0.101)	95
39	Three Randomly Superimposed Screens (Open Area, 0.03)	96
40	Elimination of Short Track Lengths: Spheridized 20% Monte Carlo Plot (Conversion of Figure 23)	99
41	Track Length Distribution at 15% Concentration	100
42	Pore-Size Distribution of Simulated Filters (Simulated in Figure 78)	104
43	Simulated Random Array of Particles in an Airstream	106
44	Reflectivities of Brass Plates of Different Surface Quality	111

INVESTIGATION OF LIGHT SCATTERING  
IN HIGHLY REFLECTING PIGMENTED COATINGS  
Volume 1  
SUMMARY

I. INTRODUCTION

The principal objective of this program was to apply light-scattering theory to real and simulated particle arrays in order to explain the scattering behavior of polydispersed, highly pigmented coatings, especially highly reflecting pigmented coatings. The program was aimed at an elucidation of the light-scattering parameters associated with the multiple-scattering events that operate in highly pigmented systems. Definition of these parameters should eventuate in the development of pigmented coatings that reflect a maximum of solar and other broad-band radiation.

This report, which is Volume 1 of the three-volume final report, is the Summary report on the subject program. Sections II and III are taken from the discussions presented in Volume 2, entitled "Classical Investigations; Theoretical and Experimental." Sections IV through XII are taken from Volume 3, entitled "Monte Carlo and Other Statistical Investigations." Although we refer liberally to the details presented in Volumes 2 and 3, Volume 1 is a comprehensive review of the studies undertaken during the course of the research and, as such, may require the use of Volumes 2 and 3 to clarify and amplify only.

The research during the first year consisted of theoretical and experimental investigations of essentially a classical nature. The theoretical studies were concerned first with a review of applicable light-scattering theory and second with the construction of theoretically simulated arrays of particles having, on the one hand, infinite refractive indices and, on the other, real (high) refractive indices with finite absorption coefficients. The experimental studies consisted of the preparation and optical evaluation of suspensions and arrays (films)

of carefully sized silver bromide particles. Monodisperse and bimodal suspensions and arrays were studied.

The Monte Carlo and statistical approaches delineated in Sections IV through XII (and in Volume 3) were first begun seriously at the commencement of the second year's activities. They were initiated when it was realized that the approaches being undertaken along classical lines of investigations were not productive in the elucidation of multiple-scattering phenomena. Indeed, it became increasingly evident that the complexity of these investigations would, in itself, eventuate in essentially insoluble (self-limiting) problems before much could be learned about the multiple interactions occurring in highly pigmented, polydisperse systems. The last year and a half of research was therefore limited to the Monte Carlo and statistical methods outlined above.

The Monte Carlo and statistical techniques outlined herein are well known as tools in mathematics and statistics. However, to the best of our knowledge, they have not before been employed in explaining the behavior of highly reflecting paint systems. In this context, these methods have contributed to new techniques for evaluating highly pigmented coatings, among several other physical systems. Regardless of the value that future research will assign to these studies, the studies have largely been of a pioneering nature. While we are certain that many errors, inconsistencies, and invalid conclusions exist, it is our hope that these studies will not only aid in the treatment of the fundamental nature of light scattering in highly pigmented coatings but will also serve to excite other workers to use these techniques in simulation studies involving other complex problems (such as filtration theory, composite materials, etc).

Finally, the above discussion of the potential of simulation studies has not been intended to infer that classical investigations such as described in the first two sections of this report are without merit. Rather, the complexity of the multiple-interaction problem associated with highly pigmented systems does

not readily, if at all, lend itself to treatment by classical methods. Indeed, the classical studies reported in Volume 2 and summarized in this volume are entirely valid for dilute suspensions and will find utility in many areas of technology.

In conclusion, the reader is referred to the Appendix of this volume, which contains an errata to Volumes 2 and 3 of this final report.

## II. CLASSICAL LIGHT-SCATTERING THEORY

### A. Concept of Light Scattering by Particles

When light or a related electromagnetic radiation impinges on a particle, the interaction leads to a redistribution of the radiant energy. The resulting radiation, which may be regarded as originating at the particle, is the light scattered by the particle. The particle is differentiated from the medium in which it resides by its refractive index. This refractive index may be real or complex -- a concept requiring further consideration.

Solution of the electromagnetic wave equation for transparent and absorbing material leads to a generalized expression for the refractive index. The expression includes terms for both refraction and absorption. For greatest generality, the refractive index is written as a complex number; the real part corresponds to the refractive index as it is usually written, and the imaginary part is related to the absorbing properties of the scatterer. The complex refractive index,  $n^*$ , is defined by:

$$n^* = n(1 - ik) \quad (1)$$

For a substance whose absorption coefficient is  $\mu$ , it is shown (ref. 1) that  $k$  in Equation 1 is defined by:

$$\mu = \frac{4\pi k}{\lambda} \quad (1a)$$

where  $\lambda$  is the wavelength of light.

The  $n$  in Equation 1 is not analogous to the refractive index defined by Snell's law. Snell's law is not obeyed for transmitting media with absorption (ref. 2). In the limit, as the absorption diminishes to zero and the medium becomes transparent,  $n^*$  becomes equal to  $n$  and Snell's law applies.

In addition to systems with real and complex refractive indices, a third case exists, that of a perfectly reflecting surface. Expressed in terms of electromagnetic theory, this condition can be described (ref. 3) as the upper limiting value of  $n$ , i.e.,  $n \rightarrow \infty$ .

Three special cases can therefore be considered:

- (A) When  $k = 0$ ,  $n^* = n$ , and the particle is transparent at that wavelength.
- (B) When  $k$  is a finite number, the particle both scatters and absorbs incident light. The absorption coefficient,  $\mu$ , is related to  $k$ :

$$k = \frac{\lambda \mu}{4\pi}$$

- (C)  $n^*$  can approach infinity by one of two routes:

$$n \rightarrow \infty$$

or

$$k \rightarrow \infty$$

A detailed examination of the theory for these three cases is presented in Volume 2 of this report (Section IIB). The total scattering of light by spherical particles is therefore a function of three parameters: the particle size, the refractive index of the particle in relation to the surrounding medium, and the wavelength of the light.

## B. Application of Classical Theory to Multiple Scattering

### 1. Introduction

In Volume 2 (Section B), we discussed light-scattering theory with reference to single particles. Single-particle theory can be used to describe the light-scattering characteristics of a colloidal or aerosol suspension in which the particles are very widely dispersed. For the present application of scattering theory to the design of a coating material, it becomes necessary to attempt to set a lower limit to the separation distance that still permits application of scattering theory.

The theoretical problem of computing the scattering of light by a multiple array of particles in terms of the interaction of an electromagnetic wave on a multiple discontinuity does not appear to have been analyzed rigorously. Van de Hulst (ref. 4) noted the problem in 1946 and commented then on its



complexity. A number of references in the literature give an empirical or an estimated partial solution of the problem. Sinclair (ref. 5) suggested a spacing of 10 or preferably 100 times the radius of the particle for independent scattering. However, Berry (ref. 6) studied the scattering of light by cubic silver bromide crystals embedded in gelatin and reported that the approximation to single independent scattering appears to be quite satisfactory when the separation of the grain centers is more than about twice the grain size.

In previous reports, we defined the term  $S$  as the effective scattering area of a single particle.  $K$ , the scattering coefficient per unit cross-sectional area of the particle, is therefore equal to  $S/\pi r^2$ . A plot of  $K$  against the parameter  $\alpha = 2\pi r/\lambda$  for several real refractive indices is presented in Figure 1 of Volume 2.

In the absence of a more exact procedure, it is proposed that for particles whose scattering coefficient,  $K$ , is greater than unity, the scattering cross section,  $S$ , governs the limit of particle spacing for effective application of light-scattering theory. The electromagnetic fields that define the scattering cross sections will interfere if the particles are spaced more closely. Also, in the case of very small particles when  $K$  is less than unity, the scattering cross section is smaller than the geometric cross section and the physical dimensions of the particle will dictate the limits of particle spacing.

## 2. General Considerations

We shall next consider the formation of a theoretical film consisting of a transparent matrix in which the light-scattering particles are embedded. Since the system is theoretical, it is possible to visualize such convenient factors as fully monodisperse particle assemblies, complete freedom of choice of refractive index, etc. The analysis is handicapped by the limited availability of numerical data. Total and radial scattering data are available for transparent spherical particles

over a wide range of conditions. On the other hand, the information for fully reflecting particles with infinite refractive index is fragmentary, and only a few cases involving complex refractive indices have been computed. Practically no data exist for nonspherical particles, although a number of these appear to have some value in the present context.

In formulating this model, one should note that the Mie theory of light scattering was developed for the case of a parallel light beam impinging on an isolated particle (ref. 7). It has often been stated that the argument is applicable to particle clouds in which the separation distance is "large," and it has also been noted that the viewing optics must be located at "infinity." The second condition is realized adequately when the viewing distance is a few tens of wavelength equivalents separated from the scatterer. The first, the separation distance, is a problem of some magnitude in the present context, where we are attempting to replace a diffuse cloud with a close-packed array.

### 3. Theoretical Films of Spherical Particles of Infinite Refractive Index

The first system consists of a suspension of spherical particles of refractive index  $m = \infty$ , i.e., perfectly reflecting surfaces. It should be recalled that particles for which the ratio  $r/\lambda$  is very small have a very low effective cross section. At the other extreme, large particles show the usual preponderance of forward scatter over back scatter. Blumer (ref. 8) has computed the total and radial scatter for a number of cases. For the case where  $\alpha = 0.5$ , the ratio of the back-scattered intensity of a single particle to the forward scatter is 9:1. Thus extinction of the incident beam in the forward direction is only slightly compensated by forward scatter; we therefore omitted consideration of forward scatter.

We computed  $N$ , the number of particles, per unit area, required to attenuate the beam to 1%; we obtained  $6.7 \times 10^8$  particles/cm<sup>2</sup>. In a volume of 1 ml, this would correspond to

a uniform lattice of particles with center-to-center distances of  $10 \mu$ . If we use a particle spacing of  $4 \mu$  in direction 1, i.e., 2 diameters, as suggested by Berry (ref. 6) as the limit for the application of scattering theory to closely spaced systems, the films would be 4 mm thick.

The calculation was carried a stage further by determining the attenuation of light of other wavelengths by this film. By substituting the values for  $K$  corresponding to various wavelengths while keeping  $r$  equal to  $1 \mu$ , it is possible to determine  $I/I_0$ . Some representative values are shown in Table 1. It is seen that a film containing, per square centimeter,  $6.7 \times 10^8$  particles of  $1\text{-}\mu$  radius and infinite refractive index will back-scatter all radiation below  $12.5 \mu$  and will be highly transparent to wavelengths at  $21 \mu$  and longer.

Table 1

ATTENUATION OF LIGHT BY A FILM OF PARTICLES  
OF  $1\text{-}\mu$ -RADIUS AND INFINITE REFRACTIVE INDEX  
AT A CONCENTRATION OF  $6.7 \times 10^8/\text{cm}^2$

$\alpha$	$\lambda, \mu$	$K$	$I/I_0$
0.3	21.0	0.028	0.48
0.4	15.6	0.086	0.16
0.5	12.5	0.22	0.01
0.6	10.4	0.47	$1.6 \times 10^{-5}$
0.8	7.8	1.26	$2.0 \times 10^{-16}$

A number of other systems have been computed, by using as the reference point the particle concentrations for  $\alpha = 0.3$ ,  $0.8$ , and  $1.0$ , at which the transmission is 1%. The results are shown in Figure 1. When  $\alpha = 1$ , a film of  $7.2 \times 10^7$   $1\text{-}\mu$ -radius particles/ $\text{cm}^2$  will back-scatter 99% of the  $6.28\text{-}\mu$  wavelength radiation. All shorter wavelengths will be back-scattered, and the film will be transparent to longer wavelengths.

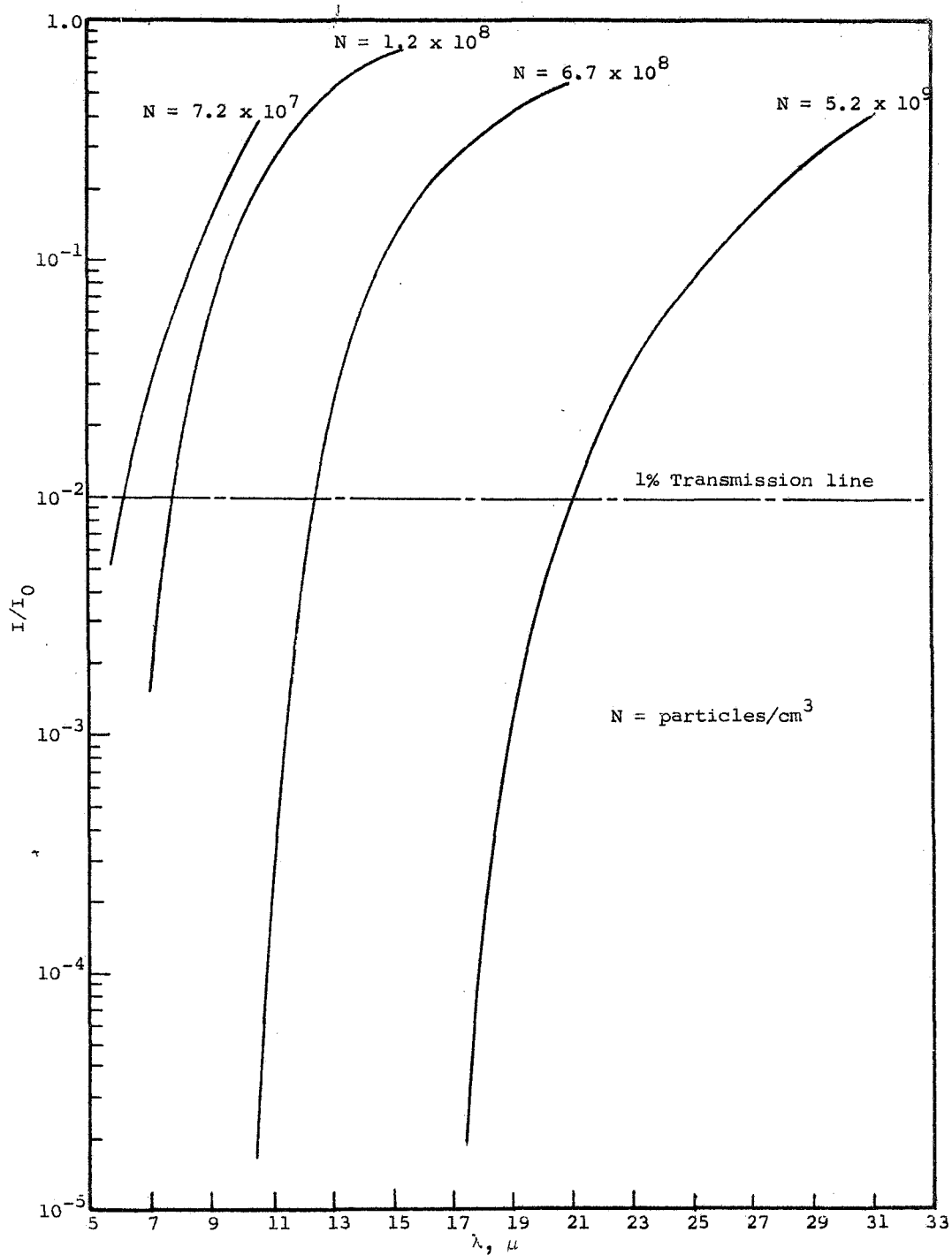


Figure 1  
TRANSMISSION FOR  $1-\mu$ -RADIUS SPHERES WHEN  $m = \infty$

The computations are presented in Section IIB3 of Volume 2 of this report.

#### 4. Theoretical Films of Spherical Particles of Real Refractive Index

The system consisting of an array of monodisperse particles of infinite refractive index represents a theoretical limit that is approached but never reached in real systems. We will next present a parallel analysis of particle systems with real refractive index; i.e., all incident light energy is scattered, and none is retained by absorption.

The radial scattering intensity is given in Equation 8 of Volume 2 of this report; the attenuation per individual particle is:

$$I = I_0 e^{-K\pi r^2 N}$$

In the case of highly reflecting particles, only a small part of the energy incident on the particle undergoes forward scatter, and Equation 2 describes this attenuation very well. However, a large fraction of the energy is scattered in the forward direction by transparent particles. Equation 2 is satisfactory for attenuation of the forward beam in a long path with near-parallel optics, but in the case of a thin film all the energy in the forward direction within the critical angle (the angle of total reflection) is transmitted. This is illustrated in Figure 2, in which the index of refraction\* is  $1/\sin \theta$ , and all light outside the cone subtended by the angle  $2\theta$  undergoes either back scatter or total reflection.

An exact determination of the forward-scatter component is obtained by integration of the radial scattering function over the solid angle of forward scatter. This is a formidable task, and we did not undertake its rigorous solution. Instead, approximation methods were used by employing averaged values of the radial scattering terms. Lowan's modified form of Figure 2 is:

---

\* Note that this is the refractive index between the film and air, not the refractive index of the particle.

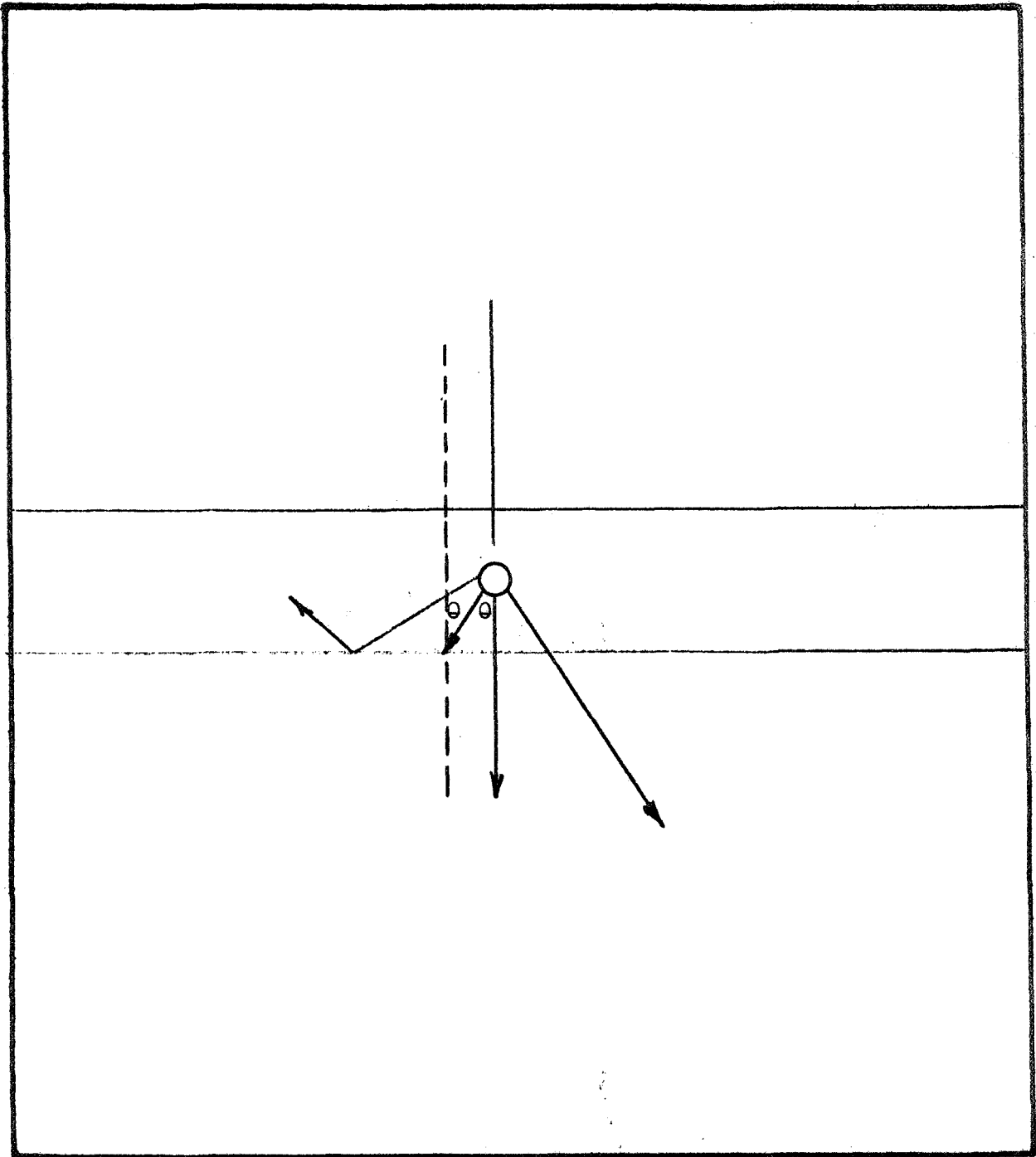


Figure 2

LIMITS OF FORWARD- AND BACK-SCATTER IN FILMS

$$I_{\theta} = \frac{I_0 \lambda^2 (i_1 + i_2)}{8\pi^2} \quad (3)$$

where

$I_0$  is the incident energy per unit area

$I_{\theta}$  is the scattered intensity per unit solid angle in the direction  $\theta$

$i_1$  and  $i_2$  are the angular distribution functions for the two plane polarized components scattered by a transparent particle illuminated by natural light.

We first considered a system of particles embedded in a film. The refractive index of the particles in the medium was 1.44; the angle of total reflection (Figure 2) was  $45^\circ$ . The forward-scattered cone therefore subtended an angle of  $90^\circ$ , i.e., a solid angle of 1.84 steradians.

For spheres of  $1\text{-}\mu$  radius, the number of particles,  $N$ , per unit area required to attenuate the incident beam to 1% was determined to be  $2.0 \times 10^8$  particles/cm<sup>2</sup>. In a film of 1-cm<sup>2</sup> area with a mean particle spacing of  $10\text{ }\mu$ , i.e., 5 particle diameters spacing between adjacent particles, the film will be about 2.0 mm thick.\*

In the application of this method, the refractive index of the particles was referred to the surrounding medium, which is the film material. The critical angle for total reflection is a function of the refractive index of the film in its surrounding medium, i.e., air or vacuum.

The maximum scattering cases, in which  $m = 1.33$ ,  $1.55$ , and  $2.00$ , is examined by using the radial scattering data of Lowan (ref. 9). The case in which  $m = 1.44$  is also reviewed.

Conditions for maximum scatter as a function of the parameter  $\alpha = 2\pi r/\lambda$  have been given by Sinclair and LaMer (ref. 1). For the cases indicated, the conditions shown in Table 2 apply.

---

\* This calculation was made with no attempt to correct for the boundary condition in which particles are very close to the totally reflecting surface.

Table 2  
CONDITIONS FOR MAXIMUM SCATTERING  
BY 1- $\mu$  TRANSPARENT PARTICLES

Refractive Index, $m$	Maximum Scattering Cross Section, $K$	$2\pi r/\lambda$ ( $\alpha$ )	$\lambda$ , $m$
1.33	3.9	6.3	1.0
1.44 <sup>*</sup>	4.0	4.8	1.31
1.55	4.4	3.6	1.74
2.00	5.2	2.4	2.62

<sup>\*</sup>The data of Section II-B-4 were recalculated from comparison in the present series.

By using Lowan's data, the scattered intensities in the forward-directed cone of 90° included angle were integrated numerically by minimizing the average intensities of the scattered light in the 10° zones between 0 and 50°. These scattered intensities correspond to the  $i_1$  and  $i_2$  term of Equation 3 and can be applied in Equation 3 to determine the fraction of incident energy if scattered into the forward cone. By comparison with the total scattering cross section, the back-scatter for one particle was determined; the attenuation,  $K_a$ , was then determined as a function of the particle's true cross section. All these calculations have been made and are tabulated in Table 3.

The attenuation cross sections,  $K_a$ , were then used to determine the concentration needed to attenuate an incident source by a standard amount. A multiple array of particles that do not interfere with each other was assumed. By using the data of Table 3 and assigning a value of 100 to  $I_0/I$ , i.e., attenuating the source to 1%, the values shown in Table 4 are obtained. The tabulated data emphasize the increased attenuation efficiency of particles with high refractive indices.

A more complete analysis is presented in Section IIB4 of Volume 2 of this report.



Table 3

SCATTERING PROPERTIES OF  $1\text{-}\mu$  PARTICLES OF VARIOUS REFRACTIVE INDICES  
AT WAVELENGTHS CORRESPONDING TO MAXIMUM SCATTERING CROSS SECTIONS

Refractive Index, $m$	Scattering Cross Section, K	$\lambda, \mu$	$i_1 + i_2$	$I_f \times 10^8$	Total Scattered Intensity, $\times 10^8$	Back- Scattered Intensity, $\times 10^8$	Attenuation Cross Section, K
1.33	3.9	1.0	440	10.2	12.3	2.1	0.67
1.44	4.0	1.3	260	10.3	12.6	2.3	0.73
1.55	4.4	1.7	155	10.9	13.8	2.9	0.92
2.00	5.2	2.6	43	6.9	16.4	9.5	3.0

Table 4

CONCENTRATION OF  $1\text{-}\mu$  PARTICLES AND FILM THICKNESS REQUIRED  
TO ATTENUATE THE INCIDENT SIGNAL TO 1%

Refractive Index, $m$	Attenuation Cross Section, $K_a$	Particle Radius, $\mu$	Particles/cm <sup>2</sup> , N	Film Thickness, <sup>a</sup> mm
1.33	0.67	1	$2.2 \times 10^8$	2.0
1.44	0.73	1	$2.0 \times 10^8$	2.0
1.55	0.92	1	$1.46 \times 10^8$	1.5
2.00	2.00	1	$7.3 \times 10^7$	0.7

<sup>a</sup>Film thickness for an idealized system of noninterfering particles spaced  $10 \mu$  apart.

### III. EXPERIMENTAL STUDIES OF SILVER BROMIDE DISPERSIONS

#### A. Introduction

Methods of preparing monodisperse silver bromide (AgBr) precipitates have been reported by a number of workers. Berry and co-workers (ref. 6 and 10) prepared monodisperse AgBr precipitates and reported turbidity measurements of dilute suspensions and transmittance measurements of thin films. The radial distribution of the intensity of scattered light and methods of preparation of AgBr have been discussed by Napier and Ottewill (ref. 11).

The studies reported here consisted of attempts to establish quantitative relationships between both inherent (refractive index) and induced (film thickness) physical and optical properties of the films. The experiments were limited to transmittance and reflectance measurements of various particle-suspension media configurations. It is hoped that this study will be useful in elucidating the radiative interactions that occur in highly pigmented reflective coatings. In the design of such coatings it is important to know when the single particle (Mie) theory begins to fail and multiple interactions become dominant.

General references to light-scattering theory and notation throughout the following paragraphs were taken from publications by Van de Hulst (ref. 3) and Penndorf (ref. 12). The optical densities given are to the base of natural log.

#### B. Experimental Procedures

A description of apparatus and a discussion of the procedures employed in preparing sized AgBr suspensions and films are presented in Section IIIB of Volume 2 of this report.

## C. Results and Discussion

### 1. Measurements of Particle Size and Concentration

Before we could initiate a study of the optical properties of concentrated thin films, it was necessary to consider how closely the measurements under idealized laboratory conditions would approach the values predicted by the Mie theory. At this point, it may be useful to reconsider the physical assumptions implicit in the Mie theory and their relationship to experimental measurements.

Light scattering is defined as a change in the direction of a light wave after its interaction with a scattering particle. An inherent but significant assumption in experimental measurements is that the theory is valid for infinitely dilute suspensions of monodisperse spheres that are illuminated monochromatically.

In traversing a dispersion of uniform spherical particles, the intensity of a parallel beam of light is reduced according to the transmission equation:

$$\frac{I}{I_0} = e^{-K\pi r^2 n L} \quad (2b)$$

or, in terms of optical density:

$$D = K\pi r^2 n L \quad (3)$$

where

K is the Mie scattering coefficient

n is the particle concentration

r is the particle radius

L is the optical path length.

The spectral transmittance curves predicted by the Mie theory are therefore oscillatory with the minima and the maxima of transmittance, which correspond inversely to the oscillations in K. Since K is a function of the size parameter, where  $u = 2\pi r/\lambda$ , the minima and the maxima occur at different wavelengths for monodisperse particles of different radii.

The radii of the particles were determined from the wavelength positions of the minima and the maxima by using spectral transmittance measurements and Equation 3. The first transmittance minimum (measured from the long-wavelength side) corresponds to the first scattering maximum, the first transmittance maximum corresponds to the first scattering minimum, etc. The number (concentration) of scatters can be determined from absolute transmittance measurements at any given wavelength.

Figure 3 shows the spectral transmittance curves for the majority of batches of AgBr particles used. The water suspensions contained approximately equal weights (0.707 g/ml) of AgBr particles, and a 2-cm path length absorption cell was used.

Graphical particle-size measurements from light scattering are summarized in Figure 4. The wavelength positions of the extrema were derived from the theory for a refractive index of 1.7, the effective refractive index of AgBr in water. A consistent increase in measured radii at higher lobes can be seen in Figure 4. This deviation could be due to the following effects.

- (a) The absorption coefficient of AgBr increases significantly at shorter wavelengths, and the effective refractive index becomes a complex number. These factors are not considered in our assumption of constant refractive index (1.7).
- (b) The deviations due to nonuniformity of the particles would be significant at higher lobes.

## 2. Transmittance of Suspensions Containing Two Particle Sizes

To approximate a suspension containing a wider distribution of particle sizes, a series of bimodal mixtures was prepared. The spectral transmittance curves of a typical mixture is compared with those of the components of the mixture in Figure 5. The mixtures were prepared to contain 50/50 wt. % AgBr particles.

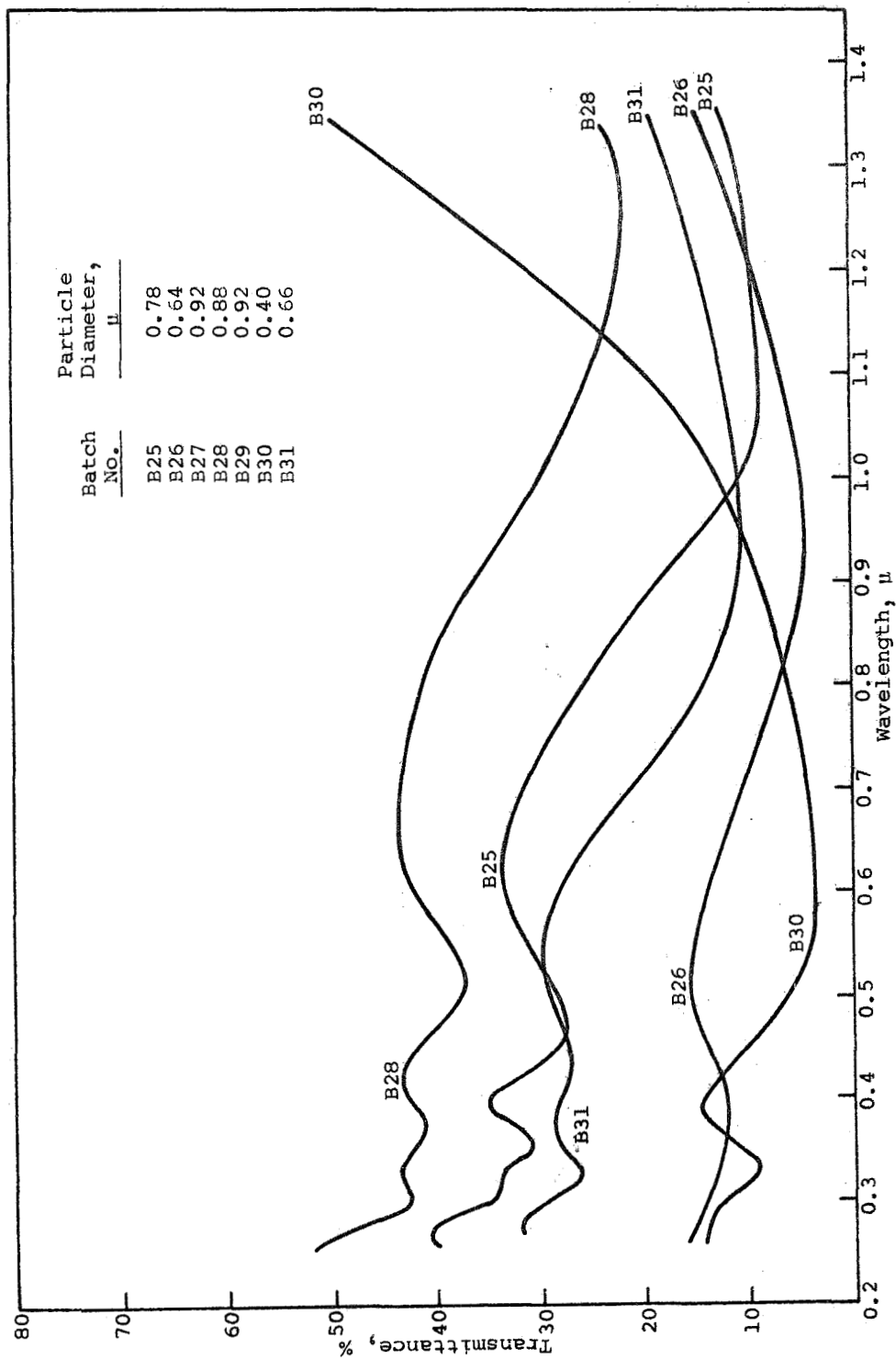


Figure 3  
TRANSMITTANCE OF AgBr SUSPENSIONS IN WATER

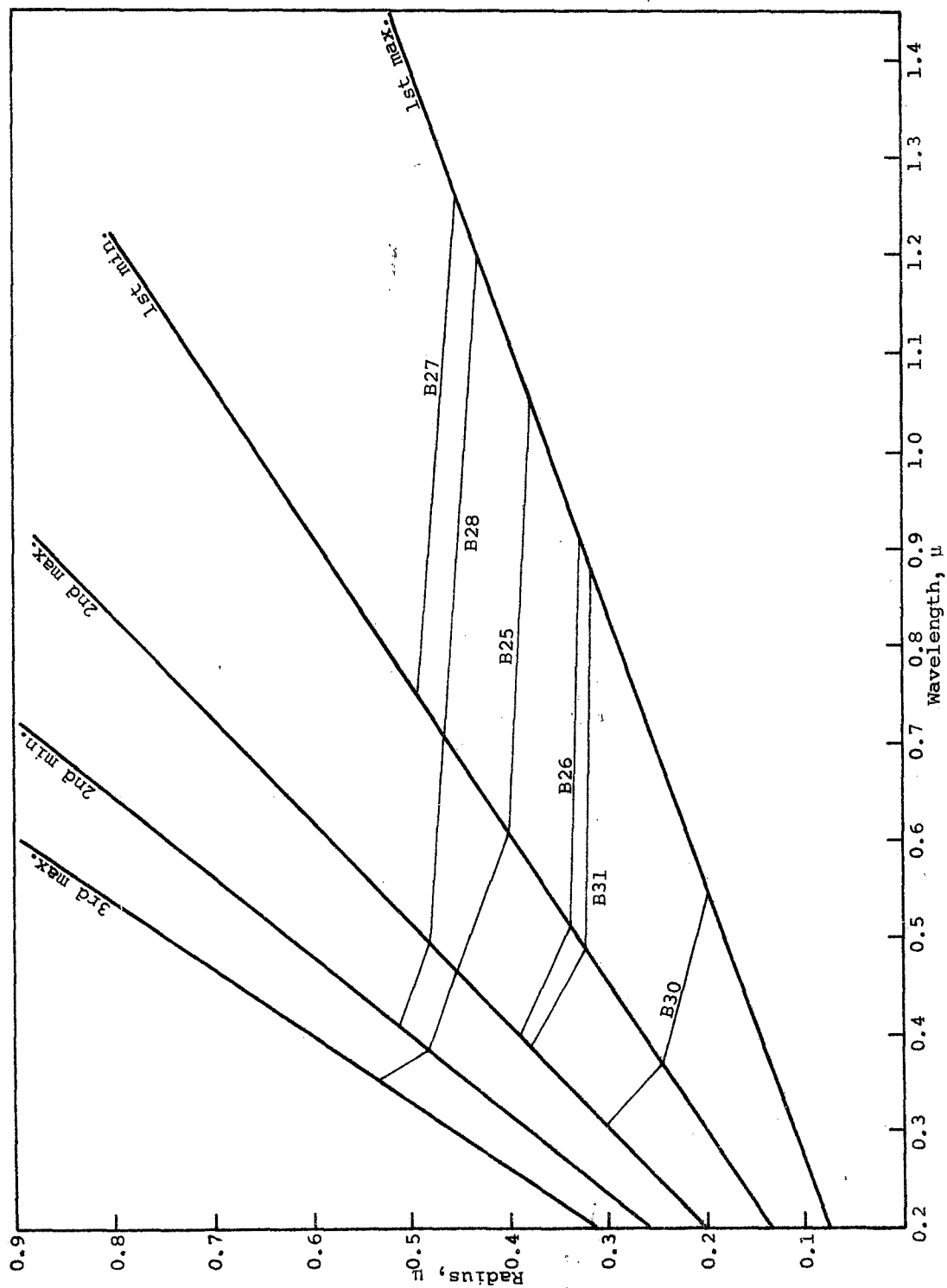


Figure 4

PARTICLE-SIZE MEASUREMENTS FROM LIGHT SCATTERING

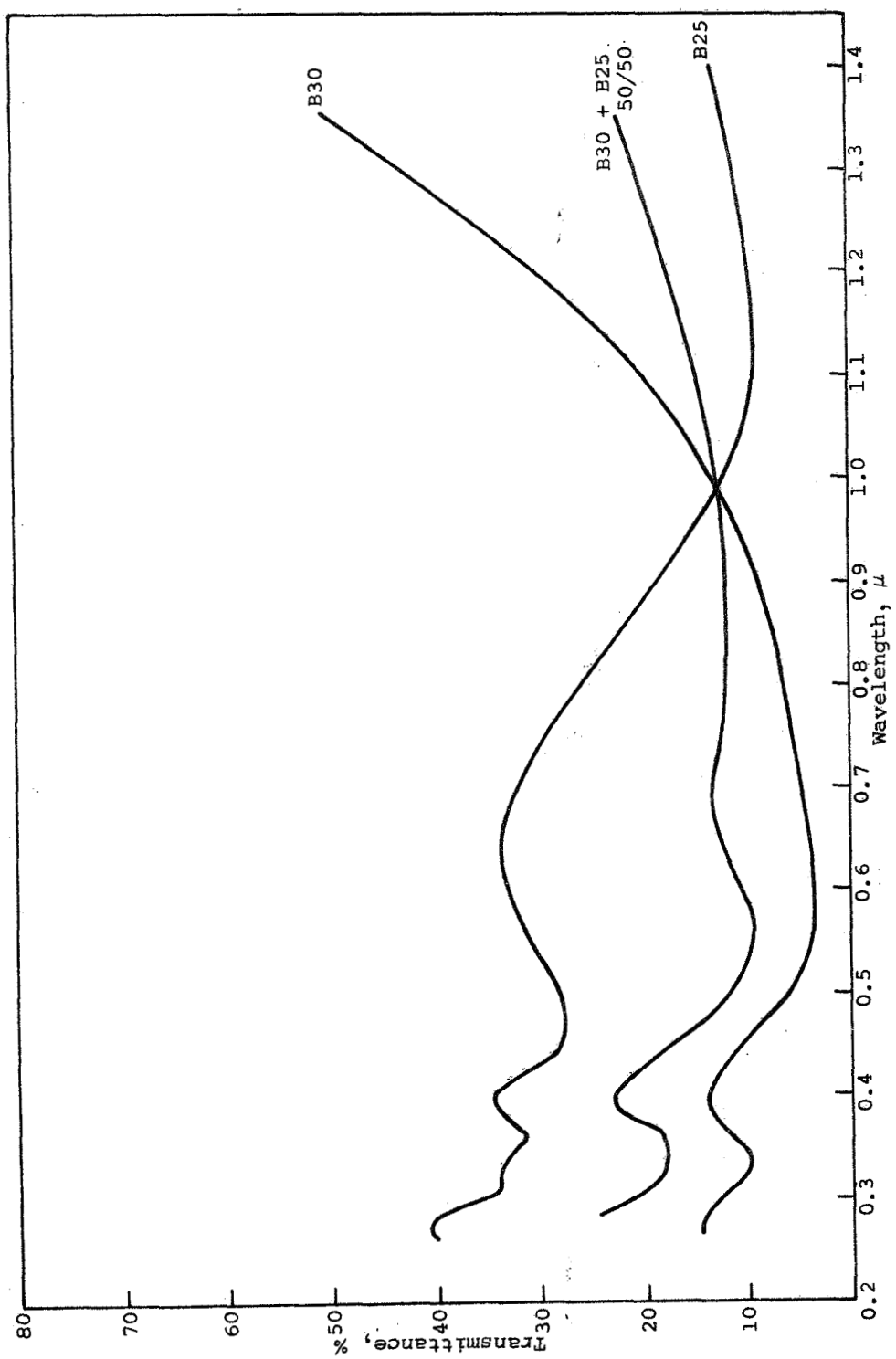


Figure 5

TRANSMITTANCE OF DILUTE SUSPENSIONS OF AgBr MIXTURES (BATCHES 25 AND 30)

The data indicate that particles of two sizes act as independent scatterers in dilute systems. The data show that independent transmittance curves for each particle size intersected with the transmittance curve of the mixture. It can be shown algebraically from the transmission equation (Equation 2b) that the transmittance of the mixture equals the transmittances of two components at this single wavelength, although the optical densities are additive at any wavelength.

Thus the optical densities would be expected to be additive for each single energy-loss mechanism, e.g., scattering (transmission equation) or absorption (Lambert-Beer law). These mechanisms apparently prevail at shorter wavelengths.

### 3. Transmittance of Concentrated Monodisperse Suspensions in Thin Films

In considering the transmittance characteristics of monodisperse closely packed suspensions of gradually increasing thickness, it is necessary to reconsider the physical mechanism of energy loss. It would be unreasonable to expect that the transmittance losses of parallel light in thick layers of concentrated suspensions would be similar to the losses in dilute suspensions, i.e., that they would be due only to changes in the direction of photons.

Theoretical considerations predict that, as the number of closely packed layers increases, the number of scattering events (changes in the direction of incident photons) also increases. Thus, increasing amounts of light in the deeper layers are lost by absorption and are converted to thermal and molecular energy modes. An increasing number of scattering events leads to an increasingly effective absorptive path length for each penetrating photon. Thus, even at low absorption efficiency (as is the case with AgBr), if the absorption path is long enough, the absorption mechanism of energy loss (Lambert-Beer law) predominates in the deepest layers of the suspension. As a result, a gradual decrease in the amplitude of the scattering minima and maxima and finally a transition into a continuous function are observed.



Figure 6 shows the change in the amplitude of the scattering extrema for various film thicknesses. In the longer-wavelength region, where the scattering is minimal, the effective absorptive path length corresponds to approximately a single pass of the photon. Since there is not appreciable change in direction of the photon due to scattering, the absorptive losses are very slight, and the transmittance increases significantly.

An actual increase in transmittance at wavelengths corresponding to the first scattering maximum with increasing concentration can be observed in several intermediate thicknesses (Figure 7). This phenomenon is also thought to be caused by multiple scattering events. In the intermediate cases, the decrease in the amplitude of transmittance minima and maxima is probably the best indication of when the single-scattering mechanism begins to fail and multiple scattering and absorption becomes the dominant mechanisms of energy loss.

#### 4. Transmittance and Reflectance Properties of Concentrated Bimodal Suspensions in Thin Films

In Volume 2 of this report (Section IIIC4), it was shown that

$$\frac{D_1 + D_2}{2} = D_{1+2} \quad (4)$$

where  $D_1$  and  $D_2$  are the optical densities of two monodisperse films and  $D_{1+2}$  is the optical density of a 50/50 (wt. %) mixture of films 1 and 2.

In the set of experiments reported here (and more fully in Section IIIC4 of Volume 2), each film was measured, and the optical densities of the components (monodisperse films) were normalized to the thickness of the bimodal mixtures. A comparison of the observed transmittance of a bimodal mixture with that constructed from the measurements of monodisperse films is shown in Figure 8. The greatest source of error in our measurements is the determination of thickness and concentration of scatterers in dry films.

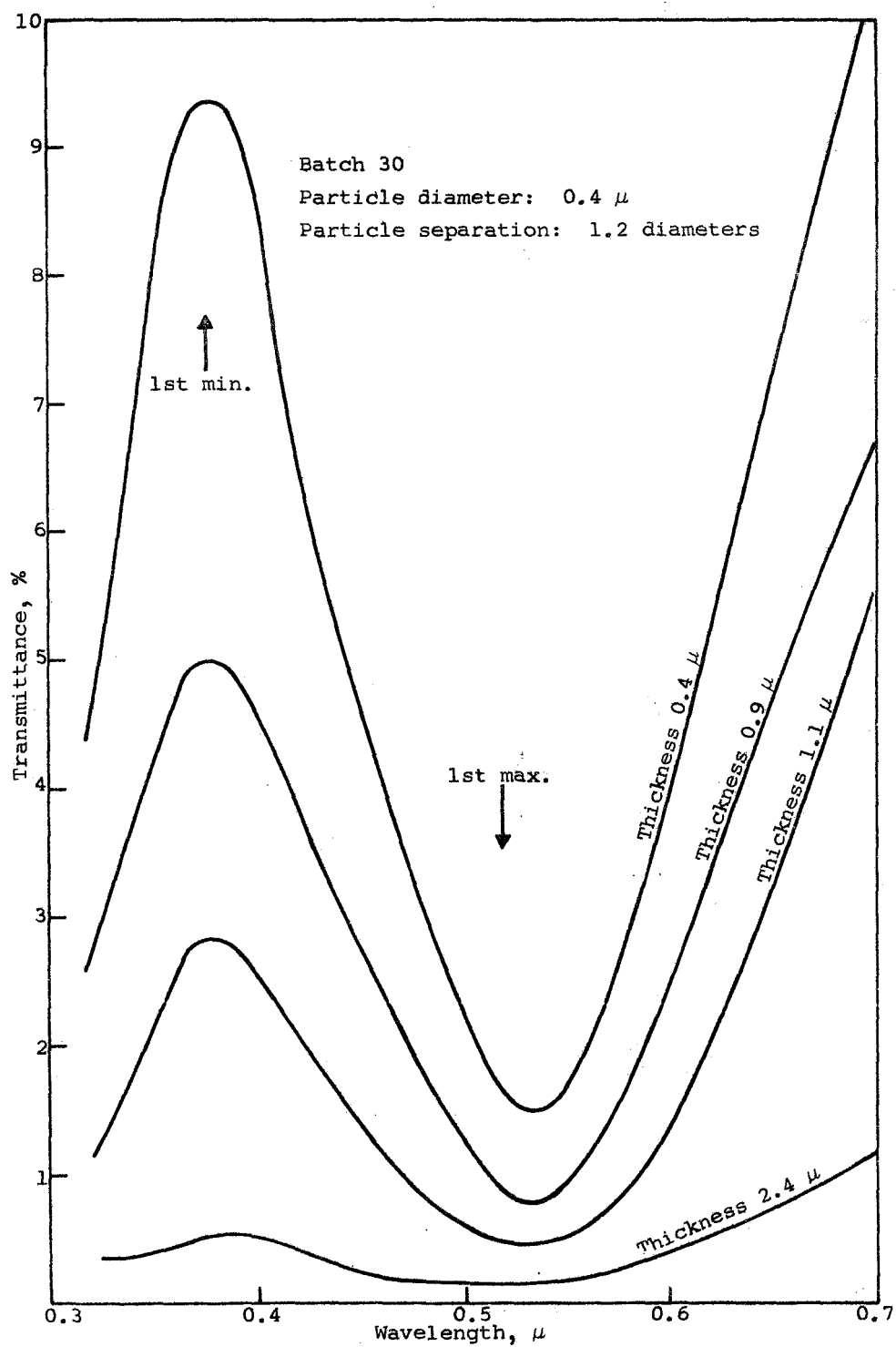


Figure 6  
SCATTERING EXTREMA VERSUS THICKNESS OF GELATIN SUSPENSIONS

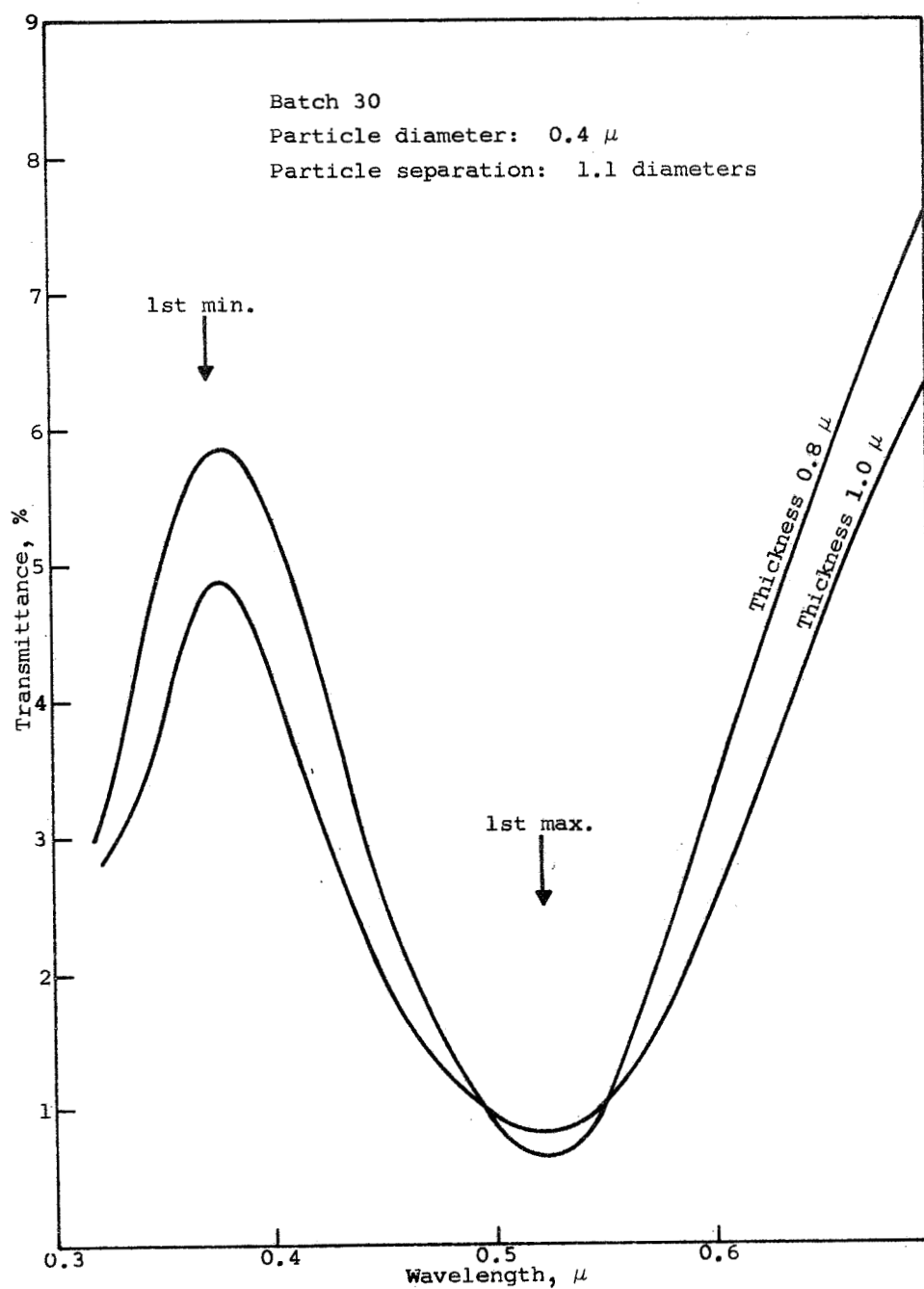


Figure 7  
TRANSMITTANCE OF CONCENTRATED GELATIN FILMS

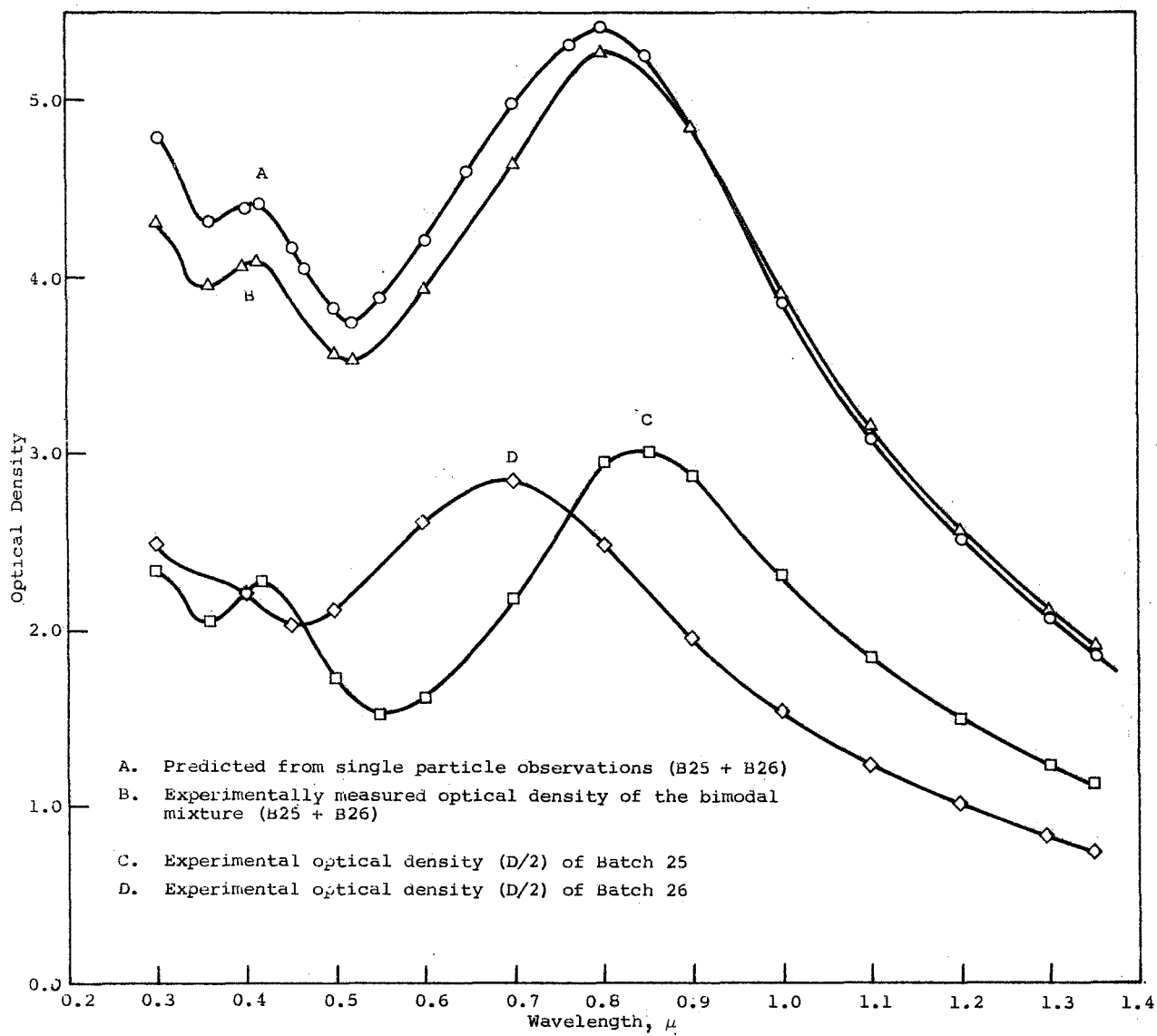


Figure 8  
 OPTICAL DENSITY OF AgBr SUSPENSIONS  
 (Batches 25 and 30)

Since a reasonable agreement was obtained between the observed transmittances of the bimodal mixtures and those constructed from observations of single particles, the above comparison was extended to include a theoretical bimodal coating constructed on the basis of Mie scattering theory. An inherent assumption in such a case is that the particles are completely uniform; i.e., there is no size distribution whatsoever for any given particle size.

Theoretical variations in the amplitude of minima and maxima with the width of the distribution were reported by Stevenson, Heller, and Wallach (ref. 13). Their data were used to construct theoretical curves at the estimated concentrations of monodisperse thin films.

The optical densities observed and theoretical bimodal coatings are compared in Figure 9. The data indicate that although there is some loss of fine structure, the agreement between observed and calculated curves is quite good. The loss of one lobe, which was predicted by the theory, is obviously due to the width of the distribution curves of the particles used in the bimodal mixture.

The back-scatter intensity, which is represented by the reflectance measurements, is given for a typical set of films in Figure 10. A set of films that was identical to the set transmittance measurements was used for the reflectance measurements. The back-scatter intensity is given in extinction units for a direct comparison with the transmittance (optical density) measurements:

$$\text{Back-scatter intensity} = \ln \frac{1}{100\% - \% \text{ reflectance}} \quad (5)$$

The reflectance measurements indicate that the back-scatter intensities due to each particle size are additive, and therefore in back-scattering the particles in their films tend to act as independent scatterers.

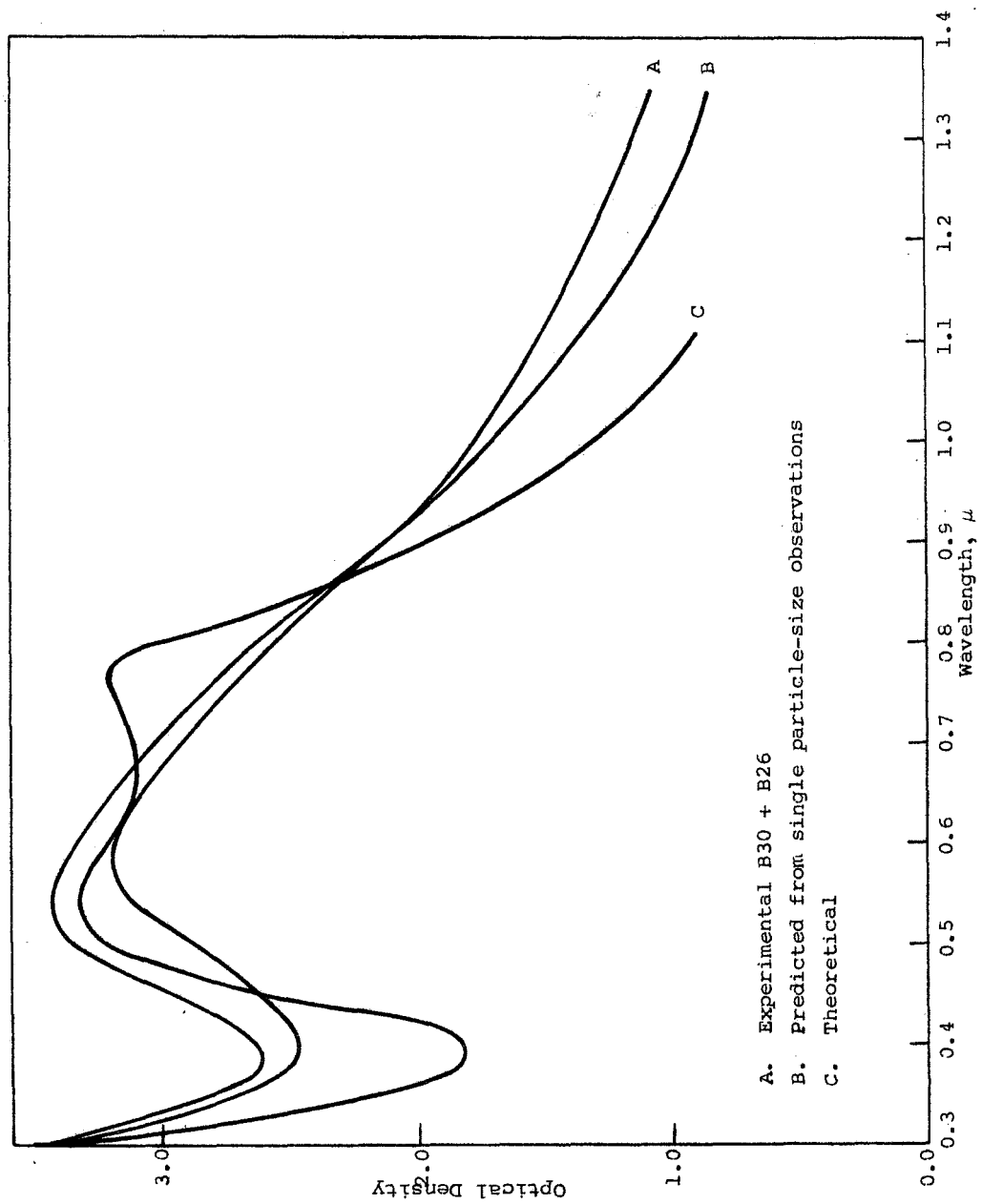


Figure 9  
 OPTICAL DENSITY OF A MIXTURE OF BATCHES 26 AND 30

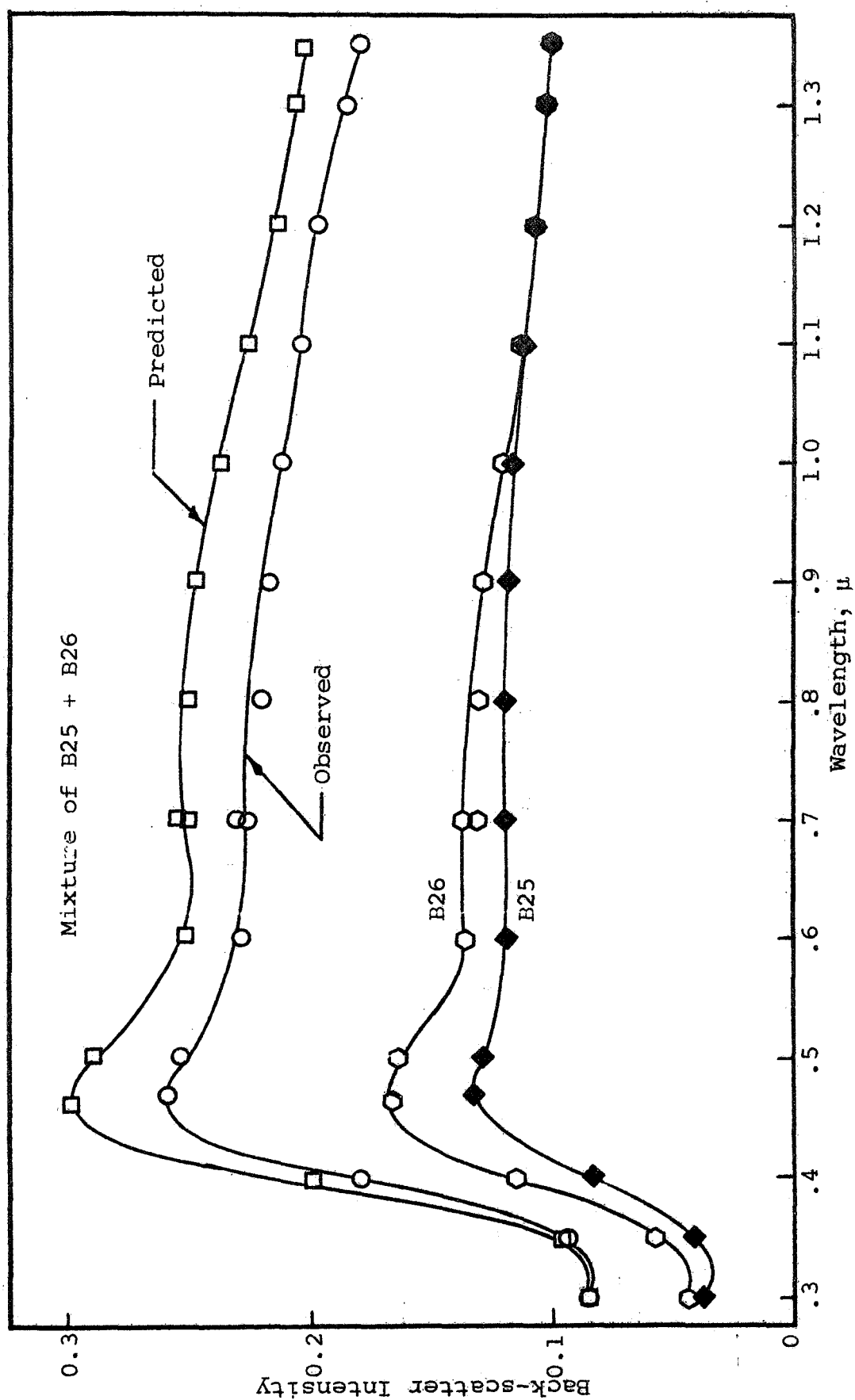


Figure 10  
 BACK-SCATTER INTENSITY OF AgBr SUSPENSIONS  
 (Batches 25 and 26)

## 5. Optical Properties of Films of Various Thicknesses

A set of monodisperse films of intermediate thickness was prepared first and permitted the measurement of both transmittance and reflectance. The reflectance measurements of a set of films are given in terms of back-scatter intensity in Figure 11.

During the reduction of the data, it was noted that a linear plot of back-scatter intensity, BI, versus  $\ln t$ , where  $t$  is the film thickness, could be obtained. The data are presented in Figure 12 for the back-scatter intensity at a wavelength of  $0.46 \mu$ .

Since Figure 12 is a linear plot, the following relationship between reflectance and thickness can be established.

$$\ln \frac{1}{100 - R_{\lambda}} = C_1 \ln t + \ln C_2 \quad (6)$$

$R_{\lambda}$  is the percent reflectance

$t$  is the film thickness

$C_1$  and  $C_2$  are experimental constants corresponding to the slope and the intercept.

$C_1$  and  $C_2$  depend on the particle size, effective refractive index and the system, and the wavelength of measurements.

Equation 6 can be written as:

$$\frac{1}{100 - R_{\lambda}} = C_2 t^{C_1} \quad (7)$$

or, in terms of reflectance,  $R$ :

$$R_{\lambda} = 100 - \frac{1}{C_2 t^{C_1}} \quad (7a)$$

## D. Summary and Conclusions

Previous experimental results indicate that a theoretical model based on the Mie scattering theory or a semiempirical model based on single-particle observations can predict the spectral transmittance properties of thin pigmented films to a fairly close approximation. The effects of absorption and interface reflection have not yet been considered directly in



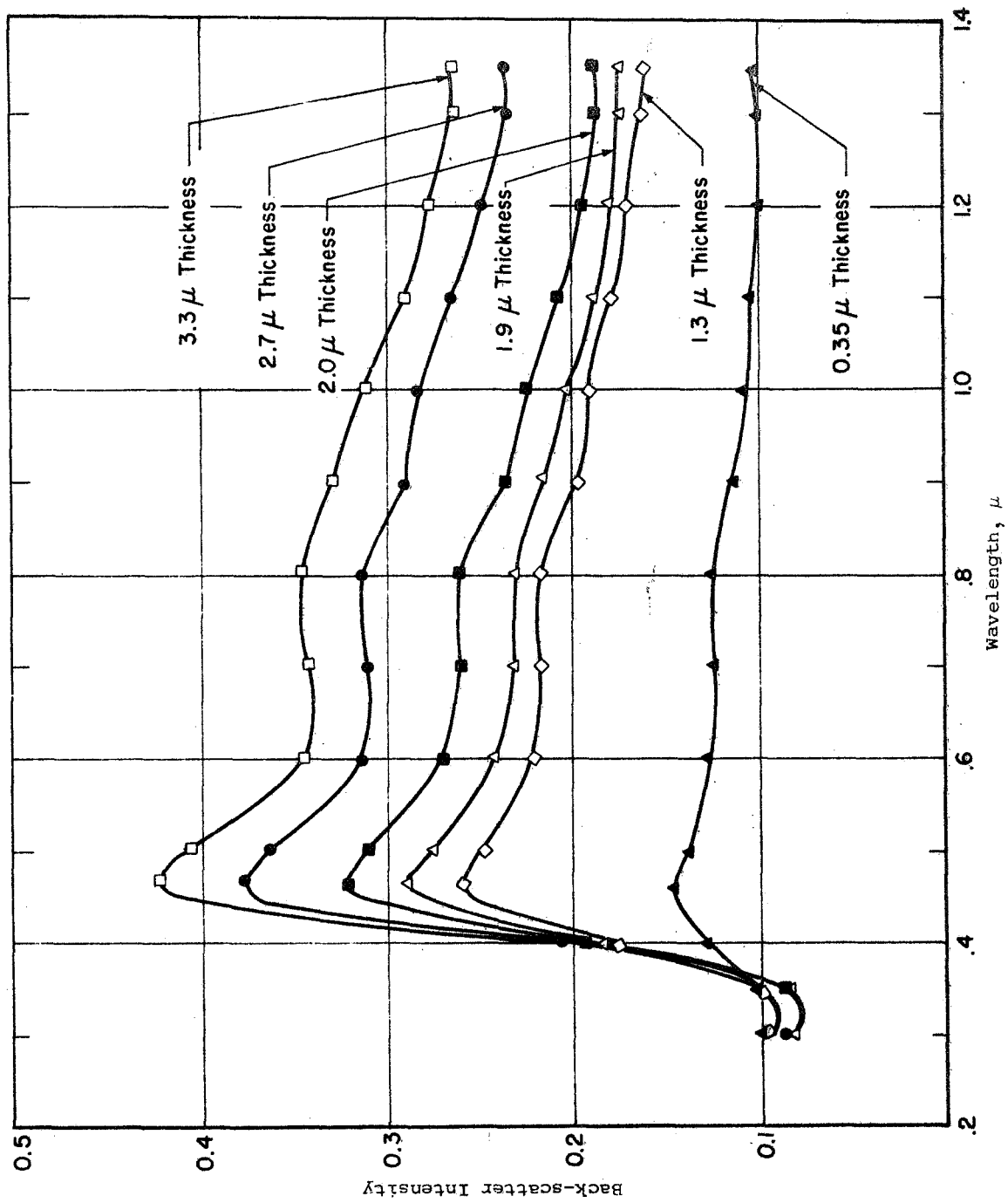


Figure 11  
BACK-SCATTER INTENSITY AT VARIOUS THICKNESSES (BATCH 26)

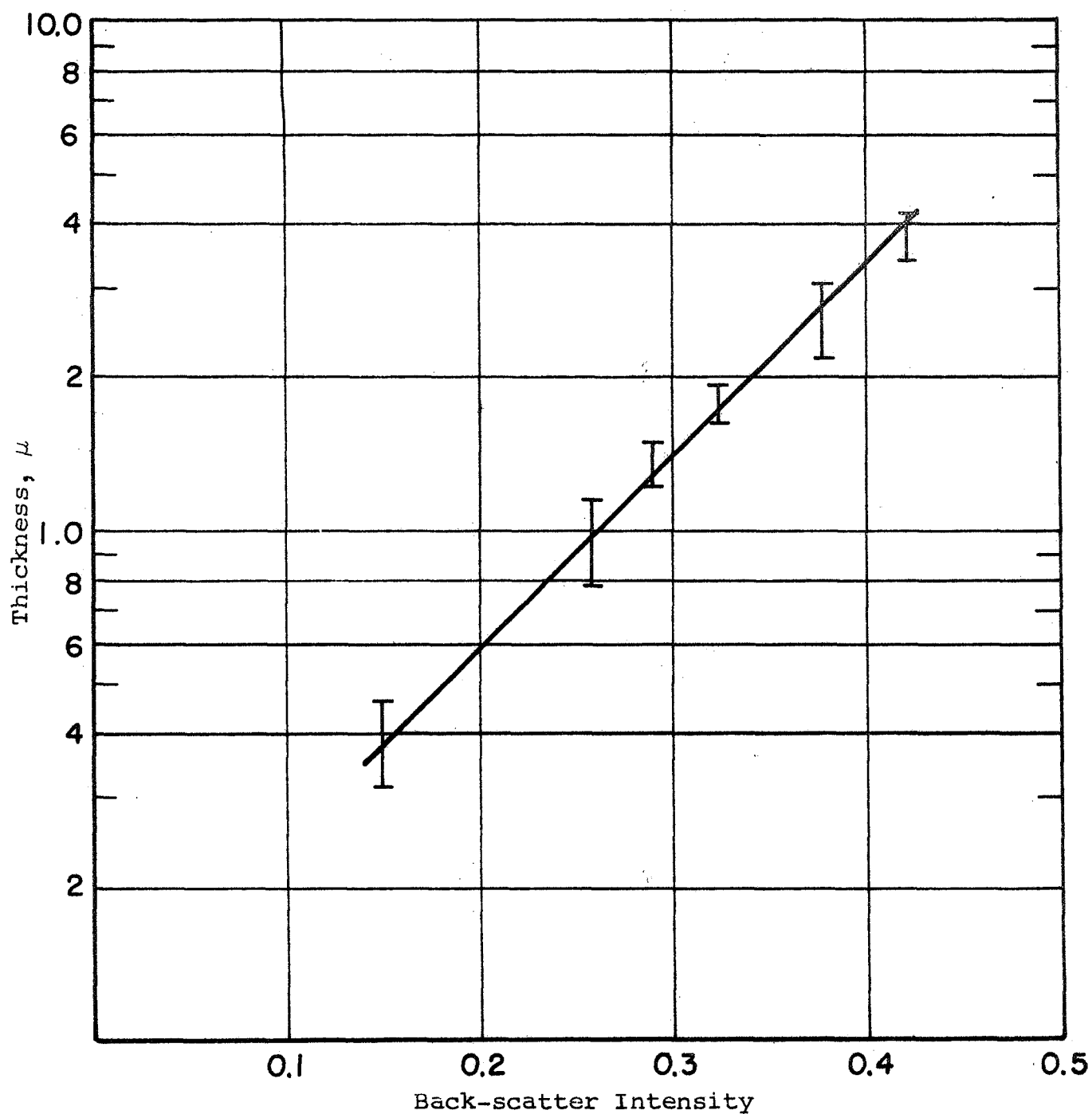


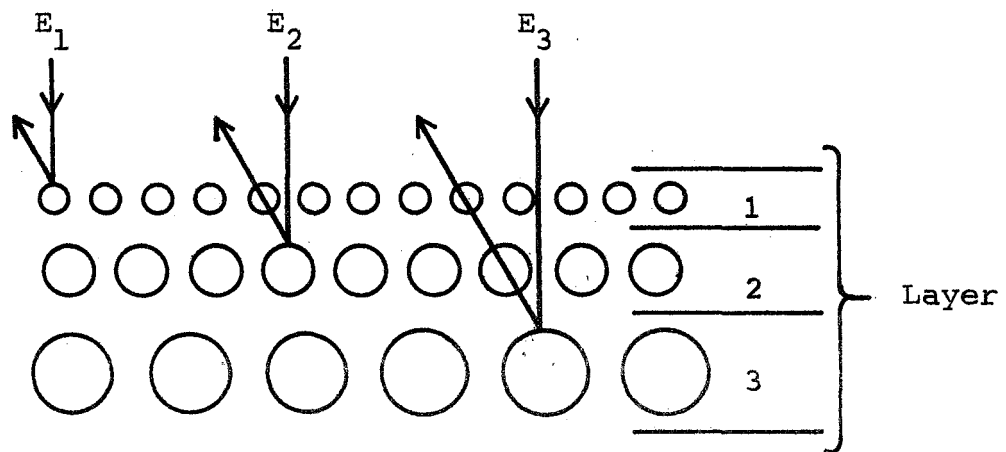
Figure 12

THICKNESS VERSUS BACK-SCATTER INTENSITY (BATCH 26)

the experimental studies. It appears that the absorption effects are closely related to multiple scattering events. The effects of multiple scatter and absorption become quite significant in films of several layers (more than 5) of scatterers. Thus, in any real pigmented paint system some degree of multiple interactions and absorption will always be present, but these effects are minimized in thin layers of monodisperse suspensions.

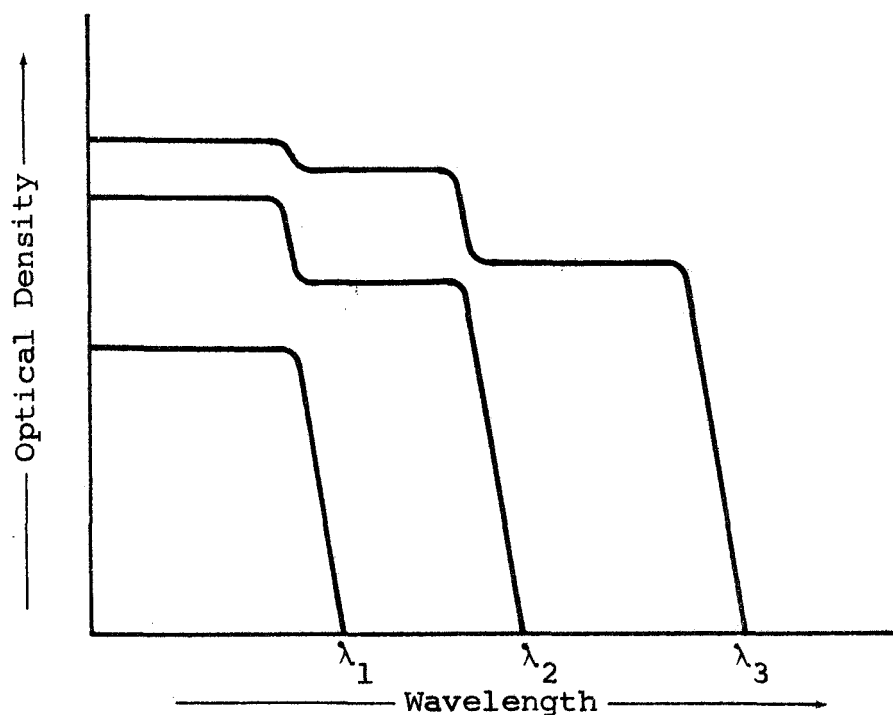
The back-scatter coefficient of thin films tend to be slightly higher than that of the thick ones. The back-scatter intensity obtained from bimodal mixtures was less than that predicted from measurements of monodisperse films. These two observations tend to support the ideal coating model proposed in Figure 13.

To attain minimum interactions between the scatterers, it is suggested that the particles should be packed in exceedingly thin layers containing particles of uniform size. The distribution of layers with respect to the incident beam should be such that each layer contains increasingly larger particles. The top layer, containing the smallest particles, will interact only with shortest wavelengths, allowing longer wavelengths to pass undisturbed in both directions. In this manner, each succeeding layer will interact with radiation of increasing wavelength. Such a coating is illustrated schematically in Figure 13.



Interactions between protons and layers at increasing particle size.

$$E_1 > E_2 > E_3, \text{ or } \lambda_1 < \lambda_2 < \lambda_3.$$



Optical density due to successive addition of layers.

Figure 13

SCHEMATIC OF MULTILAYER COATING  
AND RESULTANT OPTICAL DENSITY OF LAYERS

#### IV. RELEVANCE OF MIE THEORY FOR PREDICTING REFLECTIVE PROPERTIES OF PAINT FILMS

The scattering power of a single smooth spherical particle placed in the path of a plane parallel beam of noncoherent monochromatic light can be studied by the theory developed by Mie (ref. 7). The variations in scattering power of a single sphere with refractive index and particle diameter/wavelength ratio has been computed from the Mie theory, and this curve is often used to justify the claim that optimum opacity is obtained with a pigment-particle size of about  $1/5$  the wavelength of the incident light. When the relevance of the Mie theory to the physical phenomena occurring within the paint film is considered, it is found that even if the maximum-opacity pigment size eventually proves to be  $1/5$  of the wavelength, this fact cannot possibly be deduced from the Mie theory. Any agreement between fact and speculation stimulated by considering Mie theory can only be fortuitous.

The relationship between Mie theory and phenomena occurring within a paint film can be understood by considering several aspects of interference and Fraunhofer diffraction patterns of long single slits for plane parallel beams of monochromatic noncoherent light. First consider the Fraunhofer diffraction pattern of single slits of various widths. These patterns are shown in Figure 14. These patterns are observed on a screen at infinity (by using simulated lenses). Now consider that the screens are replaced by a photoelectric device that receives all scattered light. We are not concerned with the spatial distribution of the energy, and we observe that the total energy from the three slits is simply proportional to the slit widths, i.e., 1:5:10. From this point of view, we are not troubled by the fact that geometric optics does not apply to the system.

$\lambda$  = Slit width

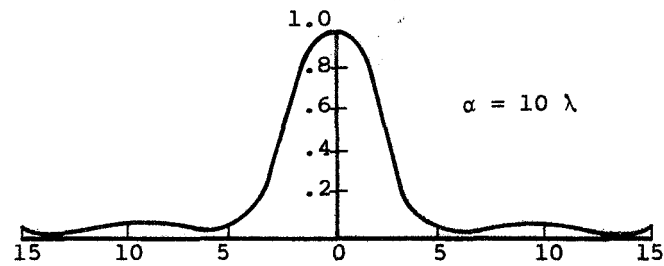
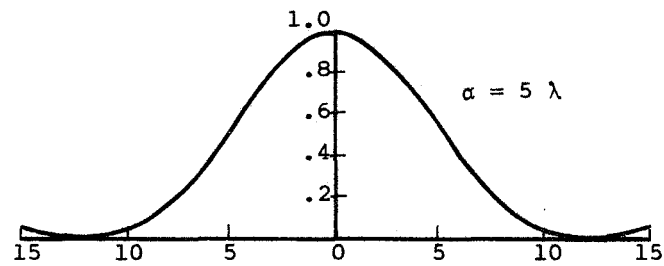
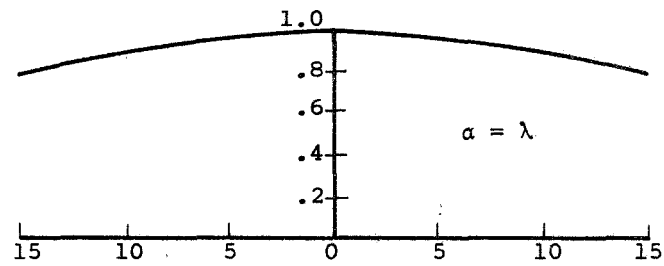


Figure 14

RELATIVE INTENSITY IN SINGLE-SLIT DIFFRACTION  
FOR THREE VALUES OF SLIT WIDTH OF THE RATIO  $\alpha/\lambda$   
(Reproduced from Physics for Students and Engineers,  
by D. Halliday and R. Resnick, John Wiley and Sons)

Next consider the diffraction pattern of a set of slits each 5 wavelengths wide but 50 wavelengths apart. The resultant pattern is shown in Figure 15. The interference fringes lie within the envelope of the diffraction pattern for the single slit. Familiarity with these diagrams in school textbooks on optics tends to obscure the important point. Although the relative intensity pattern is dominated by the system predicted from the single slit, the total energy passing through the slits is proportional to the number of slits. Again, if the screen is replaced by a photoelectric detector capable of receiving all the diffracted light, the measurement device would not be able to differentiate between 20 slits 2 wavelengths wide or 40 slits 1 wavelength wide, even though the spatial distribution of the energy for the two systems would be very different.

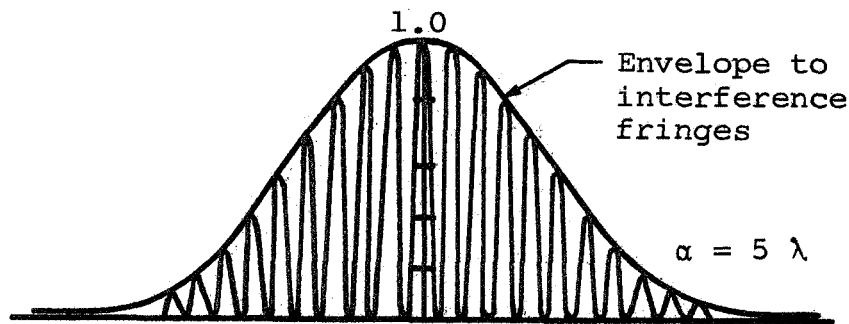


Figure 15

COMBINED INTERFERENCE AND DIFFRACTION PATTERN  
FOR SLITS 5 WAVELENGTHS WIDE AND 50 WAVELENGTHS APART  
(Reproduced from Physics for Students and Engineers,  
by D. Halliday and R. Resnick, John Wiley and Sons)

Now consider what would happen if we had 50 parallel slits each 5 wavelengths wide but spaced randomly across the diffraction screen. Any pair of lines would produce an interference pattern modulated by the diffraction envelope, but the peaks for each pattern would be separated by a factor related to the separation of the two slits. The argument holds for any pair of slits, so that the peak for each pair would fall at different points within the same diffraction envelope. Averaged out for the 50 lines, the net effect would be relatively uniform illumination modulated by the diffraction pattern for the single slit width. This results in the important observation that the diffraction pattern for 50 randomly spaced slits is undistinguishable from that of 1 slit if the power of the beam for the single slits is 50 times that of the beam passing through the 50 random slits. Physically what happens is that the random positioning of the lines obscures the fine structure of the combined interference diffraction pattern.

So far, we have considered only the effect of a single beam. If two beams at two different angles pass through the same slit, the system will be as outlined in Figure 16. A screen placed on the axis of the first beam would show the diffraction for the specific slit width. If a second beam at an angle  $\theta$  is passed through the screen, a screen placed on the axis of this second beam would have a slightly different pattern, since the effective slit width is now  $a \cdot \sin \theta$ , so the prime diffraction lobe will be somewhat wider than that for the first beam. If, however, the screens are replaced by a semi-circular photoconductive device, the power received by the device will be proportional to  $a + a \sin \theta$  if the beams are of equal strength.

---

\* The distances in Figure are not to scale. Either the screen is placed at a relatively great distance from the screen, or lenses have to be used to produce the pattern.



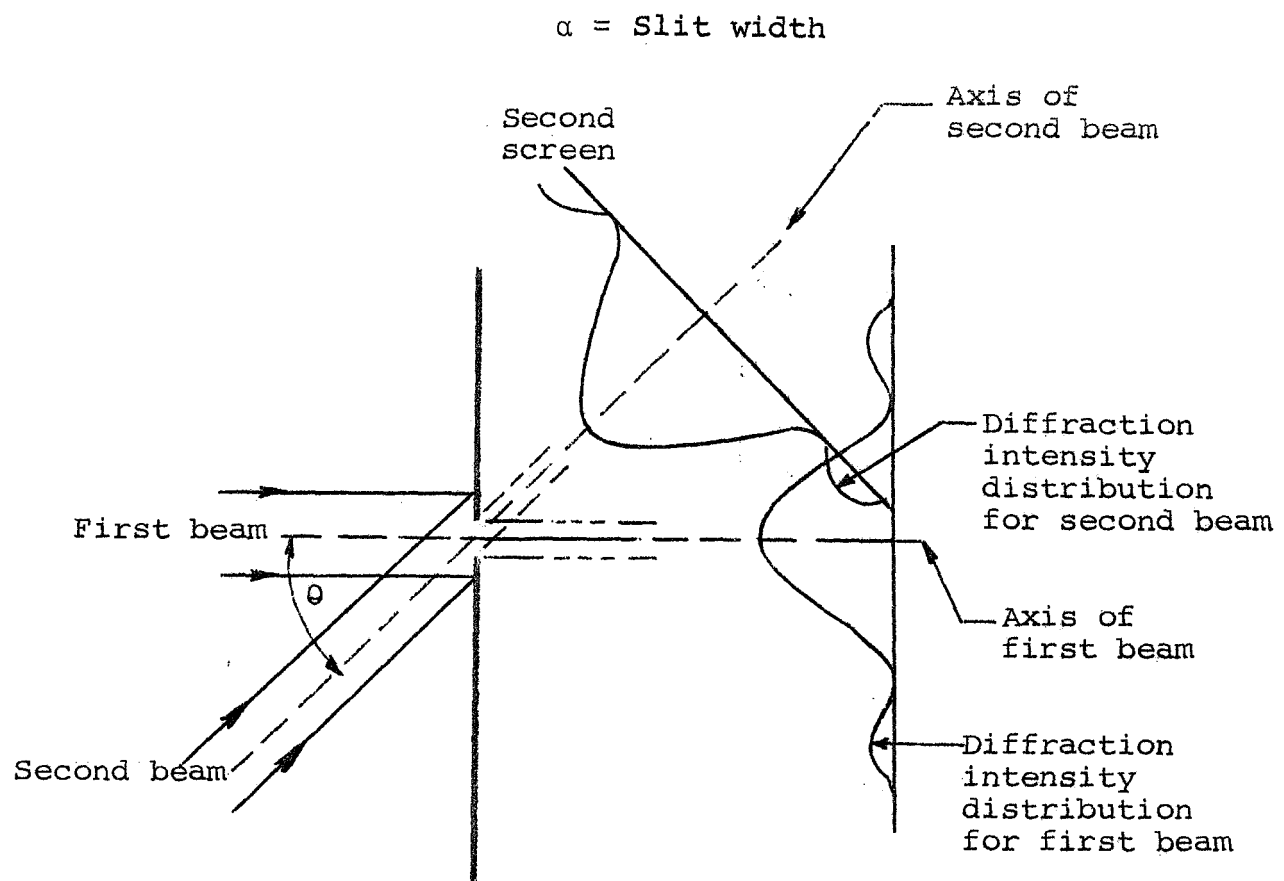


Figure 16

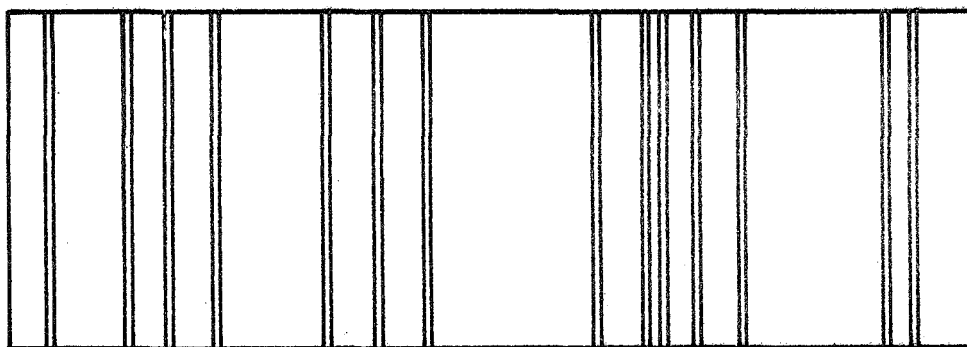
DIFFRACTION PATTERNS FOR TWO BEAMS PASSING THROUGH THE SAME SLIT

If there are beams at a whole range of equally spaced values of  $\theta$ , the calculation of the diffraction pattern on a screen perpendicular to the axis of the prime beam would be very complicated. Again, if the screen were moved so that it would be only several wavelengths from the slit, the simplified theory of Fraunhofer would no longer apply and the calculation of resultant diffraction patterns would be exceedingly complex.

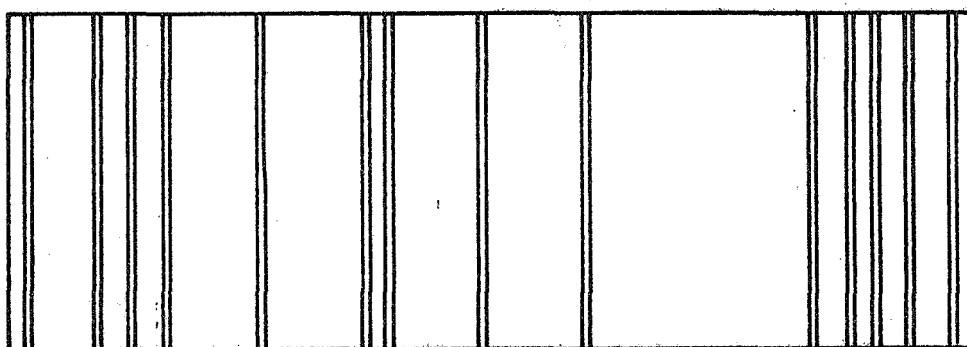
If the system is extended to consist of randomly spaced parallel slits of the same width and if all the beams are polychromatic, the calculation of diffraction patterns is, in practice, impossible. However, the power penetrating the screen is still a function of the available area in the diffracting screen, and if the width of the screen is of the order of the wavelength of light, it is probable that we could treat each hole as a source of light.

Now consider screens as shown in Figure 17. Consider that the 14 slits shown are a wavelength wide and that the portion between the slits is painted with a completely absorbing black paint. Again, if one screen were placed in the path of a plane parallel beam of monochromatic light, the diffraction pattern observed on a screen placed at a distance large compared to the wavelength of light is the diffraction pattern of a single slit and the power is 14 times that for a single slit.

Now, however, consider the problem of studying the passage of diffuse white light through 100 of these screens placed three slit widths apart when the surface of the screen between the slits is 80% reflective. From one point of view, the diffuse light can be considered to be a multiplex of parallel equipowered beams of light at equally spaced units of solid angles in space. By considering the complications arising from the combined effects of multiple-wavelength light and multidirectional beams, it is obvious that knowledge of the Fraunhofer diffraction pattern of a single screen containing randomly spaced slits will be of very little use in solving the partially reflecting multi-screen problem involving diffuse white light.



(a)



(b)

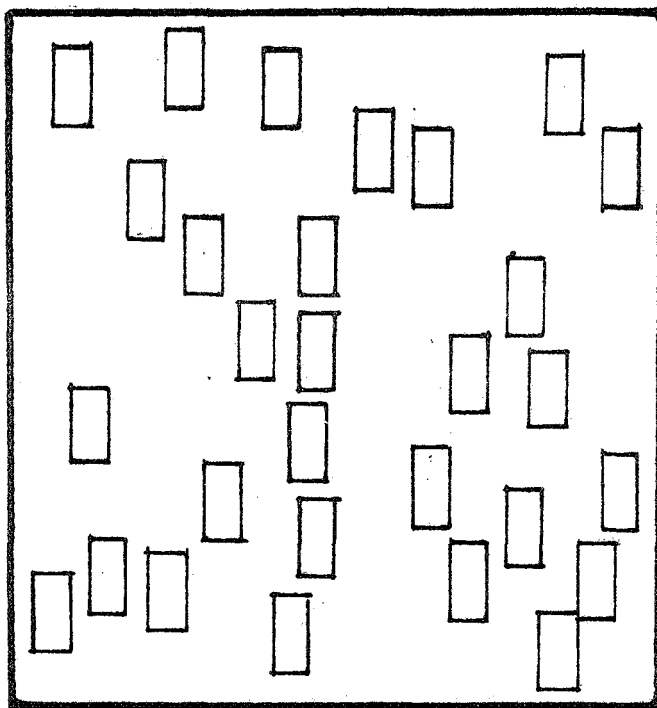
Figure 17

SCREENS CONTAINING RANDOMLY SPACED PARALLEL SLITS OF EQUAL WIDTH

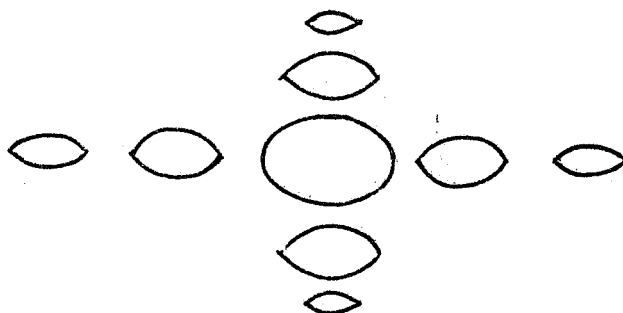
However, it can be shown that the Mie theory studies are related to paint film phenomena in approximately the same manner as the Fraunhofer pattern of a single screen containing randomly positioned slits is related to the multiscreen problem.

In order to gain an appreciation of the relevance of some of the published studies of the optical properties of pigment particles to the general problem of paint reflectance, it is necessary to extend the discussion of diffraction phenomena to the case of a screen containing randomly positioned regular apertures. This problem has been discussed by Andrews (ref. 14). He considered Fraunhofer diffraction of monochromatic non-coherent radiation for the screen shown in Figure 18. He states: "If a very large number of identical rectangular apertures with identical orientation in a plane screen are randomly scattered about on the screen, the interference pattern of the combination will be smoothed out to constant intensity, but the diffraction pattern will be the same as that for a single rectangular aperture." The bright spots of the Fraunhofer pattern for the single aperture are shown in Figure 18. The screen in Figure 18 is, in fact, a two-dimensional extension of the essentially one-dimensional case of the randomly spaced slits discussed earlier, and the considerations leading to the conclusions given by Andrews are, in fact, extensions of those given for the random slits to two dimensions.

Andrews also points out that the same type of result is obtained for the diffraction pattern produced by random spheres located in one plane perpendicular to the forward direction of the forward beam. Thus, if human blood corpuscles are placed on a glass slide and the Fraunhofer diffraction pattern is studied, a series of concentric rings typical of the diffraction pattern of the single spheres is obtained (ref. 15). In fact, the structure of the rings is sufficiently well defined that the average diameter of the blood corpuscles can be deduced from the dimensions of the diffraction rings. A clinical device that makes use of this phenomenon is called Young's eriometer.



Randomly distributed identical apertures



Schematic of light regions in Fraunhofer diffraction patterns of a rectangular aperture

Figure 18

# DIFFRACTION BY RECTANGULAR APERTURES

Thus, a random array of uniform spheres confined to a single plane should have a Fraunhofer diffraction pattern the same as that for a single sphere (ref. 16).

Mie theory represents a general solution for the scattering properties of a single sphere. When the sphere is very small compared to the wavelength of light, the scattering is symmetrical in front of and behind the particle. This type of scattering is known as Rayleigh scattering. Although Mie theory covers all scattering phenomena, the term "Mie scattering" is usually restricted to the description of scattering by particles in the size range of  $0.25$  to  $10 \lambda$ . In fact, Mie scattering is the growing tendency toward forward scattering with increasing particle size (ref. 17). The boundary between classical diffraction theory and the restricted Mie theory is not well defined, and in one sense the pattern of scattered light produced by particles in the range of  $0.25$  to  $10 \lambda$  can still be called a diffraction pattern.

The Mie theory is based upon two explicit conditions. First, the incident beam is a plane parallel beam of noncoherent monochromatic light. Second, the radiation detector used to explore the scattering pattern is at infinity, i.e., at a distance large compared to the wavelength of light. In a sense, therefore, the Mie theory corresponds to Fraunhofer diffraction.

Experiments on a thin (1 or 2 particles thick) array of pigment particles have been conducted (ref. 18) with a spectrophotometer and monochromatic radiation. Optical equipment of this kind satisfied the condition of plane parallel incident radiation with the detector at a large distance. It is not surprising that these experiments demonstrated maximum scattering power for a given particle size at wavelengths predicted from the Mie theory, since it is a general principle that the diffraction pattern produced by a thin random array of identical particles perpendicular to the beam is the same as that produced by a single particle.

To conclude from this type of observation that the scattering power of the pigment in a paint film is optimum at this size is to attempt to extrapolate from (a) monochromatic single scattering from a plane parallel beam studied at infinity to (b) the behavior in diffuse polychromatic light studied at a distance of two or three wavelengths, i.e., from the next pigment particle. This is no more logical than trying to predict the behavior of the series of screens shown in Figure 17 when placed in diffuse white light at separations of a few wavelengths from Fraunhofer diffraction patterns of a single slit.

We suggested in an earlier section (Section IIID) that a multilayer system may prove to be an efficient paint surface for preventing penetration of white light.\* This suggestion was based on reasoning which extrapolated Mie theory results to the complex interactions occurring in a paint film. If radiation from diffuse light falls on the particle from all directions, any diffraction pattern rotated through  $360^\circ$  yields the same pattern. Therefore, with diffuse radiation, it is the fact that the radiation interacts with the surface that is important, not the specific diffraction pattern for a single particle in a specific direction. Should a multilayer system prove to have important properties, the properties of the system cannot be regarded as predictable from Mie theory.

---

\* See also discussion and Figure 44 in Section IIID of Report No. IITRI-U6003-19, Volume 2.

## V. SEMANTIC PROBLEMS IN STUDYING REFLECTIVE PROPERTIES OF PAINT FILMS

### A. Introduction

When considering problems associated with the development of highly reflective paints, we find that as we extend our desire to control and predict the properties of paint films many of the words used in paint technology are not defined precisely enough.

In developing and planning these studies, many difficulties arose from an inability to give definite meaning to the concepts and terms used in discussing properties of paint systems. Inaccurately defined terms that have hindered efficient prosecution of the research program are: random, diffuse, size of particle, scattering power, highly reflective, boundary, Fresnel coefficient, and reflection.

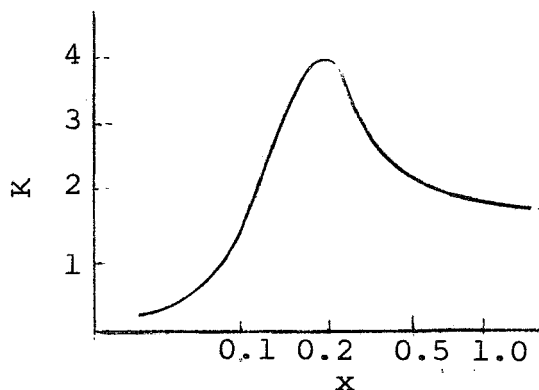
### B. Highly Reflecting Paint Films

When attempting to construct various models of paint films, it was realized that in the early reports the concept "highly reflecting paint films" was not defined. One cannot define a highly reflecting paint film without reference to the boundary conditions of the system being studied. For example, does one attempt to maximize radiative properties with respect to unit weight or unit volume of the film? To define reflectance of the paint, it is necessary to specify the radiation concerned. In these studies we were concerned with an environment in which the energy is direct radiation from the sun (in a vacuum). In studies concerned with paint for spacecraft, a highly reflective paint film should be optimized with respect to unit weight of film. It cannot be stated too strongly that the general concept "highly reflective paint" has no meaning unless it is applied in the operational context in which the paint film is to be used.



### C. Specification of Pigment Size

There is not sufficient awareness that the precision with which a particle size can be defined may be the limiting factor in applying light-scattering theory to the study of the optical behavior of paints. For example, the curve presented in Figure 19 has been suggested as an effective universal curve to be used in studying pigment optics (ref. 19). The merits of this curve as a valid measure of optical scattering power in a paint film need to be examined as a result of our criticisms of the use of the Mie theory and optical experiments made with parallel beams of light on dilute dispersed suspensions (see Section IIIC, Volume 2, of this final report).



K = extinction coefficient

$x = d \frac{m^2 - 1}{m^2 + 2}$ , where m is relative refractive index

Figure 19

CLAIMED UNIVERSAL EFFECTIVE EXTINCTION CURVE  
FOR PIGMENT PARTICLES

Consider the problem of predicting the performance of a pigment by using this curve. In the July 16, 1963, issue of Chemical Processing it was claimed that hydrated alumina can be used as a pigment or filler in paint systems. The measured characteristics of the powder were quoted as:

Average Particle Size, $\mu$	Method
0.12	BET
0.39	Fisher subsieve sizes
0.60	MSA centrifuge
0.30	Electron microscope

In applying the light-scattering curve of Figure 19 (even making the daring assumption that the average particle size can be used to calculate the overall properties of the paint), which value of the diameter should be used? The two extreme estimates differ by a factor of 5, and the four estimates would locate at very different regions on the scattering curve.

The other aspect of this problem is the difficulty of correlating reported data on the light-scattering properties of small particles. It is common practice to report data by drawing graphs of some measured quantity such as extinction coefficient versus particle diameter. However, the significance of the measured diameter quoted is not always apparent.

Even if we developed an ideal, foolproof method for analyzing the size distribution of raw pigment before it was used in paint films and even if all remaining difficulties were avoided, one important problem still remains: What is the operative size distribution of the pigment when it is dispersed in the film?

Studies of sections through paint films by analytical techniques for determining state of dispersion and spatial configuration of pigment locations are almost nonexistent. Consider the systems in Figure 20, in which the dispersion rate in a paint film is considered from a simplified two-dimensional system. In Figure 20a a number of circles are set at random; in Figure 20b these are collected into random clusters.

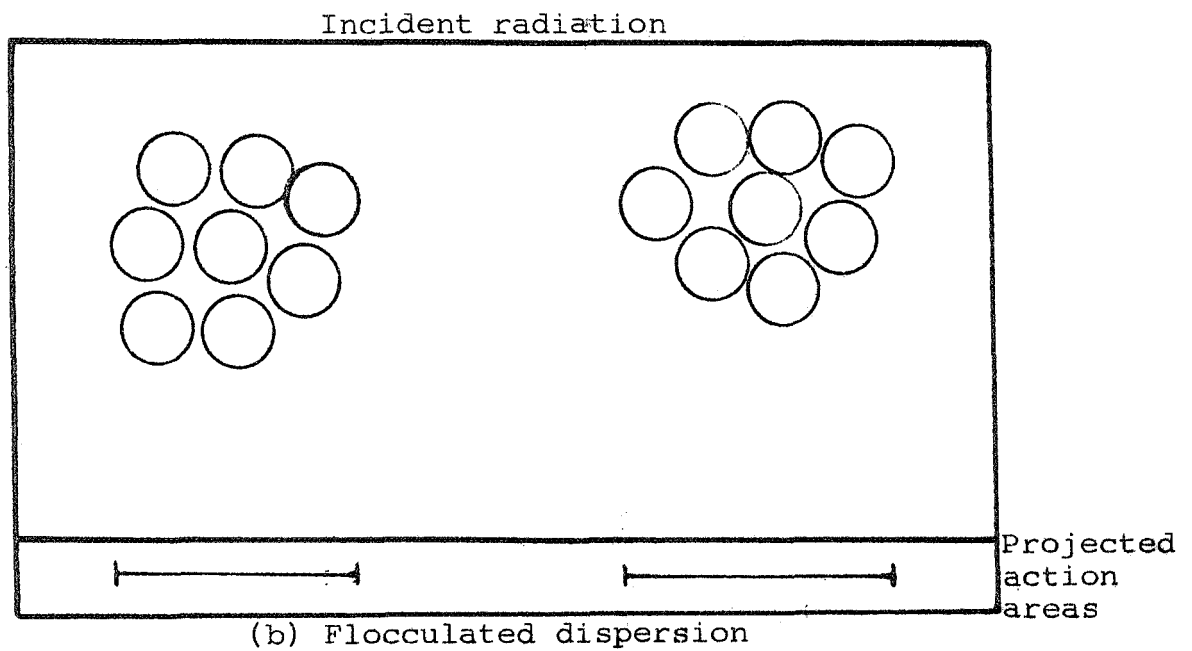
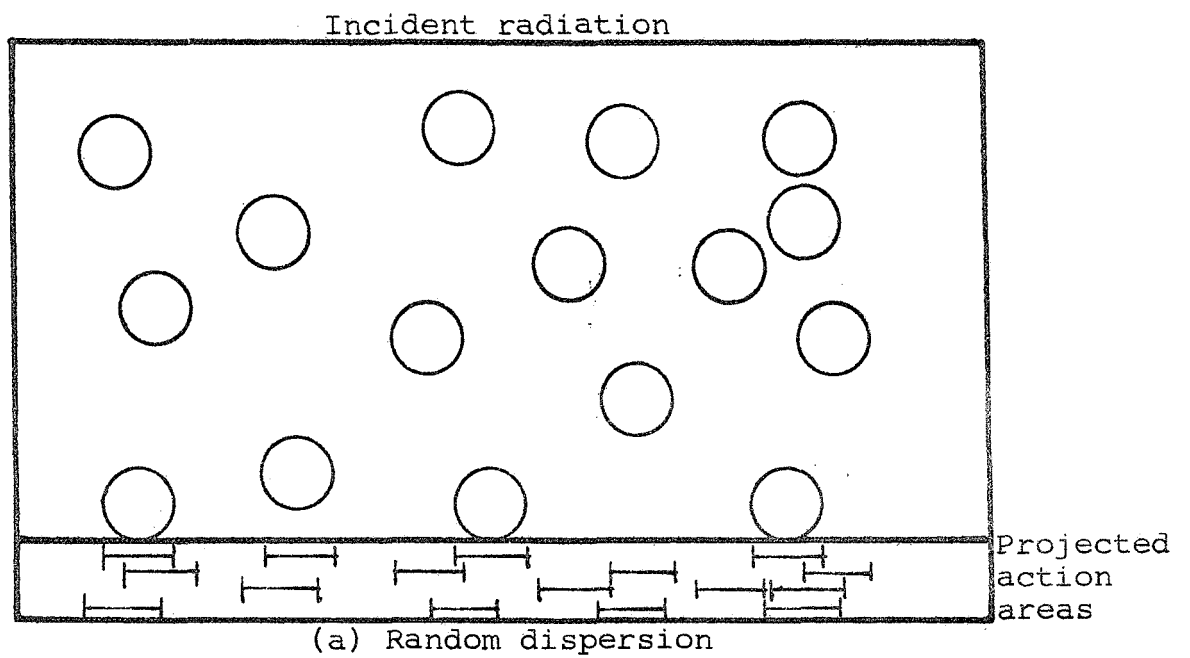


Figure 20  
DIFFERENT DISPERSION STATES WITHIN A PIGMENT FILM

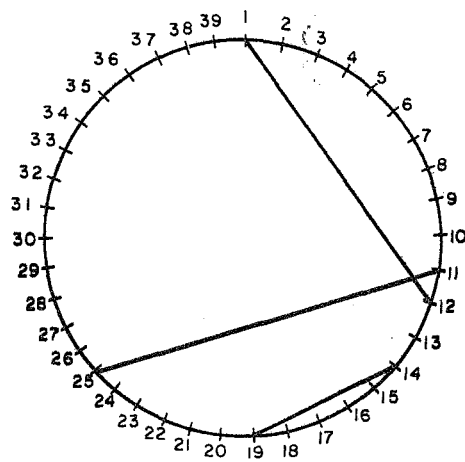
The grouping of the particles has a twofold effect. First, it reduces the area of the film in which pigment particles are available for scattering interaction. An estimate shows that the clusters are less effective. A cluster has a higher effective absorption coefficient, because its internal porosity tends to oscillate the light back and forth.

A filler improves the opacity of a high index white pigment, since random mixing of the larger inert filler particles prevents large clusters of pigment from forming by filling in the interstitial spaces available.

#### D. The Concept of Randomness

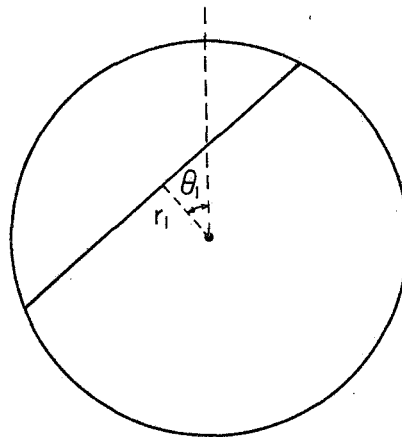
The term "random" as used in everyday speech describes a system that is not uniform or is nonsystematic. When the term is used to describe a system that has finite dimensions in space, it is necessary to be specific about the exact nature of the randomness of the system considered. Two similar systems can both be random in the technical sense and yet have different physical properties. This fact can be illustrated by considering the problem of drawing random lines across a circle. This situation arises in the study of the light-scattering behavior of paint films, since the average length of intercepts of a circle could represent the average path of photons through a spherical pigment particle.

There are four possible mathematical procedures for constructing random intercepts. In the first method, the perimeter is divided into a convenient set of intervals. Each interval is then allocated a number. To construct a random intercept, two numbers within the appropriate range are selected from random-number tables, and a line is drawn between the two corresponding points on the perimeter. This method is illustrated in Figure 21a, and an example of this type of random intercept is shown in Figure 22. Circular graph paper with the perimeter divided into 360 intervals (polar graph paper) was used. Random numbers between 1 and 360 were selected, and then 20 random lines were drawn to construct the system of random intercepts given in Figure 22.



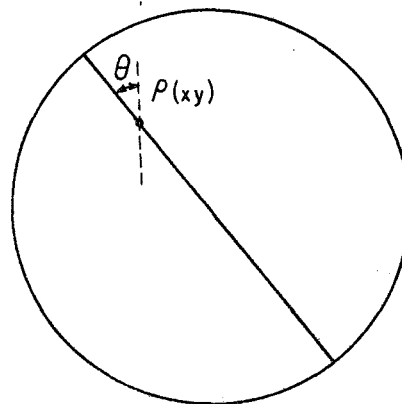
Method 1: Intercept drawn between two randomly selected points on the perimeter.

Figure 9a



Method 2: Line drawn perpendicular to radius  $r_1$  at angle  $\theta_1$  to fixed direction;  $r_1$  and  $\theta_1$  selected randomly.

Figure 9b



Method 3: Line drawn through point P of coordinates  $x, y$  in a direction  $\theta$ . The coordinates  $x$  and  $y$  are on a rectangular grid;  $x, y$  and  $\theta$  selected randomly.

Figure 9c

Figure 21

### THREE METHODS OF DRAWING RANDOM INTERCEPTS IN A CIRCLE

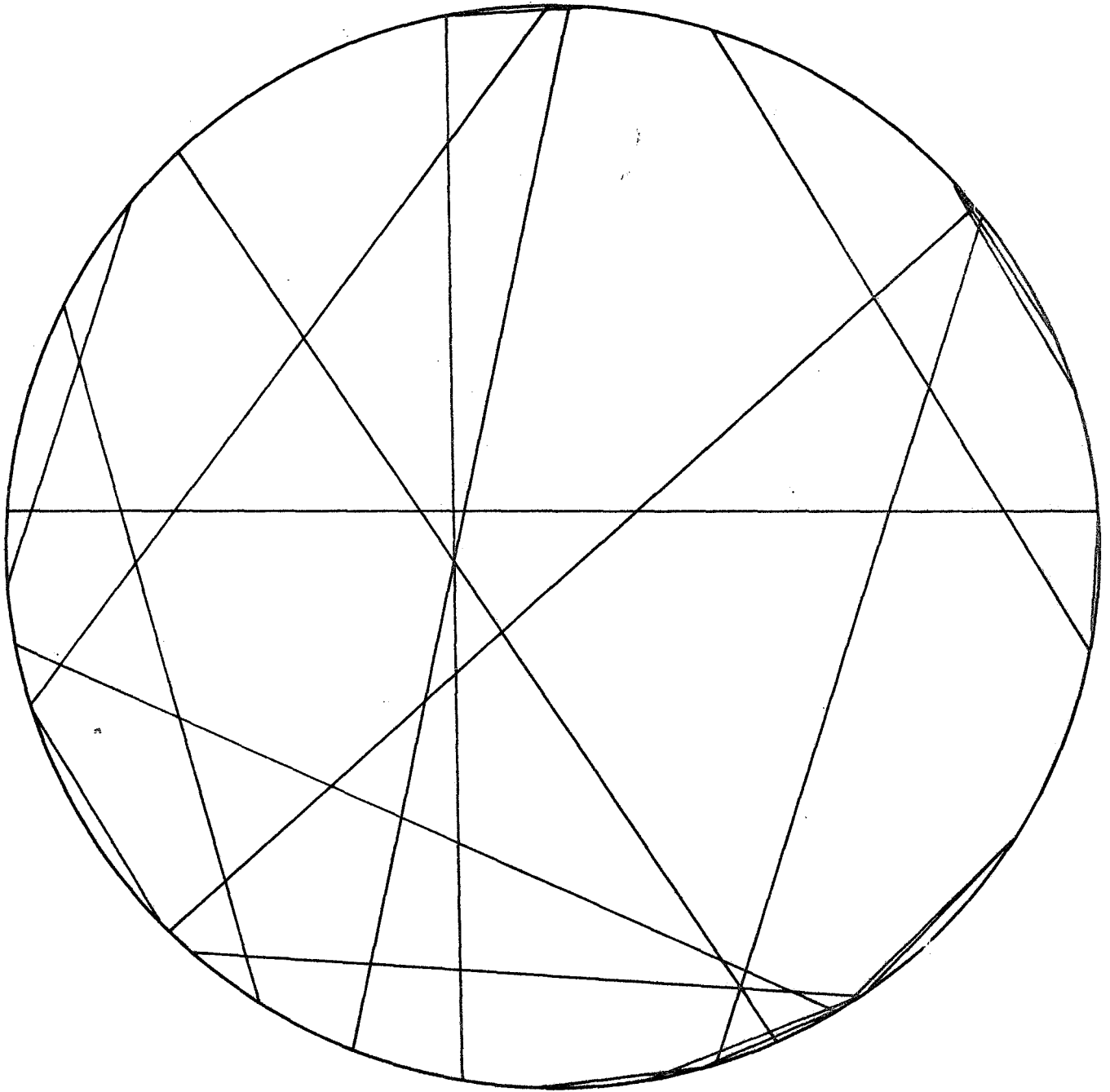


Figure 22

LINES DRAWN BETWEEN TWO RANDOM NUMBERS SELECTED ON THE PERIMETER OF A CIRCLE

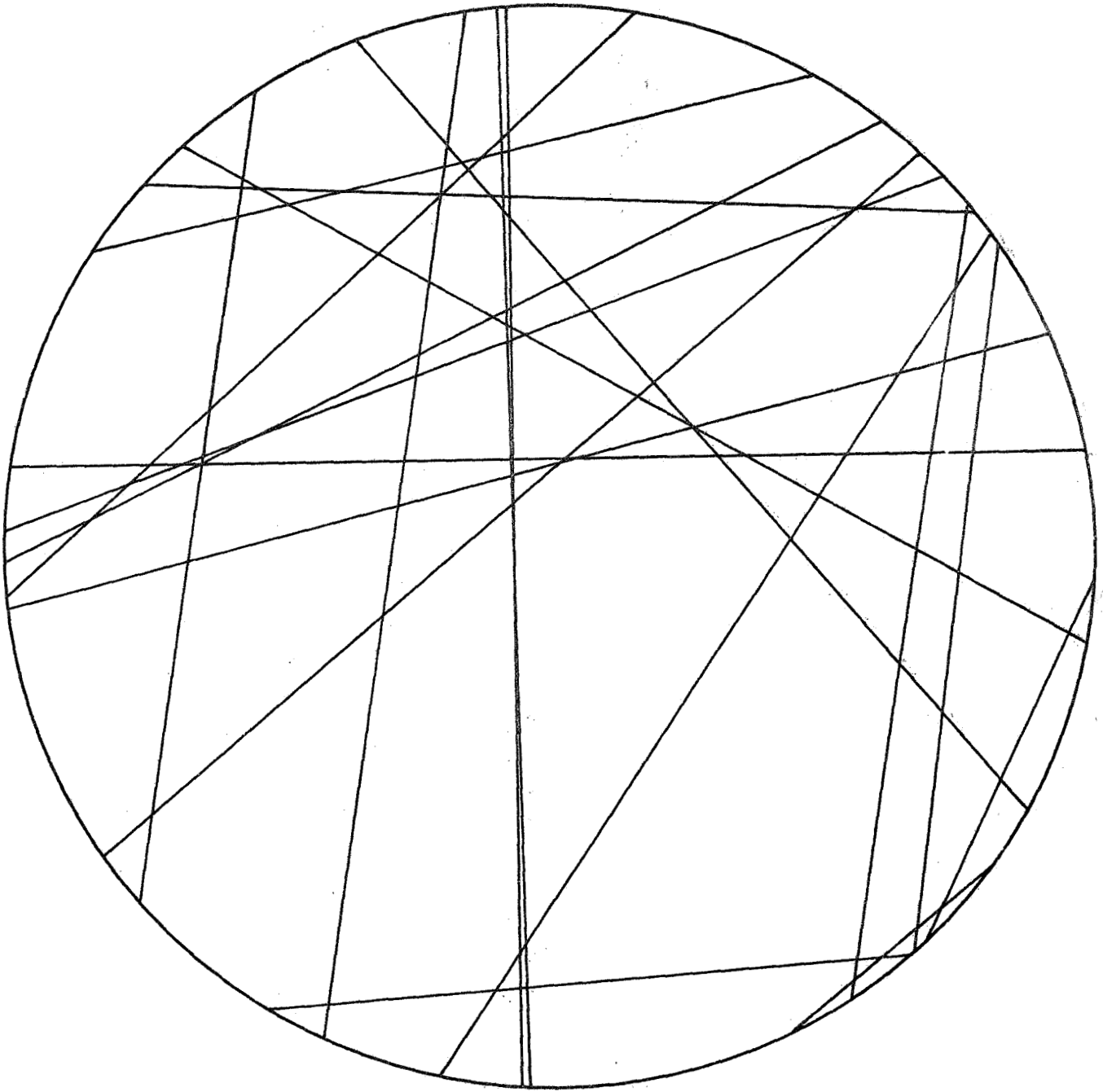


Figure 23

LINES DRAWN PERPENDICULAR TO RADIUS  
FOR RANDOMLY SELECTED ANGLES TO A FIXED DIRECTION

In the second method, the length of a radial line  $r_1$  is chosen from random-number tables, and the direction of this line with respect to some fixed direction,  $\theta$ , is also chosen at random. Then the intercept is drawn perpendicular to this radius. The method is illustrated in Figure 21b. An example of the system is given in Figure 23. Figures 22 and 23 show that shorter intercepts are more probable in method 1, and for that kind of randomness, the average intercept length is smaller in method 1 than in method 2.

In the third method, a point is specified by using a rectangular grid system superimposed upon the circle. Then the direction of the line at this point is selected at random. This method is illustrated in Figure 21c.

In the fourth method, a point on the perimeter is chosen by using random-number tables and the direction is chosen in the same manner.

Further studies of the properties of random intercepts of a circle have shown that the situation is more complex than at first anticipated. Therefore, the conclusions of these studies should be treated with caution until further data are available. We suspect, for example, that the four techniques described above reduce to three rather than two equivalent methods as suggested in Section IIID of Volume 3 of this report. For the purposes of discussion, however, it will be sufficiently accurate to refer to methods 1 and 4 as method A randomness, and methods 2 and 3 as method B randomness.

#### E. Diffuse Light

A search was made of standard optical textbooks for a definition of diffuse light. It was not possible to find a precise definition, since normally the term is used in the sense of "nondirected light" rather than in the sense of a particular spatial distribution of radiant energy. In order to begin the development of the theory of diffuse light penetration, we defined diffuse light as follows.



Diffuse light is light in which the density of photons per unit volume is the same at any location in space with all directions for the photon tracks being equally probable. By this definition, the density of photon entries at any point of the pigment perimeter is equal at all points on the perimeter. This is equivalent to saying that all points of entry for any specified photon are equally probable. The probability of directions permissible for the photon after it crosses the pigment boundary is difficult to assess, since we cannot talk about refraction phenomena unless we have an extended wave front. If equal probabilities for all possible directions can be assumed, the possible tracks correspond to the intercepts constructed by method A.

It may be possible to deduce the correct type of randomness for diffuse light by using the fact that the average branch as considered by method A is shorter than that as considered by method B. Therefore, the absorption of a colored pigment that is related to path length through the pigment particle should be related to the type of random track that occurs.

#### F. Boundary Conditions of Paint Films

To enable any postulated optical theory of paint behavior to be applied to any paint-film system, the boundary conditions of the paint film must be known. The important boundary conditions are:

- (a) Surface finish and reflectivity of the boundary between the incident energy and the pigment vehicle matrix
- (b) Surface finish and reflectivity of the boundary between the pigment-vehicle and the body to which the paint film is applied
- (c) Extent and spatial configuration of the paint film.

The surface finish of the boundary surfaces is important because it affects the energy entry, energy escape, and directional properties of radiation within the paint film. The paint industry is concerned with the surface finish of a paint, but

only gross qualitative properties such as the gloss or matt nature of a surface are measured.

In studies of the interaction of waves with a boundary, it is generally recognized that the surface is smooth if irregularities are small compared to the wavelength of light. However, there is little information on how surface irregularities affect radiation incident on a surface or on how large a smooth area must be before regular reflection occurs.

A second property of a rough surface that could increase the overall reflectivity of the surface is that directional properties of the incident radiation would be changed; i.e., part of the incident radiation would become diffuse and would be spread over a greater area of the pigment film, which therefore would be utilized more efficiently. Without quantitative information on the reflectance of directed and diffuse light from rough surfaces and also on the reflective power of smooth surfaces for incident diffuse radiation, it is not possible to develop quantitatively the statistical models for a paint film.

#### G. Size Distribution of Pigment Particles Dispersed in Paint Films

Analytical techniques for studying the particle-size distribution of a three-dimensional system from two-dimensional sections are almost nonexistent. There are some geometric probability theories that can be used as a basis for analytical procedures for deducing the particle-size distribution of a pigment embedded in a paint film. These studies are presented in detail in Section IIIG of Volume 3 of this report. They result in the development of Equation 8:

$$\frac{S}{V} = \frac{4}{\beta} \quad (8)$$

where  $\beta$  is the average length of the random intercept.

"The ratio of volume to surface per unit volume of a pigment is the average fractional length within the pigment of a random line drawn across a section through the paint film." As far as we are aware, this relationship has never been suggested in this

form for application to the study of paint films. It has been used by Bates and Pillow (ref. 20), who showed that the average path of a sound wave in an auditorium is  $4VS^{-1}$ . This relationship would seem to have great potential in the study of random paths through nonhomogeneous systems.

Also, using the symbol  $\beta$  for the average length of the random intercept and using  $\gamma$  as the average perimeter per unit section, Equation 9 was developed to calculate the average surface area exposed per unit area.

$$u = \gamma\beta \cdot \frac{\pi}{2} \quad (9)$$

## VI. MEASUREMENT OF SHAPE OF PARTICLES

In the literature on particle-size analysis the term "shape factor" has been used in the following manners. First, it has been applied to factors used to convert linear dimensions of individual particles to corresponding particle surfaces and volumes. Since powder usually contains at least a small range of shapes, these shape factors are usually averaged values for several particles.

Second, the term has been used to describe the ratio of the mean diameters measured by two different techniques. For instance, if  $d_s$  is the mean diameter determined by sieving and  $d_m$  is the mean diameter determined by microscopic examination,  $d_s/d_m$  would be a measure of the shape effects that have contributed to the difference between the diameters. Neither of these types of shape factors is appropriate to the problem of defining the shape of a particle dispersed in a paint film, particularly since the shape of a cluster is sometimes of interest to the technologist.

One other type of shape factor has been briefly mentioned in the literature. This is the use of the ratio of two statistical diameters, which have been measured by microscope count, to characterize shape. Two statistical diameters that have been used are Martin's diameter and Feret's diameter. Martin's diameter is the mean length of a line intercepting a profile boundary of the image of the particle and dividing the image into two portions of equal area. The bisecting line is always taken parallel to the direction of traverse. Feret's diameter is the mean length of the distance between two tangents on opposite sides of the image of the particle. The tangents are drawn perpendicular to the direction of traverse.

These definitions show that statistical diameters are mathematical conventions used to describe readily measured averages and not actual physical dimensions of individual particles. An apparent advantage of this type of shape factor

is that the use of statistical diameters removes the need for constant realignment of the eyepiece graticule to measure a particular dimension of a particle. The use of the ratio of statistical diameters to define shape is an attempt to define a shape factor in terms of parameters that can be measured readily.

A computer program for investigating the potential use of statistical diameters in shape factor analysis was developed. The shape factor analyses are presented in Section IV of Volume 3.

From the studies on the possibility of using the ratio of Martin's to Ferret's diameter to characterize shape factors of irregularly shaped particles, it is obvious that any method of measuring that takes into account orientation by seeking to make many measurements of a magnitude projected into a fixed direction is an inefficient measuring technique. In the following discussion, possible techniques for measuring shape factors independent of orientation are outlined.

The ratio of the radii of two circles that encircle some parameters of the particle profile could be a very useful shape factor. One possible shape factor of this type would be the ratio of the radius of the circumscribing circle whose center is on the center of gravity of the particle profile to the radius of the circle of equal area. This shape factor we define as the extension shape factor. This shape factor would be independent of the orientation of the particle and would not involve estimating the position of tangents with regard to a fixed direction. It would have the disadvantages that two operator decisions would be required: (1) the location of the appropriate center and (2) the judgment of equal areas.

It is probable that the first judgment would not be too difficult and that the second would be an easier judgment than estimating Martin's diameter, but this would have to be investigated experimentally by conducting a series of tests with a team of operators and a set of test profiles. This measurement could be carried out very rapidly by using a variable-iris

diaphragm and photomicrographs. The use of the circle of equal area is suggested because this would facilitate isolation of particles of the same size but with different shapes. This shape factor would have a value of 1 for a spherical particle, and the value would increase for an elongated particle.

Another shape factor of the same type we can call an extremity shape factor. The extremity shape factor would be defined as the ratio of the radius of the circumscribing circle to the inscribed circle when the center of both circles is on the center of gravity of the particle profile. This shape factor would also be equal to unity for a spherical particle but would increase more rapidly than the extension shape factor as the particle profile became elongated. It would reduce operator decisions to location of the particle center and to recognition of intersections. It is anticipated that these operator decisions would be relatively free from bias and cause little fatigue. However, the isolation of differently shaped particles and concurrent sizing of the particles would be more difficult.

It is probable that the extension shape factor could be measured easily by photoelectric means. The particle profile could be placed in a light beam with its center on the axis of the beam and a diaphragm opened. The radius of the circumscribing circle is the value of  $r$  at which the received light intensity begins to increase in proportion to  $2\pi r dr$ . It should be possible to visually display gain against expected gain or to have a meter indicate when this situation is reached.

To measure the circle of equal area, the particle profile is moved and the diaphragm reduced until the intensity without the particle has dropped to that with the particle. Alternatively, the optical system could be altered, and an increasing black circle could be used to measure the obscuring power of the particle. It should be possible to gain high precision for a relatively small amount of work with these shape factors, since they are independent of the orientation of the particles.

This type of shape factor could be very useful in the analysis of photomicrographs. With improved methods of obtaining photomicrographs, such as the use of Polaroid film, these types of shape factor could acquire important technical meaning.

## VII. SIMULATION OF PACKING OF PIGMENT PARTICLES IN PAINT FILMS

In order to obtain a satisfactory model for studying the penetration of light through a pigmented film, it is necessary to study the structure of a randomly packed paint film. Direct studies of the packing of powders of different shape and size distributions have been reported by various workers (ref. 21-24).

The experiments described in this section were carried out to explore the possibility of using a new technique for simulating the packing properties of small particles. This preliminary discussion will be limited to monosized spheres assembled in a random manner.

Consider sections taken at random through a sphere. All sections are equally probable. It can be shown that the fractional area of solids exposed by a section taken through a random packing is numerically equal to the volume fraction of solids in the three-dimensional packing. Therefore, it should be possible to simulate the appearance of a section through a three-dimensional packing by using the probability distribution of particle sections that can be in the plane of the section and by using some appropriate technique for locating the particle sections in the plane of the section.

We carried out a set of particle-packing-simulation experiments involving a search-circle-weighing technique which is discussed in detail in Volume 3 (Section V). Excluding edge effects, an average porosity of 18.7% was found for a simulated random packing of 2.5-in. diameter spheres. The porosity of this same simulated packing was found to be 24.2% when edge effects were included. This porosity was higher and was closer to that of real random-packings, which normally involve edge effects.

It should be stressed that the model used to simulate random packing was very rudimentary and considerable sophistication would be required before reality is approached.



A figure often quoted for randomly packed monosized spheres is 39.5% (ref. 24). The simple simulated model described here obviously does not adequately take into account the competition for space by adjacent spheres.

In Section IIIG of Volume 3 it was shown that the average track density across a field of view is numerically equal to the porosity. The formula was tested by drawing lines at random on the simulated field of view and measuring the track density per unit line, but the line was terminated 1 in. from the perimeter, so that edge effects were eliminated. The distribution of results for 20 measurements are plotted in Figure 24; it can be seen that the measured densities are distributed according to the Gaussian equation with a mean value of 81%. This value compares well with the porosity measurements made by the search-circle-weighing technique.

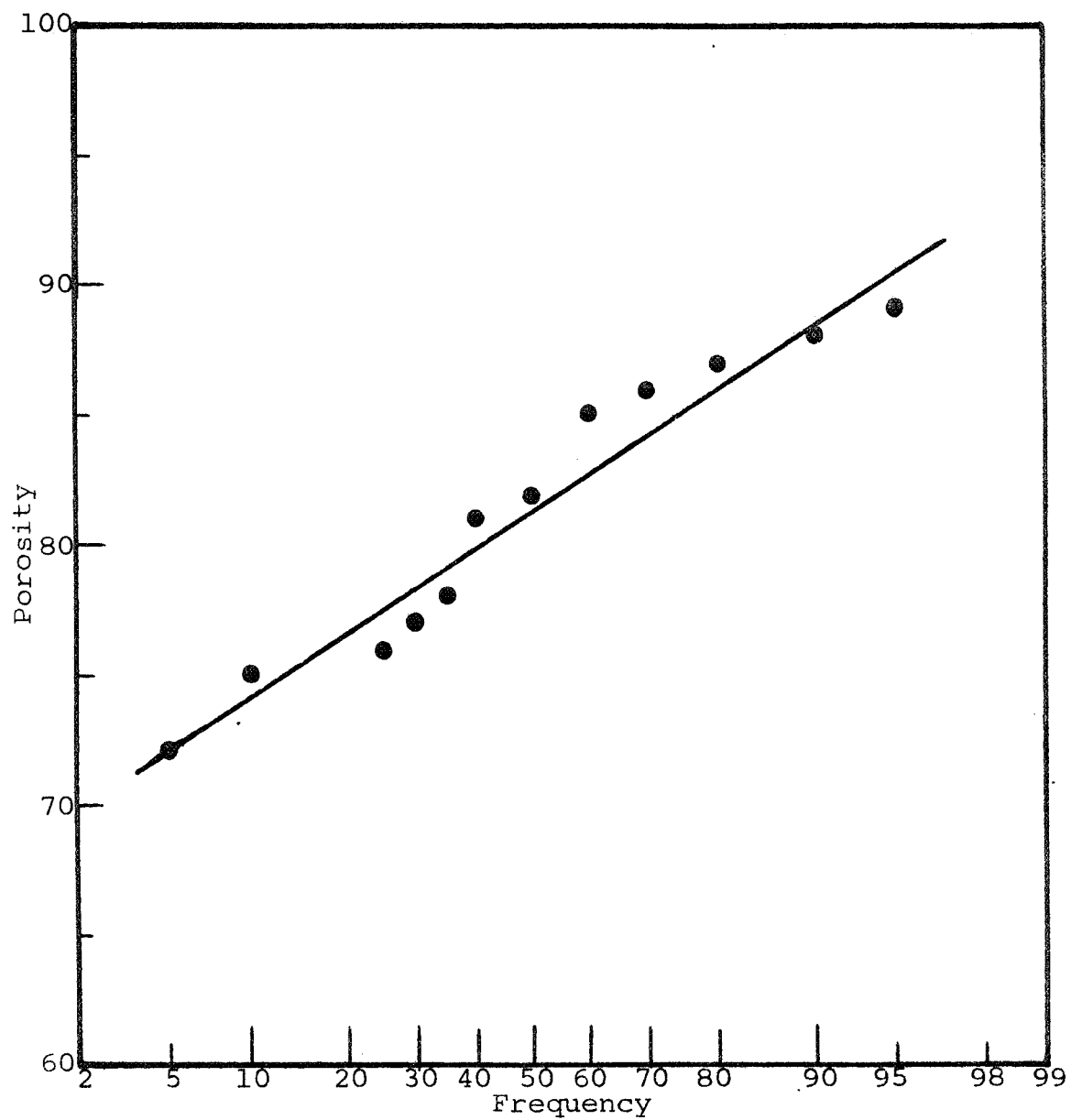


Figure 24

FREQUENCY OF OCCURRENCE OF POROSITIES LESS THAN STATED SIZE

## VIII. USE OF MONTE CARLO METHODS IN PAINT TECHNOLOGY

The Monte Carlo technique for solving complex physical problems has received considerable attention since it was used by Von Neumann and Ulam to solve the problems of neutron shielding associated with the design of atomic reactors. McCracken (ref. 25) has given an excellent introduction to the theory of Monte Carlo techniques. He points out that the basic procedure in a Monte Carlo method for solving problems is to construct a statistical model of a complex physical problem. The behavior of the physical system is then simulated by studying the behavior of the statistical model. McCracken discusses the problem of a neutron traveling through matter; and he points out that we can write mathematical formulas for the probabilities at each collision, but we are often not able to write anything useful for the probabilities of an entire sequence of collisions.

The problems associated with the study of light transmission through a paint film are somewhat analogous to the problems associated with radiation penetration through a paint film. Because the pigment particles are randomly distributed through the paint film and because their size is of the same order as the wavelength of light, we cannot use macroscopic optic theory with its associated concepts of reflection and refraction. The radiation penetration problem involves the solution of many random interactions between randomly directed photons and randomly distributed particles.

For a system of interaction of this kind, we construct probability equations; but, as in the case of neutron shielding discussed by McCracken, it is virtually impossible at the present stage of technology to write anything useful for the probability of an entire sequence of interactions.

From a study of the literature of paint film research, it appears that too many scientists have been preoccupied with studying to a high degree of precision isolated physical properties of individual constituents of the paint film and

that little research has been directed toward the interaction between physical variables within the paint film.

In an attempt to elucidate the complex phenomena occurring within a paint film, we have explored the possibility of constructing several statistical models of a paint film. The properties of these statistical models have been investigated to determine whether anything concerning the properties of real paint systems can be deduced from the models. In justification of this novel approach to solving problems of paint technology, it should be noted that Van de Hulst (ref. 26) has recently criticized current attempts to solve multiple-scattering problems. He states that "too much emphasis has been placed upon redoing with better accuracy and more refined mathematical methods the problems for which rough answers are already available." He also points to the encouraging fact that "usually, the intuitively chosen solution turns out to be the correct one." By implication, he exhorts the scientist to seek intuitive solutions to some of the more complex interaction problems.

## IX. RANDOM-WALK MODEL FOR STUDYING ENERGY PENETRATION THROUGH PAINT FILMS

In an initial attempt to construct a statistical model of a paint film we considered the possibility of studying the interaction of radiation in a cloud of particles many diameters apart. It was postulated that a study of the variation in properties of the scattering behavior of a well-dispersed cloud as the solids concentration increased could give some indication of the behavior of a paint film.

The initial idea consisted of considering the interaction between a beam of light and a particle by using Mie theory and then calculating the secondary scattering events from a knowledge of the probability distribution of particles in the cloud. This successive study of energy events cascading through the cloud is, in effect, a random-walk study.

A regular array of particles in the cloud would at first sight appear to be the simplest model for studying interaction phenomena. In a cloud of this type the density of scattering centers is not independent of the direction of the incident radiation. In fact, a random array of particles is the simplest model to treat, since the properties of the array on the average (averaged over a sufficient distance) are independent of the direction of travel. The only effect of nonnormal incidence is that a given thickness of film appears thicker. It may therefore be possible to study several random walks through a random array and average them for an average effect.

To investigate penetration of radiation through a cloud of particles, consider radiation incident on a particle. After interaction, the energy will be radially distributed about the center of the particle. Then consider possible locations of the next sphere encountered and determine how the energy is distributed.

The simplest average interparticle distance that can be calculated for a monosized system of spheres is that for a system in which the particles are assembled in a symmetrical cubic array. This simple average is a useful average even when considering the properties of a random array, because from it we can calculate the order of magnitude of particle separation within a given cloud.

In studies which are described more fully in Volume 3 (Section VIIA), we calculated the probability distribution of particle centers within such a cloud. These studies resulted in the development of the following equation:

$$y = 0.806 \sqrt[3]{\frac{1}{a}} \quad (10)$$

where

y = the number of particle diameters between particle centers

a = the volume fraction of particles

Thus, the average interparticle distance in a symmetrical array is a function of the volume concentration only.

A graph of the relationship in Equation 10 is shown in Figure 25. The volume concentration at which the particles touch is that for y = 1. For nonspherical particles in random array, the values read from the curve in Figure 25 are not exact but do indicate the order of magnitude for intersurface separation.

The probability distribution of interparticle distances within a dilute cloud of particles was developed in Section VIIC of Volume 3. An expression that is independent of the particle diameter was obtained. The results of these studies apply to the geometric relationships of particles in a cloud. However, they have not been used intensively to study paint theory because the implications of Equation 10 were that in a paint film the particles are too close for the cloud model to be valid.

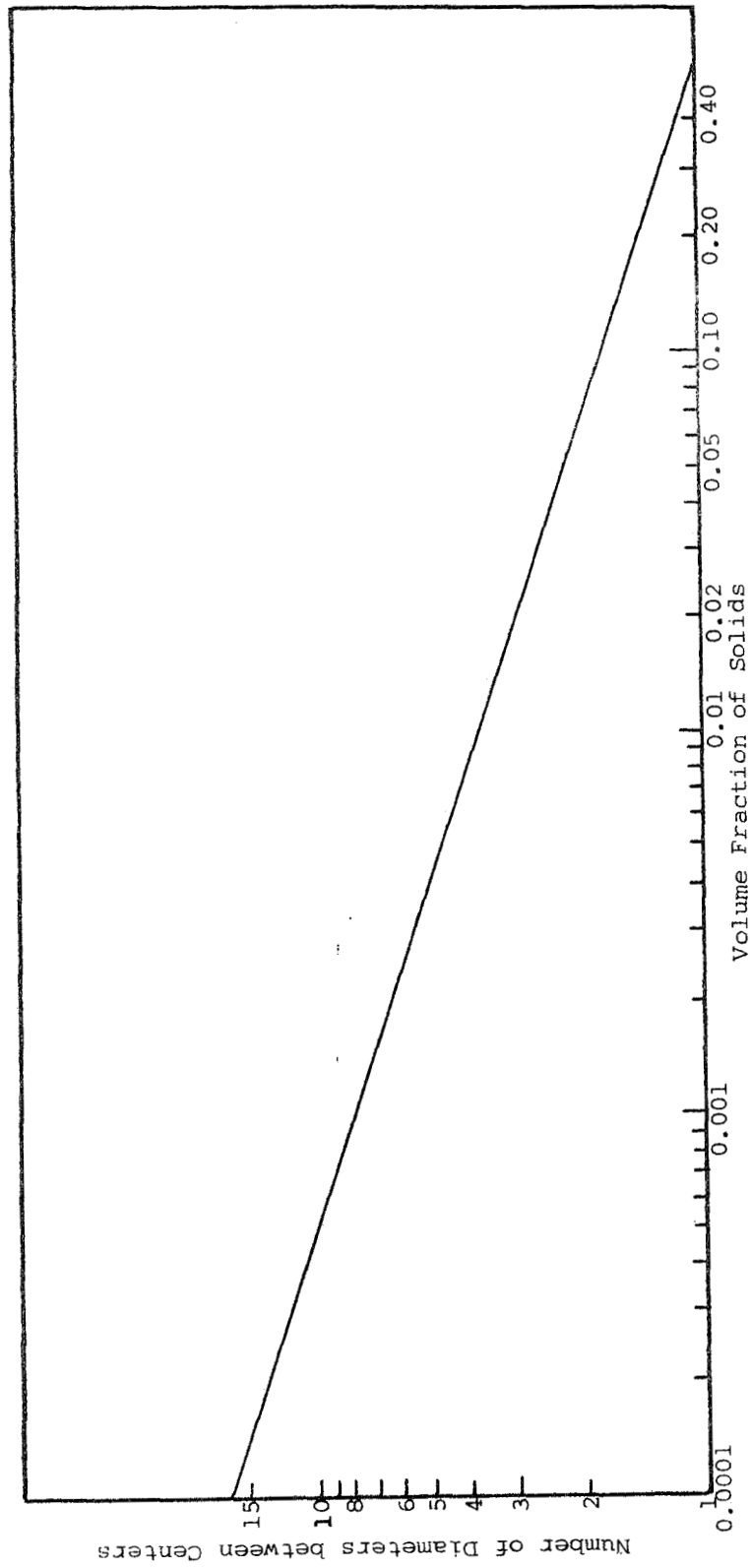


Figure 25  
RELATIONSHIP BETWEEN VOLUME FRACTION OF SOLIDS AND INTERPARTICLE DISTANCE  
IN A MONOSIZED MAXIMUM INTERPARTICLE DISTANCE ARRAY

For instance, it can be seen from Figure 25 that at the average distances between particle centers to be expected in normal paint films of about 40% by volume solids concentration, there is a high probability that many of the surfaces of the particles will be in contact. This physically resembles the situation that occurs when the cloud is completely collapsed. The special features of a collapsed cloud are loss of identity by individual particles that are in intimate contact and high density of scatterers per unit volume.

In view of these special features of a closely packed pigment particle system, it was decided that a random walk consisting of a series of discrete particle/energy encounters was not an appropriate model for current high-pigment-density paint systems. Therefore, studies of random walks through dilute cloud systems were discontinued.



## X. MONTE CARLO STUDIES OF GROWTH IN SCATTERING CENTERS AT VARIOUS CONCENTRATIONS OF PIGMENT

### A. Simple Model of Monosized Cubic Pigment without Extender

#### 1. Construction of the Monte Carlo Plot

The penetration of radiation into a dispersed particle system and the probabilities of secondary scattering within the system were first considered with specific reference to clouds of particles. For a complete random-walk treatment of energy penetration through a paint film comprising particles distributed randomly in a vehicle, the probabilities of the persistence of the forward beam have to be known. When these probabilities have been determined, the energy flux at any surface perpendicular to the direction of the original energy flow at a certain depth can be described by the equation:

$$E_T = E_0 P_x + E_D \quad (11)$$

where

$E_T$  is the total energy

$E_0$  is the original energy in the parallel forward beam

$P_x$  is the probability of persistence at depth  $x$

$E_D$  is the diffuse energy flux.

Several problems arise in predicting the decay of the forward energy beam. Although formulas for light-scattering phenomena are useful in predicting the total energy removed from the forward direction, it is not easy (sometimes it is impossible) to determine the area of the wave front disturbed by the particle. Another major problem is prediction of the statistics of persistence of the forward beam, e.g., the number of particles that are effective scattering centers and the probability that particles along the direction of traverse will occur in line with particles nearer to the source. The following experimental system was devised to study this type of problem.

Consider a rectangular grid. Along the x-axis let there be  $N_x$  units, and along the y-axis,  $N_y$  units. Therefore, within the major grid there are  $N_x N_y$  small squares. If we now consider the path of a plane parallel beam of light passing through the plane of the grid, the z-axis perpendicular to the plane of the grid represents the direction of travel. If an observer looks along the z-axis and if dispersed particles are placed between the observer and the source of light, the observer is not aware of the z coordinate of the particles. The projected representation of the particles on the x-y plane represents their appearance to the distant observer. Also, the fraction of open area seen by the observer represents the fraction of the initial forward beam penetrating the system if diffraction effects are negligible.

Therefore a series of experiments was conducted to simulate the appearance of a dispersed monosize-particle system. A piece of graph paper with 70 units along the x-axis and 100 units along the y-axis was selected. A pair of coordinates was selected from random-number tables, and the appropriate square on the grid was filled with black ink. This blacked-out square represents the shadow of the particles. If the particles are small, the square represents their effective area.\* If the particles are large, the square represents their geometric shadow.

It can be argued that the use of square particles that cannot partially overlap (only completely, or not at all) is an artificial system. It is, but the generalizations obtained from this study are very informative and probably qualitatively correct. After all, the simple kinetic theory of gases is artificial, but it served as a useful tool in the development of the physical sciences.

---

\* The exact meaning of "effective" depends upon the system considered and is not defined further.

In this study we consider particles larger than the wavelength of light, so that only the geometric shadow needs to be considered. To simulate the light-obscuring behavior of particles, the appropriate number of particles is plotted on the grid. When coordinates occur for a position that is already occupied, this represents a particle that is ineffective in destroying the forward beam. The fact that an overlapped particle has occurred is recorded, and plotting continues. The number of particle coordinates plotted represents the concentration of particles in the beam, and the number of spaces remaining represents the open area persisting. Therefore, a record of the two numbers simulates the efficiency with which the forward beam is diverted.

At measured particle concentrations, the grid was examined visually for squares that were touching, and the number of squares within any cluster of profiles was recorded. Figure 26 shows a typical grid at 35% coverage.

The implications and importance of these data are discussed below.

## 2. Rate of Overlapping within a Paint Film (Simulation of Lambert-Beer Law)

Increasing the number of pairs of coordinates considered for plotting on the master grid is equivalent to two physical procedures. Either it is equivalent to studying the changes in attenuation for a unit volume of the beam as the concentration increases, or it is equivalent to studying the increased attenuation caused by increasing the path length through a film of constant pigment volume concentration.

The Lambert-Beer law can be written in the form:

$$\log \frac{I_T}{I_0} = A + N \quad (2c)$$

where A is a constant.



Figure 26  
MONTE CARLO BLOCK PLOTTING EXPERIMENT AT 35% CONCENTRATION

If the simulation experiment described in the previous section is in agreement with empirically determined knowledge, then

$$\log \delta = B + N$$

where

$\delta$  is the logarithm of the fractional open area

N is the number of pairs of coordinates (particles) chosen

B is an arbitrary constant.

Since a plot of the logarithm of  $\delta$  against N was a straight line, it was demonstrated that a Lambert-Beer equation for attenuation of a light beam can be deduced from statistical reasoning alone.

### 3. Cluster Configuration

For verification of the Lambert-Beer law, the basic grid of the Monte Carlo experiment can be considered to be an end-on view through a paint film in which monosized particles are dispersed. Now consider the plot to be a slice of a paint film one unit thick and the particles to be located exactly in the plane of the section. Again, although this is an idealized paint system, the information derived from it is qualitatively in accord with measured properties of actual paint systems. For this interpretation of the plotting experiments, the overlapped particles are regarded as particles that try to occupy positions already filled. They are not considered in studying the distribution of particles or the configuration of clusters in the film section, since they represent nonpermissible particles.

Therefore, the important parameter is the number of spaces occupied. It seems reasonable to regard the cluster as the scattering unit. In fact, it has generally been assumed in paint technology that a badly dispersed pigment has low scattering efficiency because the effective pigment particles are larger and therefore less effective in scattering light.

If we treat a cluster as the scattering unit, we can calculate the total number of scatterers in the paint film at each volume concentration. In Figure 27 the number of scatterers achieved is expressed as a fraction of the number of particles placed in the section. This curve offers a statistical explanation of the fact that a higher volume concentration of pigment dispersion yields a lower hiding power of a given amount of pigment.

If, instead of plotting percentage scattering centers, we plot the absolute number of scattering units per unit volume at various volume concentrations, the data appear as shown in Figure 28. Note that at 17% volume concentration there is an absolute maximum of scattering centers and that further additions of pigment particles only serve to create larger clusters. This suggests the possibility that there is an optimum pigment volume concentration at which maximum numbers of scatters per unit volume are achieved. A survey of the literature indicates that this statistical reasoning may explain the experimentally determined peak in the scattering power/PVC relationships of paints discussed by several investigators (ref. 27-29).

If the growth of clusters of different size is plotted (Figure 29), the reason for the drop in the scattering centers achieved with rising concentration is confirmed; i.e., further addition of particles creates bigger clusters and fewer scattering centers. Thus the number of doublets initially increases at a rapid rate and then declines as further single particles convert doublets into triplets.

#### 4. Edge Effects

In the original investigation of the number of scattering centers per unit area and in the experimental determination of the size distribution of clusters, the fact that clusters touching the boundary of the grid represented only partial clusters that possibly extended beyond the edge of the grid was ignored.

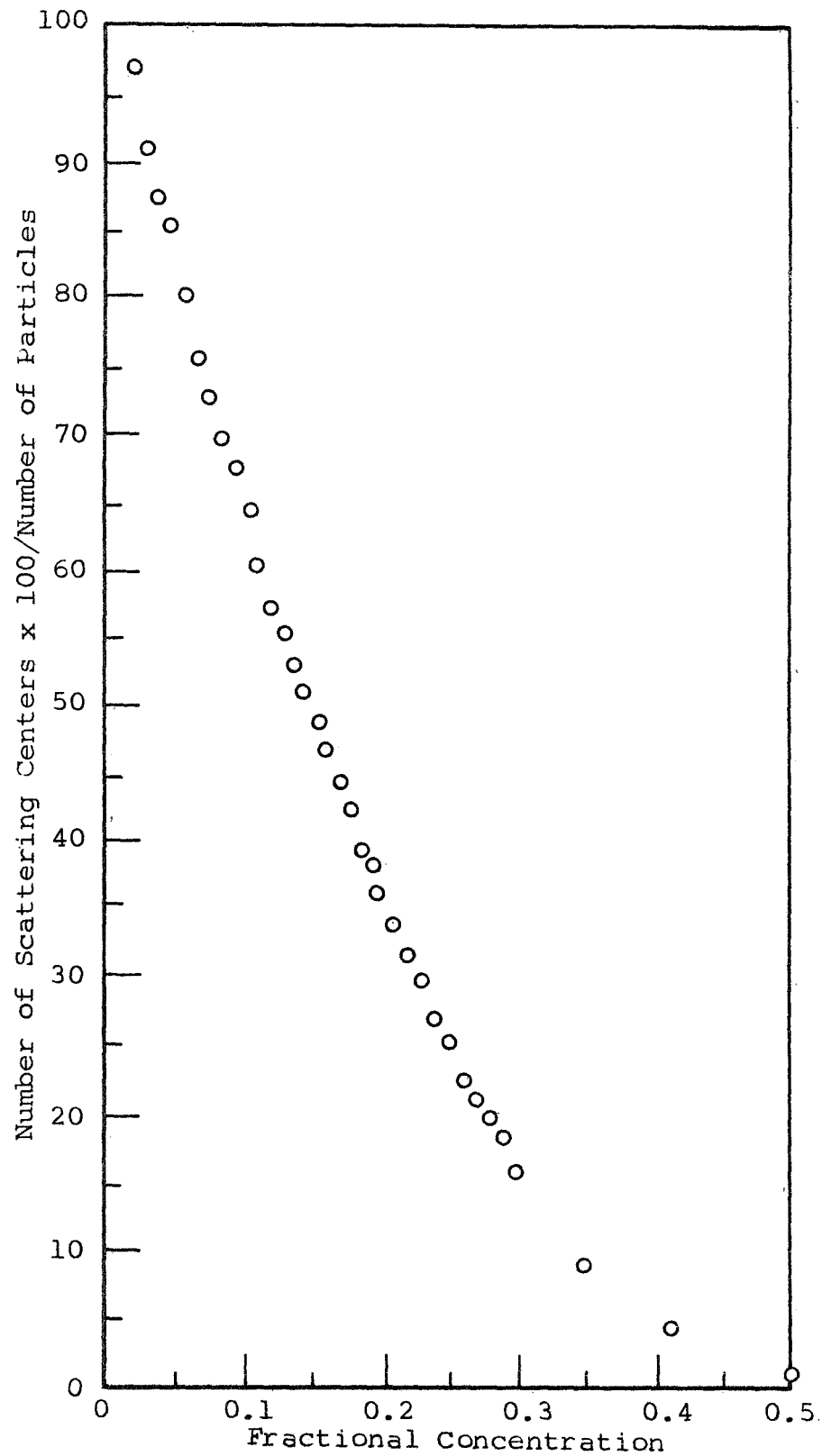


Figure 27

NUMBER OF SCATTERING CENTERS AT VARIOUS VOLUME CONCENTRATIONS  
FOR RANDOMLY DISTRIBUTED MONOSIZED PARTICLES

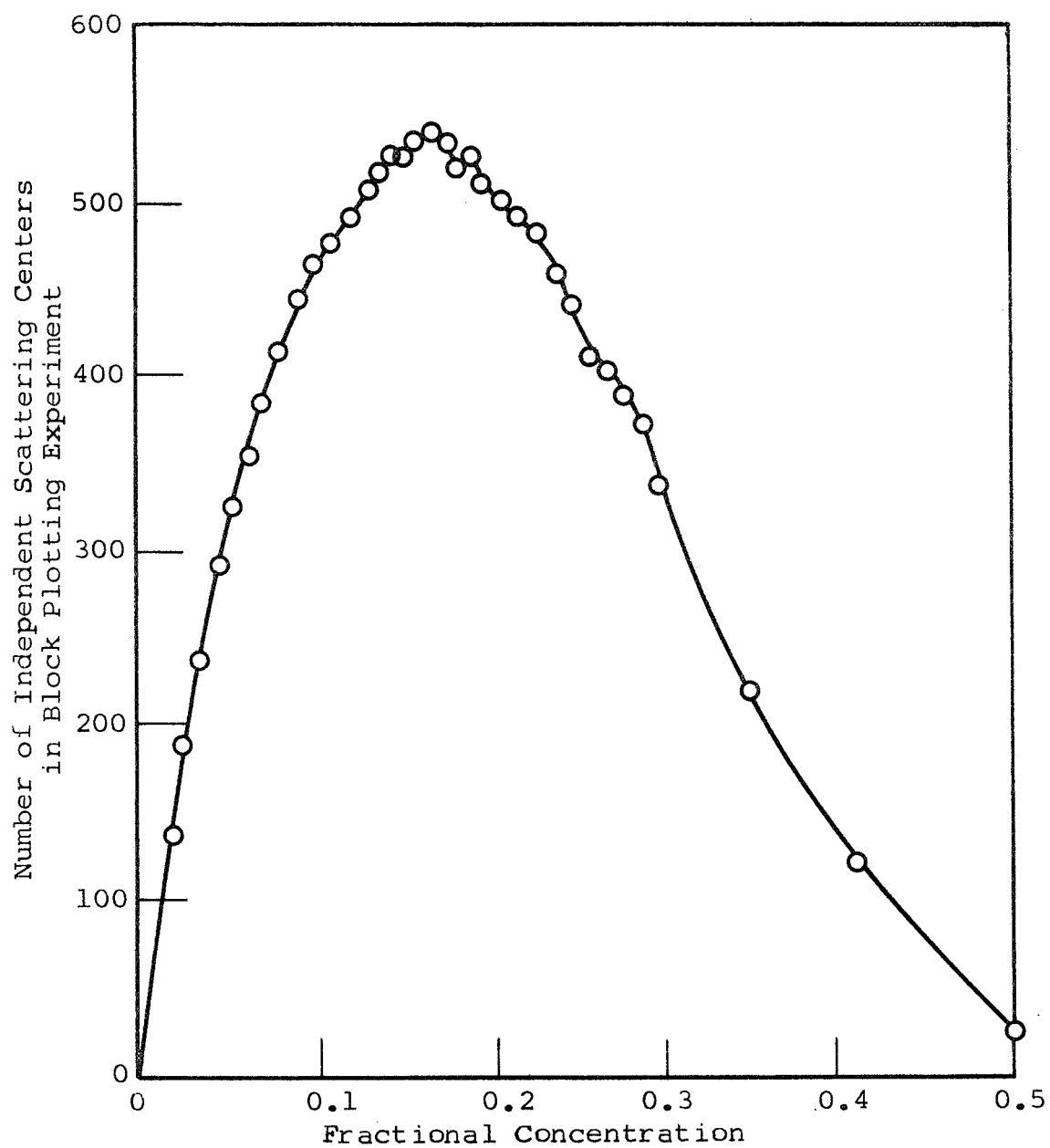


Figure 28

ABSOLUTE NUMBER OF SCATTERING CENTERS PER UNIT VOLUME



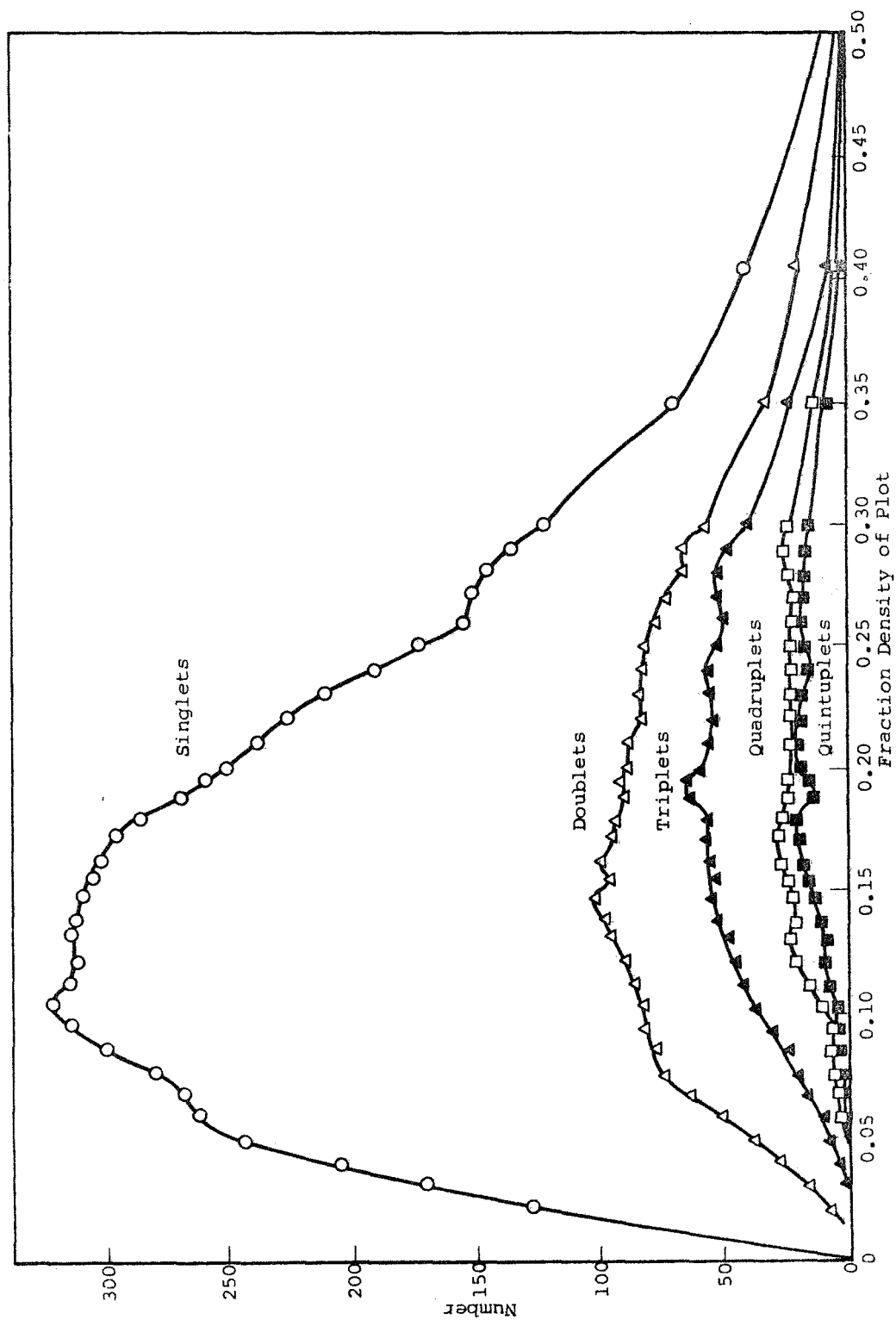


Figure 29

NUMBER OF DIFFERENT SIZED CLUSTERS AT VARIOUS VOLUME CONCENTRATIONS FOR RANDOMLY DISTRIBUTED MONOSIZED PARTICLES

For low equivalent volume concentrations, i.e., low density of coverage, the error involved in ignoring edge effects is negligible. For high equivalent volume concentrations, the error can be considerable.

A simple technique for calculating the correct size distribution of clusters is to eliminate from the data used to calculate the size distribution all clusters touching the boundary of the grid. This technique has the disadvantage that it rejects information available in the simulated field of view.

Techniques for calculating the true cluster density for unit area were investigated. These studies are discussed in detail in Volume 3 (Section VIIIA4). However, one result of these studies is the plot of the total number of scattering centers against fractional concentration shown in Figure 30. The top curve is uncorrected for edge effects and is identical to the curve presented in Figure 28; the bottom curve is corrected for edge effects. Since correction in this case is essentially exclusion of intercepted clusters, it is to be expected that the total number of scattering centers at a given concentration will be reduced.

#### B. Simple Model of Noncubic Pigment without Extender

In the simulation experiments reported in Section VA, the growth of cluster formation was simulated in two dimensions by using a two-dimensional grid-plotting experiment. Although the validity of the quantitative data on cluster formation deduced from these experiments is limited by the fact that clusters are growing in three dimensions, the qualitative deductions (such as the presence of a maximum in the total number of scattering centers) appear to correlate with known empirical data on the changes in opacity of a paint film at various solids concentrations.

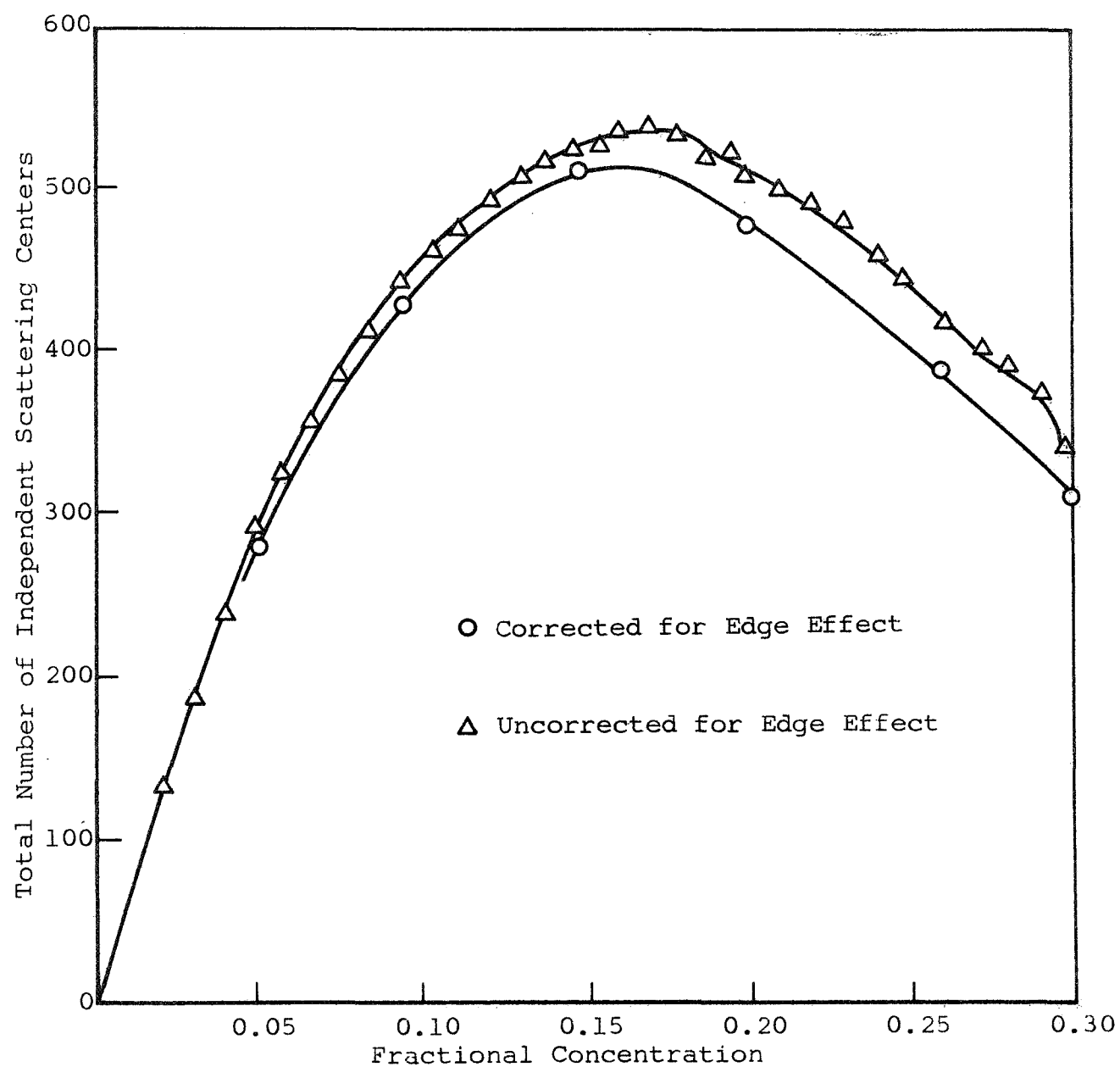


Figure 30

ABSOLUTE NUMBER OF SCATTERING CENTERS PER UNIT VOLUME

A criticism of the simple cubic-pigment-particle model used in the first Monte Carlo experiment is that the particle shape assumed is too symmetrical and that results from the plotting experiment are not valid because real pigment particles have asymmetrical shapes. The implications of this possible criticism were explored and a new plotting experiment was carried out.

A square grid containing 70 x 70 square subdivisions was marked out. On this grid particles consisting of two squares were plotted by using three random numbers. The first two random numbers selected ranged between 1 and 70 to find a location on the plotting grid. The third random number was a single digit. If it was even, the particle was plotted with its left side lower corner on the coordinate and its longer side lying horizontally. If it was odd, the left side lower corner was again laid on the selected coordinate but the long side was laid vertically.

The resultant field of view at approximately 20% coverage is given in Figure 31; other coverages are shown in Section VIIB of Volume 3.

The total number of scattering centers versus percent coverage is plotted in Figure 32. It will be observed that the growth of clusters again causes the number of independent scattering centers to reach a maximum in the region of 20% by volume. Comparison of Figure 32 with Figure 30 shows that the maximum shifted to slightly higher concentrations for the particles with a shape factor of 2:1. This phenomenon may not be real in the sense that statistical fluctuations between repeat Monte Carlo plotting experiments could demonstrate that the difference between it and 20% for the two differently shaped particles could arise purely from chance mechanisms.

Figure 33 presents the growth of the different sized clusters in the plotting experiment using particles of 2:1 shape factor. The results of the plotting experiments with the 2:1 shaped particles have important implications for paint reflectance studies.



Figure 31 .

20% COVERAGE BY PARTICLES HAVING 2:1 SHAPE RATIO

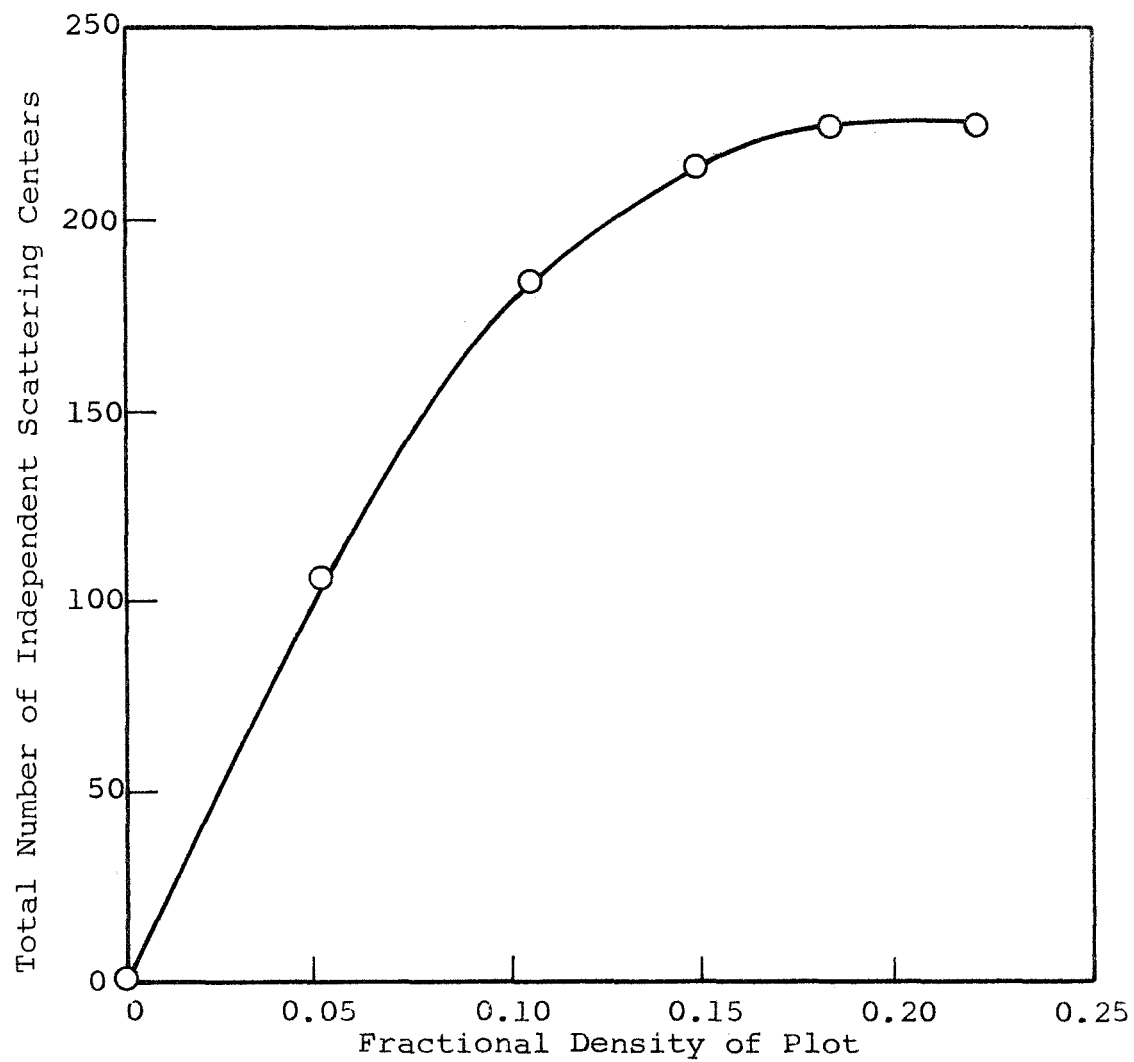


Figure 32

ABSOLUTE NUMBER OF SCATTERING CENTERS PER UNIT VOLUME  
FOR PARTICLES HAVING 2:1 SHAPE RATIO

3

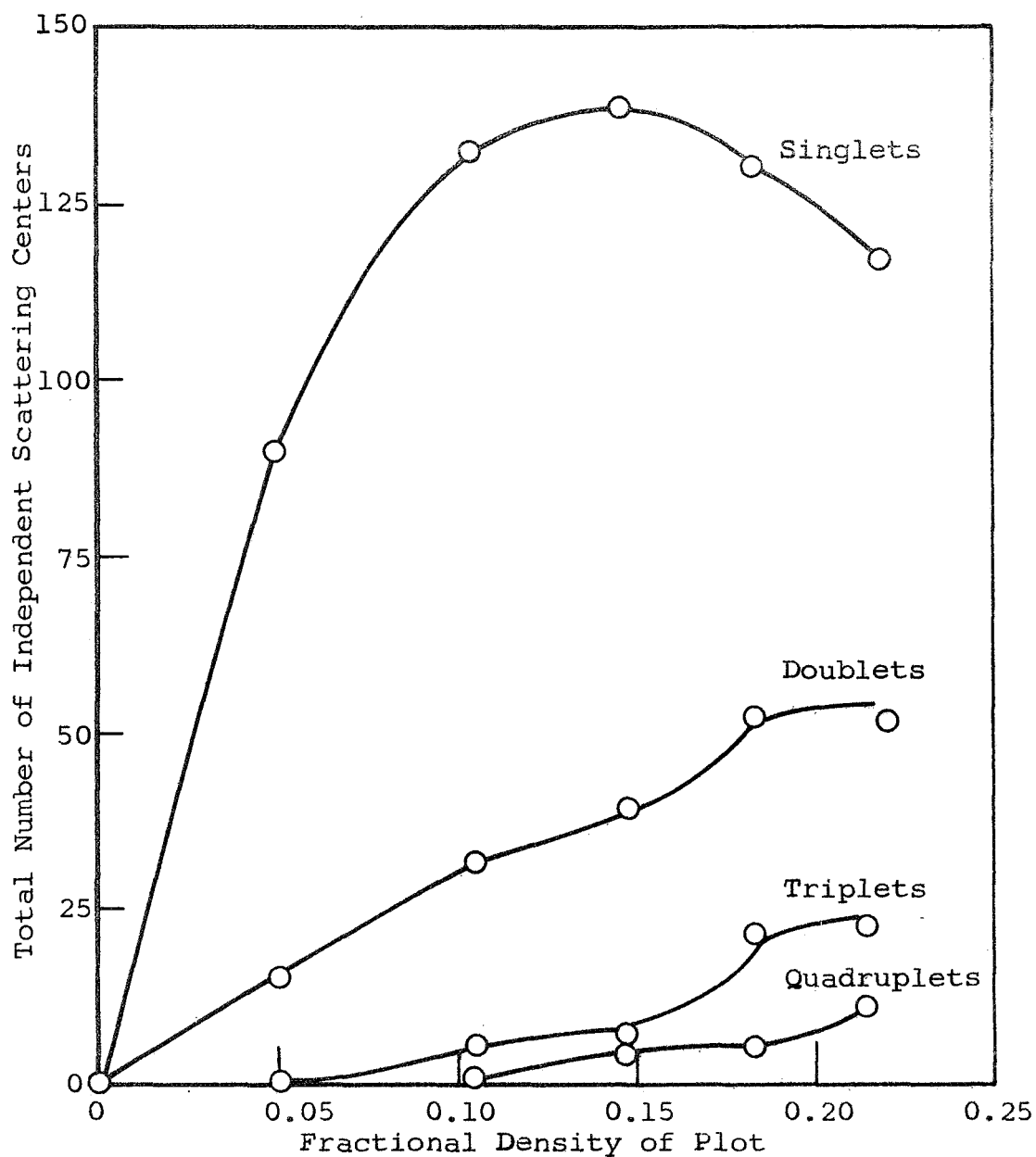


Figure 33

NUMBER OF DIFFERENT SIZED CLUSTERS  
AT VARIOUS VOLUME CONCENTRATIONS  
FORMED FROM PARTICLES HAVING 2:1 SHAPE RATIO

First of all, irrespective of the significance of the small shift from 17 to 20%, these experiments confirm that cluster formation imposes a limit on the number of scattering centers achieved and that 20% by volume is the order of magnitude for pigment concentrations beyond which there is a loss in effective scattering power.

Secondly, the concentration at which the number of independent scattering centers starts to fall off is approximately the same for both the square model and the 2:1 particles. As long as the spaces between particles is several particles wide, the chances of a particle 2 diameters wide touching another particle is not much higher than the chances of a particle 1 diameter wide.

Thirdly, it was postulated in Section IV that it may be advantageous to achieve maximum pigment surface per film thickness provided that the individual particles are still effective scattering centers. It might be argued that 2:1 or higher shape factors might be advantageous from the point of view that they have more surface per mass than a sphere. Again, this is a superficial argument and has no real meaning unless particle size is defined very carefully.

It is possible to discuss the possible influence of dispersion on the optical properties of a paint film by using the statistical considerations outlined in the foregoing paragraphs. Consider a monosized pigment. If the particles are not well dispersed in the paint film, this is equivalent to saying that the units of pigment to be dispersed are not single particles, but groups of particles containing 2, 3, 4 up to  $n$  particles. A cluster of two particles can be considered to be a particle of shape factor 2:1. The case of a cluster containing a number of particles is more complex, because of the possible configurations they can achieve in space. However, all clusters in fact represent basic units of increasing particle-shape factor as the cluster size increases.



From the statistical considerations given above, one would anticipate that in a poorly dispersed pigment the concentration of solids for maximum scattering centers is displaced toward the higher concentration but that the total number of scattering centers is low. Therefore, increasing the degree of dispersion should increase the overall opacity and should shift the maximum of the opacity/concentration curve toward lower concentrations. This conclusion is based on tentative postulations and very simple models, but its applications are sufficiently interesting to warrant investigation. If the conclusion proves to be a real description of the properties of a paint film, an interesting corollary to the hypothesis is that the location of the maximum in the concentration/maximum scattering centers curve will always be a function of the shape factor of a well-dispersed pigment.

#### C. Simple Model of Monosized Cubic Pigment with Extender

A simple modification of the original Monte Carlo plotting experiment can be used for exploring the possible role of extender particles in a paint film. Consider an idealized system in which equal quantities of equally sized pigment and extender particles are randomly dispersed.

A plot having 10% pigment and 10% extender and plots having 30% pigment and 5% and 10% extender respectively were constructed according to the procedures outlined in detail in Volume 3 of this report (Section VIIIC). The plot for 30% pigment and 10% extender is shown in Figure 34.

The number of particles plotted in each case is sufficiently close for comparison of the number and the type of scattering centers achieved for a fixed volume concentration with and without extender particles. For direct comparison, Tables 5 and 6 list the cluster distribution for pigment plus extender and that for pigment alone.



Figure 34

SIMULATED PIGMENT-EXTENDER SYSTEM: 30% PIGMENT, 10% EXTENDER

Table 5

DATA ON CLUSTER FORMATION AT 0.1 VOLUME FRACTION OF IDEALIZED MONOSIZED PIGMENT  
DISPERSED WITH AND WITHOUT THEORETICAL EXTENDER

Pigment	Number of Particles, N'	Number of Clusters								Number of Independent Scattering Centers, S
		1	2	3	4	5	6	7	8	9
Alone	784	315	86	43	15	7	6	4	-	1
Plus extender	790	387	75	45	15	6	1	2	1	-
										477
										532

DATA ON CLUSTER FORMATION AT 0.3 VOLUME FRACTION OF IDEALIZED MONOSIZED PIGMENT  
DISPERSED WITH VARIOUS CONCENTRATIONS OF THEORETICAL EXTENDER

Extender Conc., fraction	Number of Particles, N'	Number of Clusters										Number of Independent Scattering Centers, S
		1	2	3	4	5	6	7	8	9		
0.0	2100	121	56	38	27	14	9	6	13	8		338
0.05	2100	125	51	37	25	18	9	10	12	7		351
0.1	2100	132	50	33	18	17	11	14	13	5		350

The data in Table 5 show that when 10% extender is present in equal quantities with the pigment, (a) there is an overall increase of 12% in the number of scattering centers achieved, (b) there is a 23% increase in the number of single-particle centers (these are probably the most effective in scattering the light), and (c) the overall number of scattering centers is as high as the total number achieved at any higher concentration with the pigment alone (Figure 28). When cluster distributions with and without extender are plotted (Figure 35), both obey the log-normal distribution. Figure 35 also shows that when an extender is present, there is less probability that the larger clusters will occur.

On the other hand, when 10% extender or less is present with 30% pigment, (a) the increase in number of scattering centers is only 4% and (b) the increase in number of single-particle centers is less than 10%. These data show that at these relative concentrations the extender is not efficient at preventing the buildup of large clusters.

This simulation experiment strongly suggests that the extender has a definite role in light-scattering phenomena, i.e., in preventing pigment clusters by mechanical competition for possible positions. An extension to this conclusion is that most efficient use of pigment for scattering is to be gained from the use of a maximum quantity of free extender to compete for cluster sites.

#### D. Partial Encapsulation of Pigment Particles

Note that an encapsulated pigment would carry its own "built-in" extender; i.e., it would have a region surrounding it that another pigment particle could not occupy. Thus it could be a very efficient light-scattering center in a paint film.

If all pigment particles were completely encapsulated with extender before they were randomized in the vehicle, formation of pigment-particle clusters would not be possible.

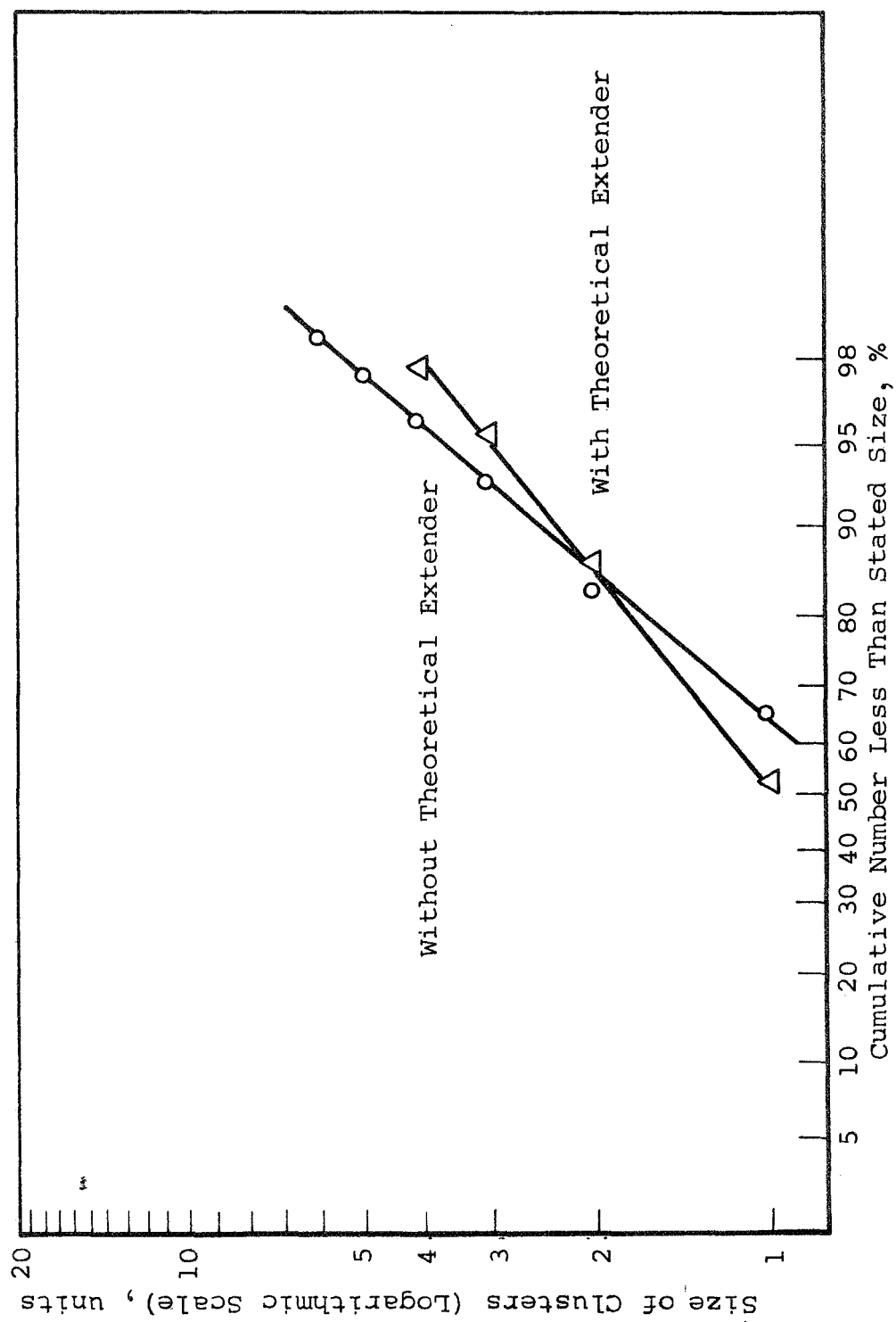


Figure 35

SIZE DISTRIBUTIONS OF CLUSTERS FORMED AT VARIOUS VOLUME CONCENTRATIONS FOR IDEALIZED MONOSIZED PIGMENT DISPERSED WITH AND WITHOUT EXTENDER

Since it may not be feasible on economic or practical grounds to fully encapsulate each pigment particle, consider the advantage to be gained from partial encapsulation of pigment.

Consider the simple two-dimensional Monte Carlo plotting experiment described in Section VIIIA, in which square particles are randomly placed upon a flat grid. Suppose each particle is modified so that one face is coated with extender without altering the size or shape of the composite particle.

The possible configurations of two such particles are shown diagrammatically in Figure 36. This figure shows that the probability of two cubes touching with a layer of extender between the pigment is  $7/16$ , i.e., 0.437. Thus, approximately half the doublet clusters will be broken up into single scatterers by encapsulation of only 1 face in 4.

If a third particle is added to the doublet shown in Figure 36, the probability of having an extender layer between at least two particles is 0.430. As the clusters are allowed to grow, the number of possible configurations increases very rapidly to the point at which it becomes impractical to predict the probability of the pigment being separated by the extender layer.

In these studies which are discussed in greater detail in Volume 3 (Section VIIIl), it is shown that a significant increase in the number of dependent pigment scattering centers developed in a paint film of given pigment volume concentration can be achieved by less than complete encapsulation of pigment with extender.

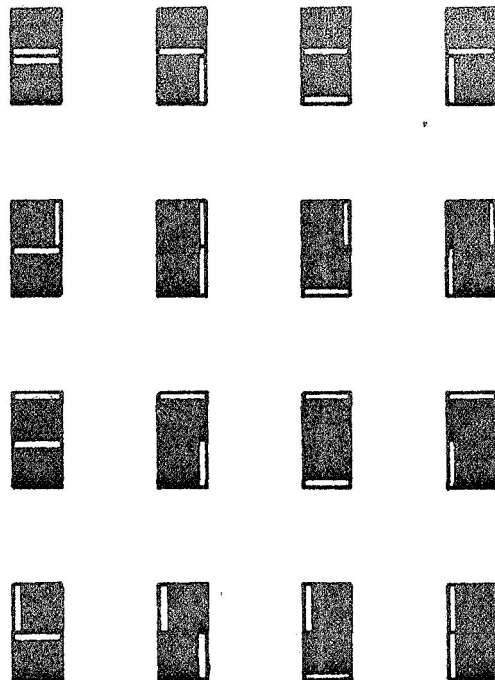


Figure 36

POSSIBLE CONFIGURATIONS  
OF TWO PARTIALLY ENCAPSULATED PARTICLES

## XI. RANDOM SCREEN MODEL FOR STUDYING PENETRATION OF LIGHT THROUGH PAINT FILMS

### A. Introduction

If a section is taken through a paint film, it can be considered to define a screen in which the pigment cross section can be regarded as relatively opaque areas distributed at random in a transparent slab of material. On this basis, we decided to study the possibility of treating the transmission of radiation through a paint film as a series of radiation/screen encounters. The properties of the screens would be related to the pigment volume concentration of the paint film. It is possible to consider events at each screen to be independent of previous encounters, since diffraction effects would diffuse the light energy between encounters. As a first stage in developing this statistical model, the properties of random screens were studied.

### B. Physical Properties of Random Screens

The first property of randomly imposed screens is the residual straight-through area, since this can be used to deduce important facts concerning the persistence of an incident plane parallel beam of light penetrating a paint film.

It can be shown that two regular screens superimposed at random should be a close approximation to random screens placed on top of each other and that the average residual exposure for two random screens superimposed should be  $f_1 \cdot f_2$ . Similarly, for a series of  $n$  screens, the residual exposure should be  $f_1 \cdot f_2 \cdot f_3 \cdots f_n$ . A master circular grid (Figure 37) containing 325 whole square openings was therefore constructed on paper. The opaque portions were covered with India ink, and the openings were cut out with a scalpel. This master was copied by Xerography. The master was then superimposed at random on this copy, and the combination again copied by Xerography. The openings common to both screens could be seen clearly on this copy.



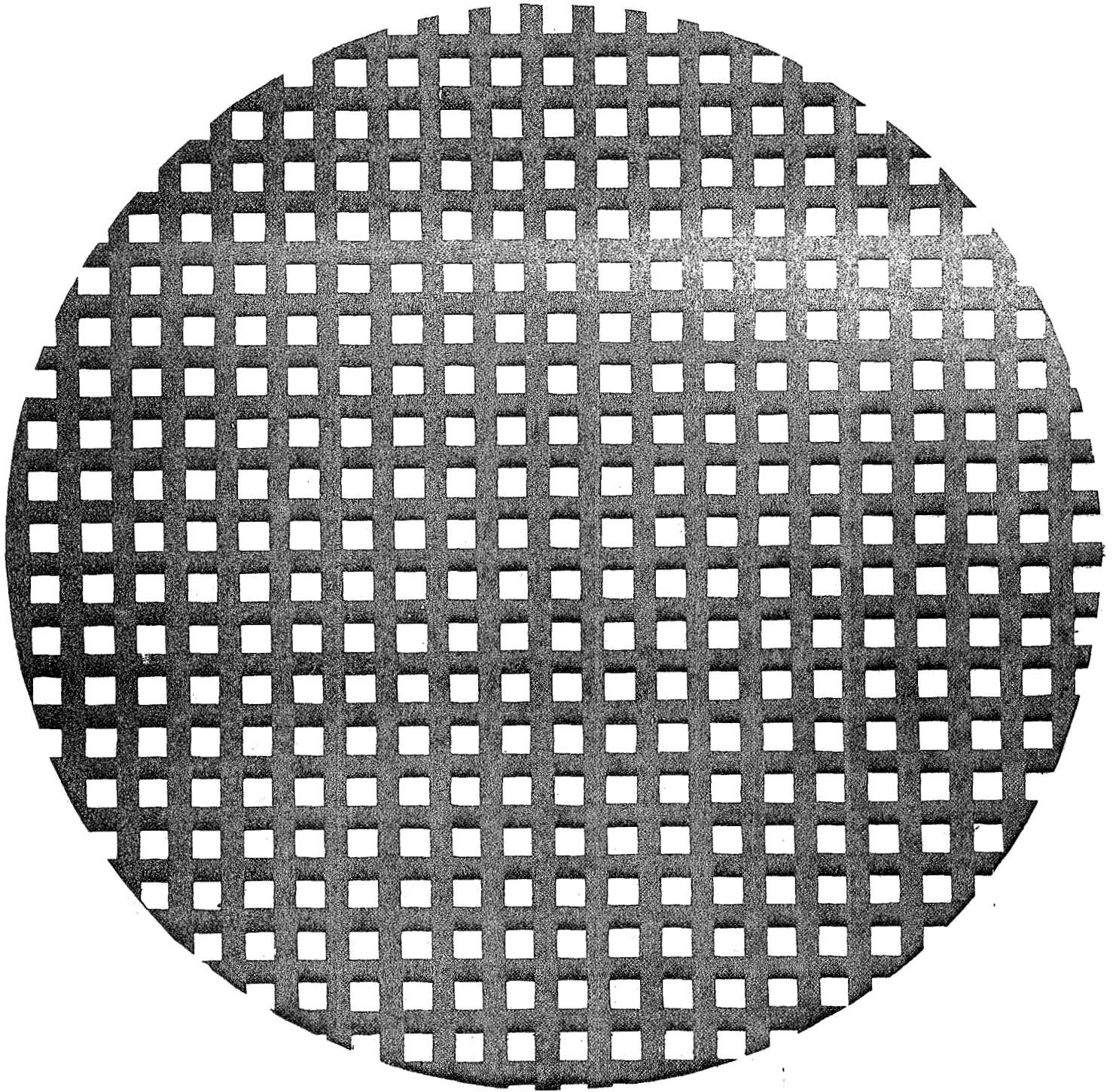


Figure 37

BASIC SCREEN (OPEN AREA, 0.303)

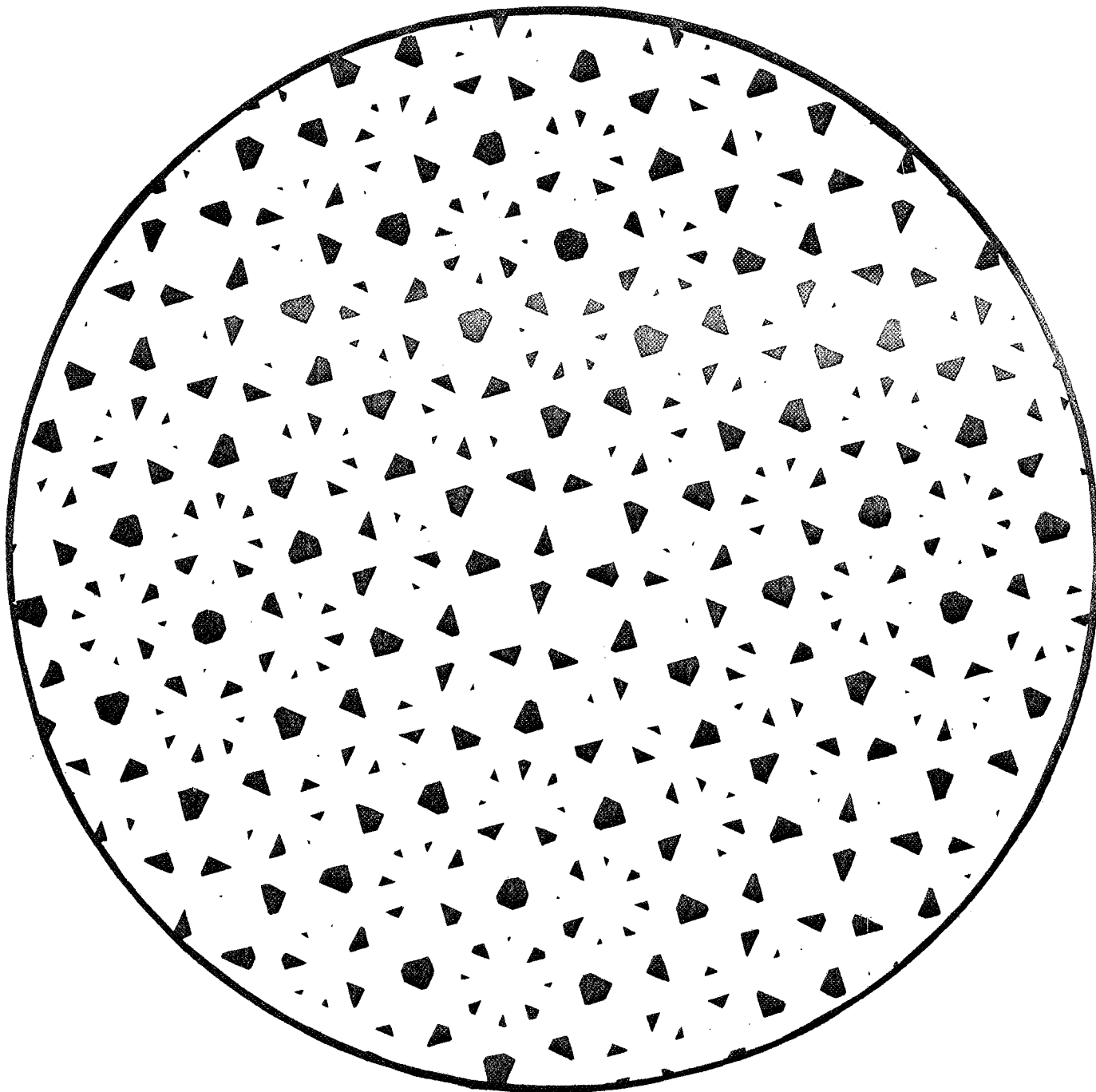


Figure 38

TWO RANDOMLY SUPERIMPOSED SCREENS (OPEN AREA, 0.101)

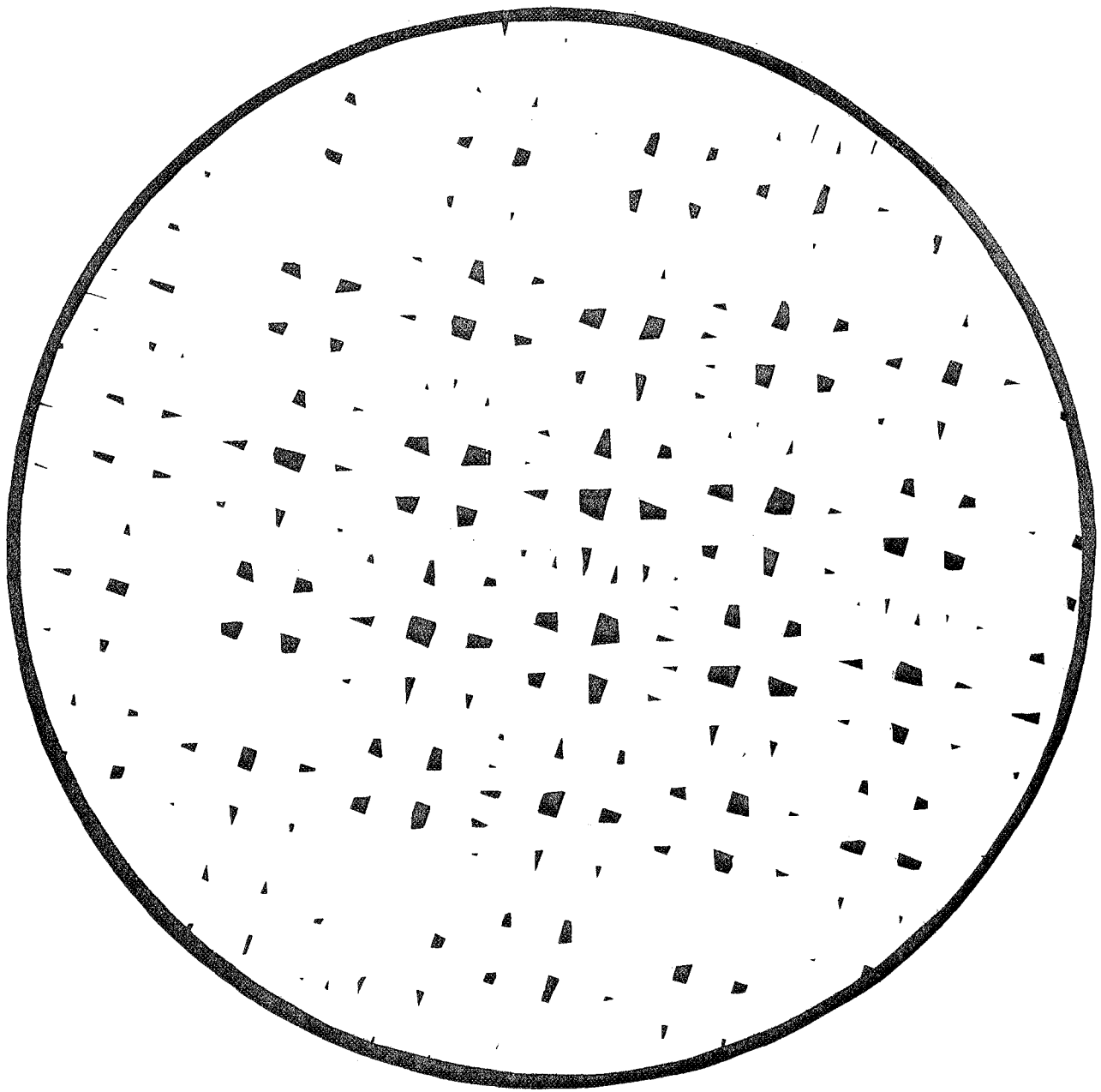


Figure 39

THREE RANDOMLY SUPERIMPOSED SCREENS (OPEN AREA, 0.03)

To measure the open area, the portions of the disk corresponding to the common open area were cut out with a scalpel. The loss in fractional weight of the disk represents the fraction of open area remaining. A typical disk obtained by the two super-positionings is shown in Figure 38.

The result of superimposing the original master screen randomly on one of the double screens is shown in Figure 39. Similar experiments were carried out to simulate four and five superimposed screens. The experimental results are summarized in Table 7. The data show that the predicted and measured straight-through fractional areas agree within the limits imposed by experimental error and statistical fluctuations. This agreement indicates that the penetration of a light beam into a pigment can be predicted by considering the random screens formed by the pigment in the paint film.

Table 7

AVAILABLE STRAIGHT-THROUGH PATHS  
IN RANDOMLY SUPERIMPOSED SCREENS  
(Open Space in Original Screen, 0.303)

Number of Screens <u>Superimposed</u>	<u>Straight-Through Fractional Area</u>	
	<u>Predicted</u>	<u>Measured</u>
2	0.092	0.092
		0.102
		0.098
		0.101
		0.105
3	0.028	0.030
		0.028
4	0.008	0.012
		0.011
		0.007
		0.010
		0.008
		0.006
5	0.002	0.014
		0.003
		0.001
		0.001

### C. Average Track Length within a Randomly Distributed Paint System

If we create a model of a paint film in which we postulate the existence of physically equivalent screens, we have the problem of deciding the number of screens to postulate and the effect of varying the screen aperture.

In an analysis described in Volume 3 (Section IXD), we have shown that the average distance between pigment/surface encounters is the reciprocal of the pigment volume concentration:

$$\bar{L} = \frac{1}{\alpha} \quad (12)$$

By a similar argument, the average track within the pigment is:

$$\bar{L} = \frac{1}{(1-\alpha)} \quad (13)$$

Figure 40 shows the redrawn Monte Carlo plot for 20% coverage (Figure 23 in Volume 3) in which each cluster has been redrawn as a circle of equivalent area. Between clusters the whole range of fractional paths is possible and reentrant surfaces have been eliminated. Two sets of 100 tracks were measured on this diagram by using random lines. The average track length for the first 100 tracks was 4.8 and for the second 5.2. Thus, for this model, the expected value of 5 is achieved within the limits of statistical fluctuations.

Figure 41 shows a typical set of tracks measured on the Monte Carlo plot at a density of 15%. Within the limits of statistical fluctuations, the average track lengths are as predicted from theory, i.e.,  $1/\alpha$  diameters.

The successful prediction that the average track length within a randomly distributed pigmented film is the reciprocal of the volume fraction times the particle diameter indicates that a satisfactory model for a paint film consists of a series of translucent slabs of pigment material separated by the average track length. Each slab is a perfectly diffusing medium of thickness  $1/(1-\alpha)$ . The total surface of the slabs is equal to the total surface of the pigment, so that probably

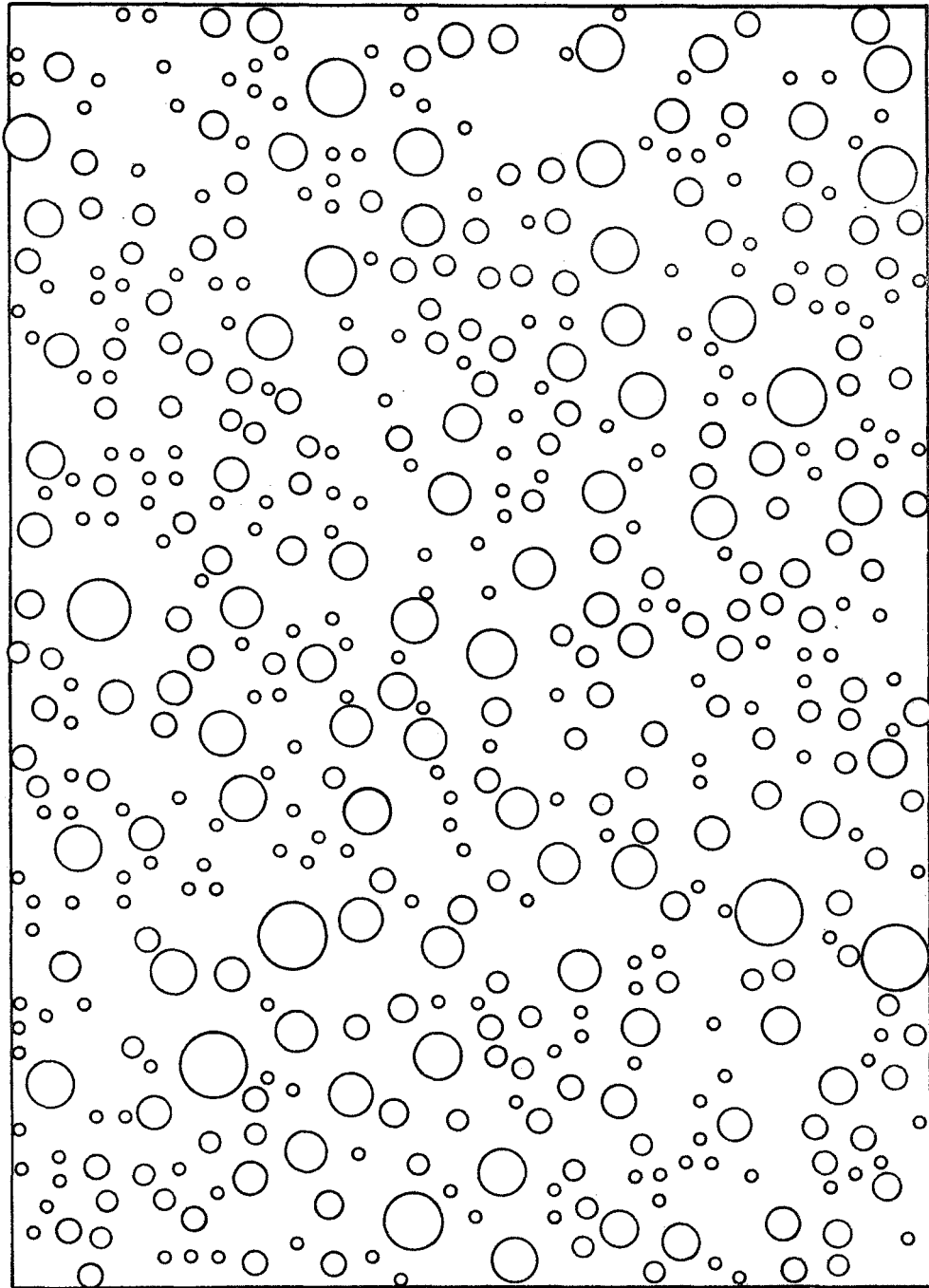


Figure 40

ELIMINATION OF SHORT TRACK LENGTHS: SPHERIDIZED 20% MONTE CARLO PLOT  
(Conversion of Figure 23)

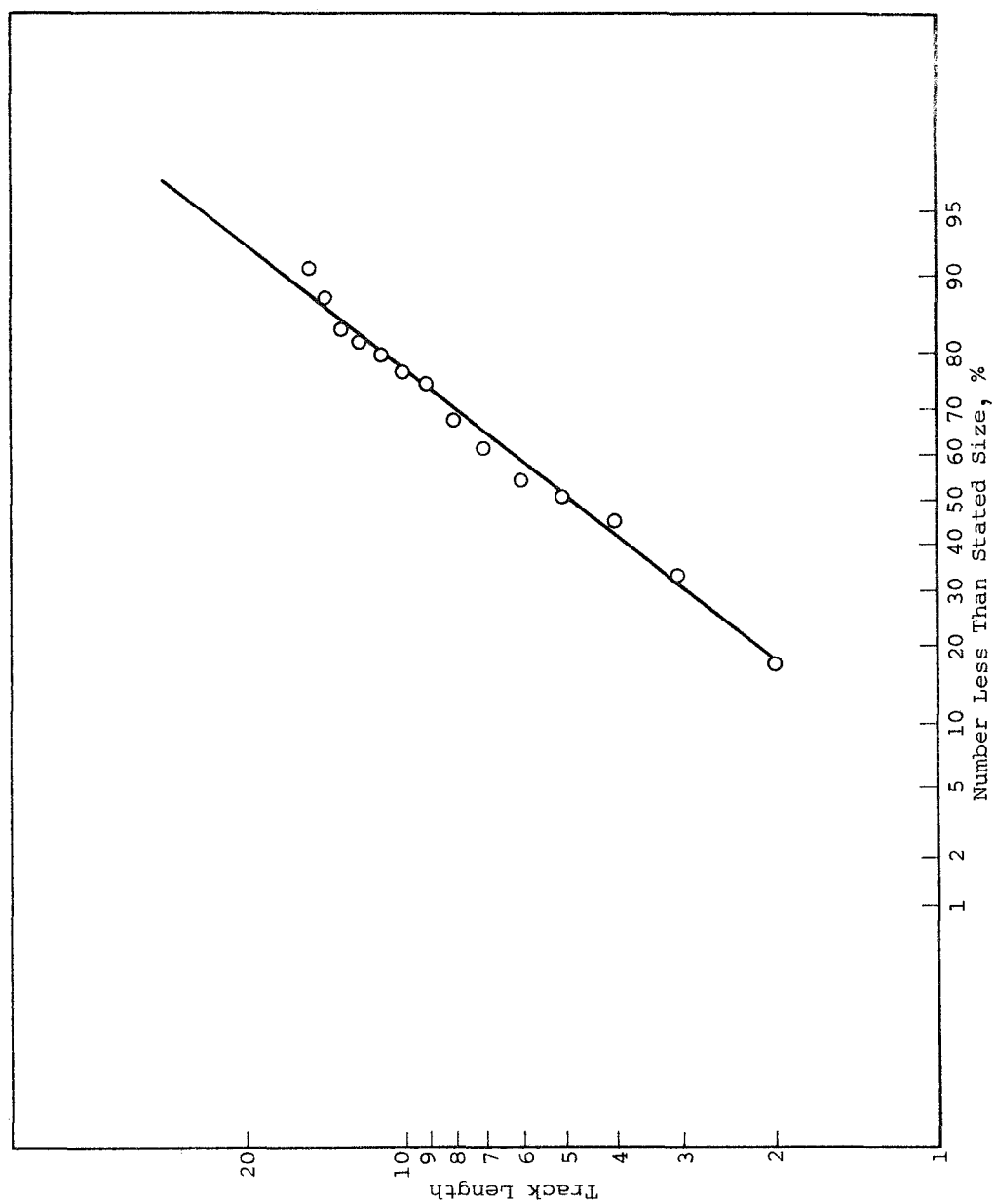


Figure 41  
TRACK LENGTH DISTRIBUTION AT 15% CONCENTRATION

the number of slabs is  $S/2d^2k$ , where  $S$  is the surface area/unit volume expressed in the same units as the average particle diameter, and  $k$  is a constant related to the spatial geometry of the particle and probably has to be determined empirically.

Treating the paint films as being constructed as a series of parallel slabs if perfectly diffusing material is equivalent to finding a physical basis for the Kubelka-Munk equations. The Kubelka-Munk theory postulates that the material can be treated as a perfectly diffusing material of given scattering and absorption power. This is difficult to accept physically, since a paint film is never large in terms of pigment diameter, so that the laws of statistical average cannot be applied without any qualification.

The treatment we have elaborated suggests that the reason statistically based laws can be applied to paint films is that the myriad of possible photon/track encounters represent a large statistical averaging system with respect to time, even though the paint film is statistically thin.



## XII. IMPLICATIONS OF MONTE CARLO STUDIES OF RANDOM TRACKS ACROSS A CIRCLE FOR FILTRATION STUDIES

### A. Concept of Randomness Applied to Fibrous Filters

Some filter systems are made by assembling an array of fibers in a random manner. The random intercepts drawn in Figures 22 and 23 can be considered as unit elements in a filter composed of randomly assembled fibers.

The fact that the two random arrays drawn by methods A and B (see discussion in Section IIID) can both satisfy the technical definition of randomness and yet have different physical properties indicates that technologists dealing with filtration theory may encounter difficulties arising from inadequate terminology. Apparently, similar fibrous mats that in a qualitative sense can be described as a random array of fibers may have been assembled in two different ways, which gave different types of randomness to the positions of fibers. The different types of randomness, unsuspected by the technologist, represent an uncontrolled variable in the experimental studies of filter performance and could cause unexpected differences in performance. The performance differences that could arise from "randomness" difference can be illustrated by the following considerations.

Two major mechanisms are used to capture particles passed through a filter: (a) direct obstruction to the passage of a particle by the pore system of the filter and (b) capture of the particle by single fibers when the particles impact onto the fiber. For both these mechanisms, random filters assembled to form systems analogous to those constructed by method B will be more efficient, since in method B the pore distribution has smaller probability for larger apertures and has more fiber per unit area when captured by the second mechanism.

The effective pore-size distribution for the fiber simulation system in Figure 22 and 23 and similar displays was measured by using a circular graticule. The largest circle that could be placed in any aperture defined by the random fibers was defined as the effective pore size for the passage of spherical particles through the filter.

The size distributions measured for the system shown in Figure 22 is given in Figure 42. The number of apertures for this and other systems drawn by method A was 70; and the number for the system drawn by method B (Figure 23) was 109. The pore structure was quite different for the system constructed by method B. These studies are discussed in greater detail in Volume 3 (Section XA).

It can be seen that random track diagrams of the type shown in Figures 22 and 23 could be used to study dependence of the performance of filters on various random types of arrays of fibers. If it were desired to simulate fiber systems in this way, the effect of the fiber diameter can be taken into account by decreasing the radius of the circle considered able to pass through the simulated aperture by the magnitude of the fiber diameter.

If a filter mat is constructed by allowing relatively short fibers to fall into position, the randomness of the fiber system will be analogous to system B, since this corresponds to the equal probability of all points in the plane of imposition having a line through them. If, however, long fibers are assembled so that the density of fibers at the perimeter is uniform, the fibrous system is analogous to system A for a circular perimeter. From the estimated pore-size distribution measurements, it can be seen that the two systems would have different properties.

It may be possible to make major advances in filtration theory by considering the exact meaning of randomness in a fiber system and devising techniques for achieving a random system with optimum properties.

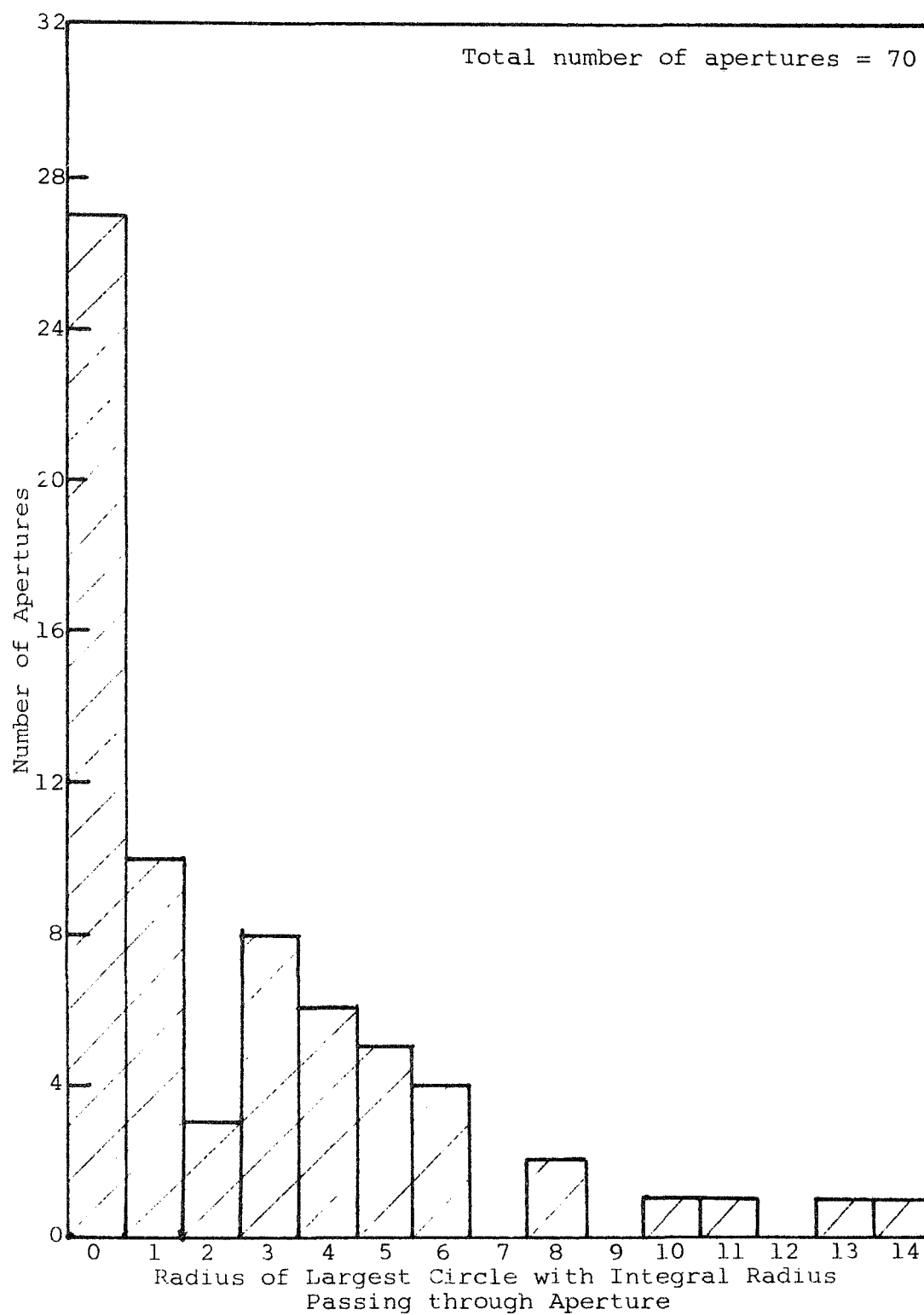


Figure 42

PORE-SIZE DISTRIBUTION OF SIMULATED FILTERS  
(Simulated in Figure 78)

## B. Use of Random Intercept Diagrams to Devise Monte Carlo Methods for Studying Aerosol Filtration

Prediction of the performance of any filtering device is complicated because of the many variables to be considered in constructing an appropriate theoretical system. Many workers have chosen to study the various factors that are known to influence filter performance in isolation. Thus, effects due to flow conditions and to electrostatic forces are studied separately. It is difficult to evaluate the usefulness of these studies for actual filtration systems because of the subtle way in which these variables interact. One way of studying the behavior of complex interacting systems is to construct an abstract model in which the major variables have been simulated and which can be used to predict the orders of importance of the various mechanisms by using the model as a basis for a Monte Carlo experiment. In a Monte Carlo routine a succession of events is simulated by using an abstract system, and the behavior of the model is studied as it undergoes these successive events.

Consider the system of Figure 22 to be a set of simulated fibers for a given filter system. To simulate particle capture, we now use a transparent sheet of paper on which a random set of particle profiles is simulated by using postulated characteristics of the distribution of particles in an airstream (Figure 43). This simulated set of particles can be placed on top of the fibers in many positions and the probability of capture simulated. In this way, the effect of the interaction of a random stream of particles encountering random fibers can be predicted. The effect of the fiber diameter can be simulated by drawing a dotted line at a distance of half a fiber width around the particle profile. This has been illustrated for several particles in Figure 43.

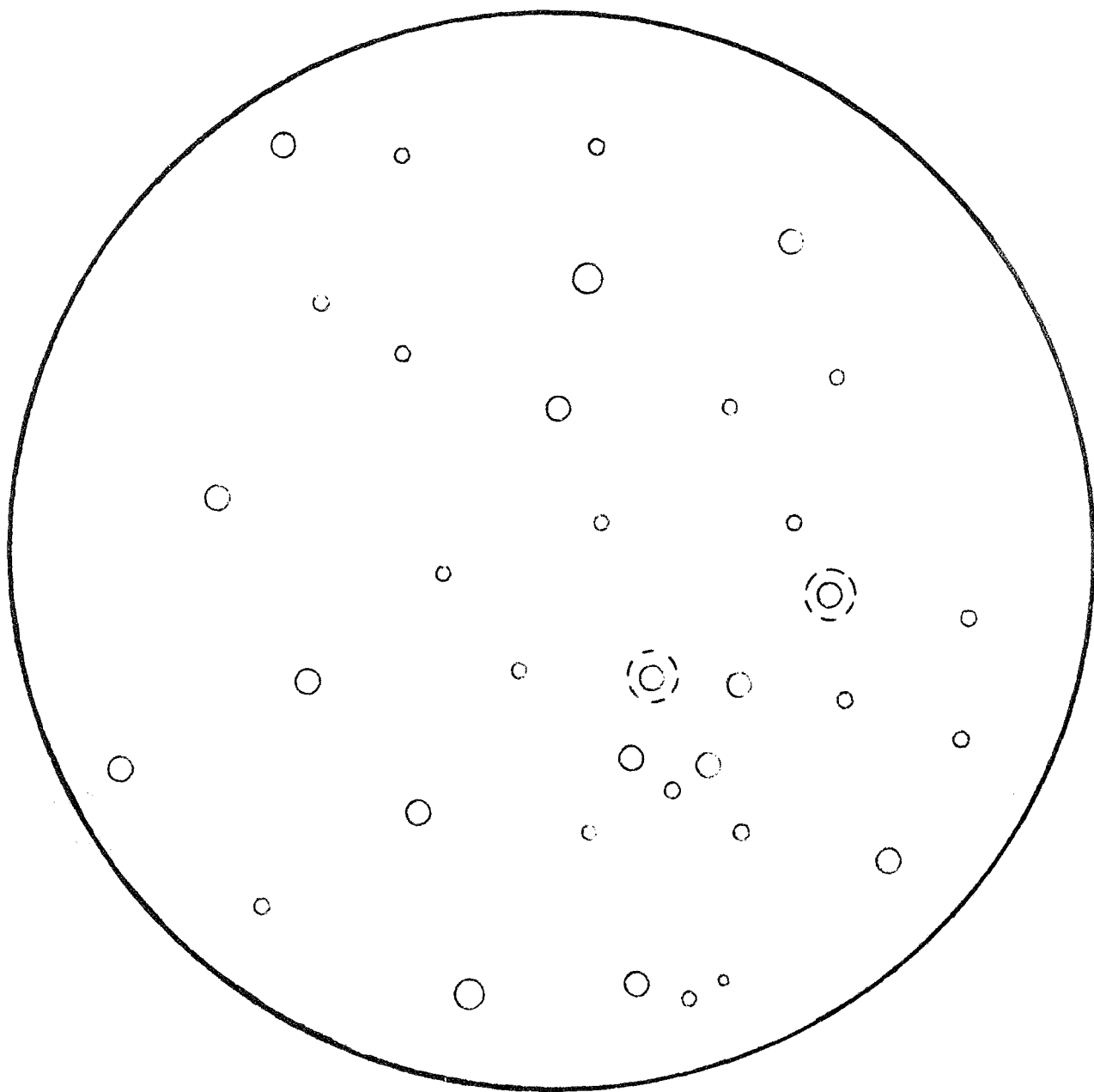


Figure 43

SIMULATED RANDOM ARRAY OF PARTICLES IN AN AIRSTREAM

Dotted line denotes encounter diameter.

It is useful to think of particles pursuing a random walk through the fibrous system. Thus, imagine that a composite filter consists of many sections like those in Figure 22 in series with each other. Imagine we wanted to predict how many filter sections would be required to capture all the particles in Figure 43. We could have a series of drawings like that in Figure 22, each of which could be placed on top of Figure 43 in many random orientations. The experiment could be repeated until all particles were captured. Each superposition of the simulated fiber system would be a step in the random walk of the particles through the filter.

The above concepts can obviously be extended to any system of fibers. It is even possible to simulate the effect of rotary motion. For instance, in the systems shown in Figures 22 and 23, the fiber system could be rotated a definite distance to simulate the movement occurring for a given movement of airstream through the system, and thus the increased capture rate could be studied.

In conclusion, it can be stated that the use of Monte Carlo techniques for simulating random walk of particles through a filter system could be very useful for investigation capture efficiency of various fiber element orientations as well as effects of rotation of the filtering mechanisms.

## REFERENCES

1. Sinclair, D. and LaMer, V. K., Chem. Rev., 44, 245, 1949.
2. Ditchburn, R. W., "Light," Interscience Publishers, Inc., pp. 441, 480, 1953.
3. Van de Hulst, H. C., "Light Scattering by Small Particles," Wiley, 1957.
4. Van de Hulst, H. C., "Optics of Spherical Particles," N. S. Drukkerij, J. J. Duwaer and Sons, Amsterdam, 1946.
5. Sinclair, D., "Handbook on Aerosols," Chap. VII, Atomic Energy Commission, Washington, D.C., 1950.
6. Berry, C. R., J. Optical Soc. Am., 52, 888, 1962.
7. Mie, G., Ann. Physik, 25, 1908; Stratton, J. A., "Electromagnetic Theory," McGraw-Hill, Chap. IX, 1941.
8. Blumer, Z. Physik, 38, 304, 1962.
9. Lowan, A. N., "Tables of Scattering Functions for Spherical Particles," National Bureau of Standards Applied Mathematics Series No. 4, 1948.
10. Berry, C. R., Marino, S. G., and Oster, C. F., Phot. Sci. Eng. 5, 332, 1961.
11. Naper, O. H. and Ottewill, R. H., "Electromagnetic Scattering," The Macmillan Co., New York, 1963.
12. Penndorf, R., New Tables of Scattering Functions, Geophysics Research Papers, No. 40, AFCRC-TR-56-204(6), Parts 1-6.
13. Stevenson, A. F., Heller, W., and Wallach, M. L., J. Chem. Phys. 34, 1789, 1961.
14. Andrews, C. L., "Optics of the Electromagnetic Spectrum," Prentice Hall, Englewood Cliffs, N.J., 1960.
15. Ditchburn, R. W., "Light," Interscience Publishers, Inc., New York, p. 28, 1961.
16. Heywood, H., "The Scope of Particle Size Analysis and Standardization," Symposium on Particle Size Analysis, published by London Institution of Chemical Engineers, p. 17, Feb. 1947.

17. Davies, C. N., "Survey of Scattering and Adsorption of Light by Particles," The Physics of Particle Size Analysis, Brit. J. Appl. Phys., Suppl. 3, Apr. 1954.
18. DeVore, J. R. and Pfund, A. H., J. Opt. Soc. Am., Vol. 37, No. 10, pp. 826-832, Oct. 1947.
19. Barnett, C. E., Ind. Eng. Chem., Vol. 41, p. 272, 1949.
20. See, for example, the work of Bates and Pillow, described in "Geometrical Probability," Kendall and Moran, Hafner Pub. N.Y., 1962.
21. Mason, G. and Clark, W., "Distribution of Near Neighbors in a Random Packing of Spheres," Nature, Vol. 207, No. 4996, p. 512, 1965.
22. Bonenali, R. F. and Brosilow, C. B., "Void Fraction Distribution in Beds of Spheres," AIChEJ, p. 359, July 1962.
23. Wise, M. E., Phillips Res. Rept., 9, p. 25, 1954.
24. Herdan, G., "Small Particle Statistics," pp. 180-200, Butterworths, 1960.
25. McCracken, D. D., "The Monte Carlo Method," Sci. Am., p. 90, May 1955.
26. Van de Hulst, H. C., "Light Scattering by Small Particles," John Wiley and Sons, New York, 1957.
27. Steig, F. B., Jr., Off. Dig. Federation Paint Varnish Prod. Clubs, Vol. 29, No. 388, p. 439, May 1957.
28. Armstrong, W. G. and Madson, W. H., Ind. Eng. Chem., Vol. 39, p. 944, 1947.
29. Zerlaut, G. A., "Utilization of Pigmented Coatings for the Control of Equilibrium Skin Temperatures of Space Vehicles," Proc. Aerospace Finishing Symposium, Ft. Worth, Tex., Dec. 8, 9, 1959.



## APPENDIX

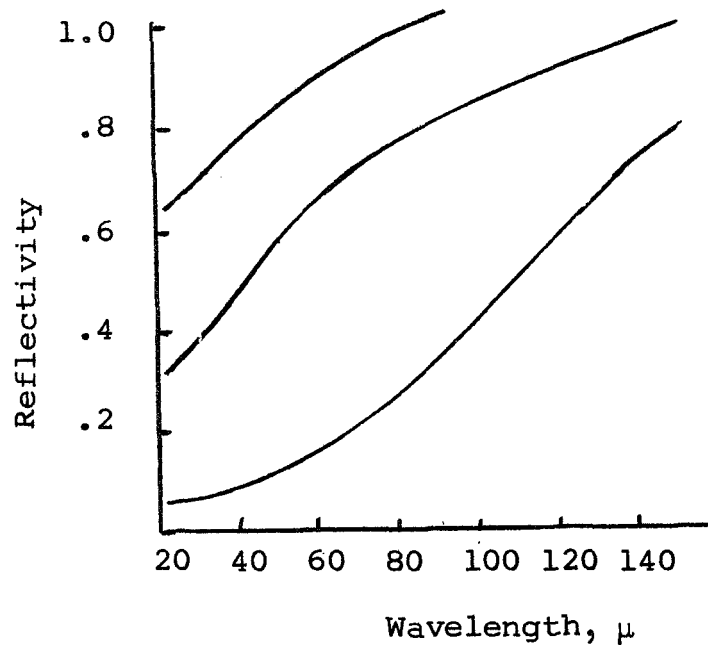
### ERRATA IN VOLUMES 2 AND 3

#### VOLUME 2

1. p. i; line 7 should read: May 1, 1963, to September 30, 1966.
2. p. 24, line 9; "particle" should be "particles."
3. p. 53, line 6 of para. 5; "approximate Figure 16 (see Figure 27)" should read "approximate figure 8's (see Figure 27)."
4. p. 82, Figure 44 caption; "protons" should read "photons."

#### VOLUME 3

1. p. 27, line 2, para. 2; the figure noted as Figure 11 is missing. The missing figure is not Figure 11 (which is on p. 24). The missing figure is enclosed herein as Figure 44 of Volume 1.
2. p. 51, line 8 of para. 2; "the measured porosities" should read "the measured densities."
3. p. 52, Figure 14; the ordinate should be captioned "Density," not "Porosity."
4. p. 54, line 10; Van de Hulst is reference 22, not reference 23.
5. p. 86; Equation 45 should be: 
$$\frac{I_I}{I_0} = \exp (-KCL)$$
6. p. 104, Figure 42; the curves are mislabeled; the top curve is uncorrected for edge effects.
7. p. 105, line 1 of para. 2; "in Section VA" should read "in Section VIII."
8. p. 127, line 2; "shown in Figure 55" should read "shown in Figure 54."



- A - Brass plate polished with fine abrasive powder  
B - Brass plate polished with medium-grade abrasive powder  
C - Brass plate polished with coarse abrasive powder

Figure 44  
REFLECTIVITIES OF BRASS PLATES  
OF DIFFERENT SURFACE QUALITY